HYDRAULIC ENERGY LOSS IN PIPE EXPANSIONS

by

GOLAM MUSTAFA

A Thesis
Presented to the University of Manitoba
in Partial Fulfillment of the
Requirements for the Degree of
MASTER OF SCIENCE
in the
DEPARTMENT OF AGRICULTURAL ENGINEERING

Winnipeg, Manitoba

MAY, 1984

HYDRAULIC ENERGY LOSS IN PIPE EXPANSIONS

by

Golam Mustafa

A thesis submitted to the Faculty of Graduate Studies of the University of Manitoba in partial fulfillment of the requirements of the degree of

MASTER OF SCIENCE

ABSTRACT

The energy loss coefficient of pipe expansions in reducing the velocity of flow from values occurring at the outlet of a centrifugal pump to values acceptable for mainline flow in an irrigation system was determined. Sixteen pipe expansions were tested in the Hydraulics Laboratory of the Department of Civil Engineering at the University of Manitoba. They were made of standard steel. Four were abrupt pipe expansions each of which featured a different combination of approach and exit diameters. Six gradual pipe expansions and six two-stage pipe expansions each featuring a gradual expansion stage and an abrupt expansion stage were also tested. A comparison of the experimental values of the energy loss coefficient reflects the impressive potential of the optimally designed two-stage pipe expansion by showing that it has an energy loss which in many applications would be only a fraction of the energy loss for the other pipe expansions.

ACKNOWLEDGEMENTS

The author is grateful to his advisor, Dr. G.E. Laliberte, who introduced the author to this field of research. The author also wishes to express his gratitude to Dr. Laliberte for his invaluable suggestions, useful guidance, helpful criticisms and continuous encouragement throughout the period of this research.

Sincere appreciation is due to the other members of the Examination Committee, Dr. A. Tamburi and Dr. F.F. Penkava, for their valuable suggestions.

The author wishes to express his sincere appreciation to Mr. J. Putnam for his valuable help in the preparation and installation of the experimental set-up and his continuous help throughout this research.

Special thanks are extended to the staff of the Department of Agricultural Engineering and the Department of Civil Engineering's Hydraulic Laboratory for their help and cooperation during this study.

The author wishes to express his heartfelt gratitude to the Department of Agricultural Engineering for the research assistantship which the author received during his studies and research.

Very special thanks are extended to Mrs. Donna Weiss and Mrs. Debby Allston for their cheerful and helpful cooperation on many occasions during this study.

Lastly, the author wishes to dedicate this thesis to his parents who have been a source of inspiration all through his life.

TABLE OF CONTENTS

LIST OF TABLES

LIST OF FIGURES

CHAPTER I

INTRODUCTION

1.1 GENERAL

In pressurized irrigation systems, centrifugal pumps deliver the water to the irrigation system with a relatively high velocity. This high velocity typically ranges from 4 to 10 m/s. The reason for designing pumps at such a high discharge velocity is to achieve higher pump efficiency.

Unfortunately, if water were transported for long distances in pipes in an irrigation system at these high velocities, a substantial amount of energy would be sacrificed due to high frictional losses in the pipes and fittings. Another problem associated with high velocities in pipelines would be the vibration and the increased hazard of failure resulting from water hammer.

For these reasons, a maximum velocity of 1.5 m/s is recommended (Uni-Bell Plastic Pipe Association, 1977) to keep the friction losses to an acceptable level. To achieve this average velocity, it is necessary to reduce the velocity of water in the mainline. This can be accomplished by using a large-diameter pipe; however a large-diameter pipe requires higher capital cost and this is a critical factor for the selection of pipe diameter. In most labour-intensive systems and in some capital-intensive systems, the mass of the pipe which is to be transported within and between fields is also a consideration.

For reducing the high discharge velocities a device called a pipe expansion (also labeled an expander, an enlargement or a diffuser) is used. A pipe expansion decreases discharge velocity by increasing the cross-sectional area of flow, in accordance with the continuity condition. To achieve this objective a certain amount of energy has to be sacrificed in the device itself, due to wall friction, turbulence and deceleration.

The challenge is to develop an acceptable design for this device which achieves a minimum energy loss.

1.2 BACKGROUND

During a field survey of 556 pumping stations in 17 Oregon counties, Shearer and Hansen[1] observed that the pipe expansion most commonly used by farm operators to reduce the velocity at the pump outlet was an abrupt pipe expansion. This type of pipe expansion configuration is comparatively easy to fabricate, requires less space and is inexpensive to buy. Unfortunately, it has a high energy loss for a given practical use.

In recent years, with increasing concern for energy conservation, the gradual pipe expansion has become more popular. A gradual pipe expansion results in a lower energy loss as compared with an abrupt pipe expansion. This type of pipe expansion is slightly more difficult to fabricate, requires more space and is slightly more expensive to buy. But for most installations, the slightly higher initial cost is offset over a relatively short time by reduced energy costs.

---

1 Shearer, M.N., and H.J. Hansen. Unpublished information. Agricultural Engineering Department, Oregon State University, Corvallis, OR 97330.

The concepts presented in this work were developed by Laliberte, et al. (1983). They proposed a pipe expansion which would be potentially even more energy-efficient than the gradual pipe expansion. Although these authors did not claim the original idea, they did propose the original solution to a design equation on which the device is based. The uniqueness of the device is that it employs a two-stage pipe expansion. The device is no more expensive to fabricate than a gradual pipe expansion. It requires less space and, for a given application, it is claimed to have a smaller energy loss.

1.3 OBJECTIVES

The main objective of this study is to test the performance of a two-stage pipe expansion.

Secondly, it is a purpose of this study to verify the design criteria proposed by Laliberte, et al. (1983) by conducting a series of laboratory tests.

Finally, the study has the objective of presenting a comparison of the energy loss coefficients K for the sixteen pipe expansions considered.

1.4 SCOPE OF THE STUDY

The two-stage pipe expansion has the potential for energy saving in irrigation systems. One of the encouraging and practical features is its simplicity of fabrication. If a flanged connection is used, the manufacturing process is similar to that for a single-stage gradual pipe expansion. In addition, the amount of material required is marginally less.

CHAPTER II

REVIEW OF LITERATURE

2.1 ENERGY LOSS IN FITTINGS

There are a number of ways to express the energy loss associated with resistance to flow in pipe fittings. One of these requires an energy loss coefficient which, if multiplied by the average approach velocity head gives the energy loss. Mathematically, it can be expressed as:

$$\Delta E = K \frac{V_1^2}{2g} \qquad (1)$$

where ΔE is the energy loss per unit weight,

K is the energy loss coefficient,

V_1 is the average approach velocity, and

g is the acceleration due to gravity.

There are a number of charts, nomographs and tables available from many sources for the energy loss coefficient for pipe fittings including bends, elbows, tees, entrances, exits, contractions, and gradual and abrupt pipe expansions. One must be careful in using values of the energy loss coefficient obtained from a chart, nomograph or table.

There are two other energy loss coefficients which are expressed as a function of both the approach and the exit velocities and applied to pipe expansions. The equations are as follows:

$$\Delta E = \frac{K_1 \ (V_1 - V_2)^2}{2g} \qquad (2)$$

$$\Delta E = \frac{K_2 \ (V_1^2 - V_2^2)}{2g} \qquad (3)$$

where K_1 and K_2 are the two other energy loss coefficients,

V_2 is the average exit velocity and the remaining terms are as defined before.

After applying the continuity condition the energy loss coefficients for pipe expansions can be related as follows:

$$K = K_1 \left[\frac{D^2 - 1}{D^2} \right]^2 \tag{4}$$

$$K = K_2 \left[\frac{D^4 - 1}{D^4} \right] \tag{5}$$

$$K_1 = K_2 \left[\frac{D^2 + 1}{D^2 - 1} \right] \tag{6}$$

where D is the ratio of the exit and inlet diameters.

2.2 ENERGY LOSS IN ABRUPT AND GRADUAL PIPE EXPANSIONS

Brightmore (1906) and Gibson (1911) experimentally demonstrated that, for an abrupt pipe expansion (Fig. 1), the energy loss coefficient K_1 can be expressed as a function of the expansion geometry by the equation:

$$K_1 = \frac{102.5 + 0.25D^2 - 2.0d_1}{100} \tag{7}$$

where D is the ratio of the exit and inlet diameters, and d_1 is the approach diameter in inches.

If d_1 is expressed in centimetres, Eq. 7 becomes,

$$K_1 = \frac{102.5 + 0.25D^2 - 5.1d_1}{100} \tag{8}$$

Archer (1913), however, experimentally formulated the energy loss in an abrupt pipe expansion by the equation:

$$\Delta E = \frac{1.098\ (V_1 - V_2)^{1.919}}{2g} \qquad (9)$$

where V_1 and V_2 are in feet per second.

As corrections for pipe wall friction losses between the points of measurement of hydrostatic head upstream and downstream from an abrupt pipe expansion were made in Archer's experiments, the energy loss ΔE in Eq. 9 represents only the component resulting from internal fluid forces.

King, et al. (1948) and Brater and King (1976) substantiated Archer's findings. Assuming the continuity condition for incompressible fluid and comparing Eq. 2 and Eq. 9, the energy loss coefficient K_1 can be expressed in terms of V_1 and D; thus,

$$K_1 = \frac{1.098}{V_1^{0.081}} \left[\frac{D^2}{D^2 - 1} \right]^{0.081} \qquad (10)$$

where V_1 is in feet per second.

When V_1 is expressed in metres per second, Eq. 10 becomes:

$$K_1 = \frac{0.997}{V_1^{0.081}} \left[\frac{D^2}{D^2 - 1} \right]^{0.081} \qquad (11)$$

The values of K_1 derived by using Archer's equations and those by using Eqs. 7 and 8 are very close. However, in practice the value of K_1 is not determined from any of the above mentioned equations, but rather is assumed to be independent of V_1, d_1 and D, and is taken to be equal to 1.00.

On the other hand, the value of K_1 for a gradual pipe expansion, is generally less than 1.00. Gibson (1911) derived an equation for the energy loss coefficient K_1 as follows:

$$K_1 = 0.0110\ \theta^{1.22},\ 6^\circ \le \theta \le 35^\circ \qquad (12)$$

where θ is the internal planar angle between the walls of a gradual pipe expansion of conical cross section (Fig. 2).

When θ is expressed in radians, Eq. 12 becomes:

$$K_1 = 1.536\ \theta^{1.22}\ ,\ 0.10 \text{ rad} \leq \theta \leq 0.61 \text{ rad} \qquad (13)$$

Eqs. 12 and 13 yield values of K_1 in the range $0.10 \leq K_1 \leq 0.84$. Eqs. 12 and 13 were derived under experimental conditions characterized by energy loss due to pipe wall friction and internal fluid forces caused by shear and turbulence. Friction losses become relatively more important than internal fluid losses for $\theta < 6°$. At $\theta \simeq 5°$, K_1 reaches a minimum; the value of K_1 increases if θ becomes either less than or greater than 5°. The angle θ which produces the minimum value of K_1 is also a function of wall surface roughness. In Gibson's experiments, a moderately smooth wall surface in sections bored from brass was used.

Andres (1909), using a smaller interior angle ($2° \leq \theta \leq 12°$) and an extremely smooth wall surface, determined the energy loss coefficient for gradual pipe expansions in terms of K_2 instead of K_1. The values of K_2 were in the range $0.033 \leq K_2 \leq 0.20$.

Using Eq. 6 for D = 1.6, these values of K_2 can be shown to be equal to values of K_1 in the range $0.075 \leq K_1 \leq 0.46$. In the range of overlap of θ in Gibson's and Andres' experiments, the results are not entirely in agreement (King, et al. 1948). The small difference is considered to be due to the influence of wall surface roughness.

King, et al. (1948) and Brater and King (1976) solved Eq. 4 for abrupt pipe expansions using a value of K_1 from Eq. 10. The results reveal that the practice of assuming $K_1 = 1.00$ for abrupt expansion is justified.

King, et al. (1948) and Brater and King (1976) also determined the energy loss coefficient K for gradual pipe expansions for different values of D over the range $2° \leq \theta \leq 60°$. Investigators are cautioned that the results at best represent approximations of the experimental work of Andres (1906) and Gibson (1911) on which they are based.

Tatarinov (1946) developed a graphical representation of K over the range $5° \leq \theta \leq 180°$ for values of D in the range $1.3 \leq D \leq 4.0$, probably based on Gibson's data. In general, Laliberte, et al. (1983) found that Tatarinov's curves for K correspond reasonably well (± 0.07) with values of K calculated using, in Eq. 4, values of K_1 determined from Eq. 12 and Gibson's other experimental values of K_1 in the range $35° \leq \theta \leq 180°$. Tatarinov's curves are applicable for both gradual and abrupt pipe expansions.

Idel'chik (1966) postulated that the energy loss coefficient should reflect both wall friction losses and internal fluid losses; thus,

$$K = K_{fr} + K_{exp} \tag{15}$$

where K_{fr} is the friction coefficient and K_{exp} is the local resistance coefficient due to the pipe expansion. For an abrupt pipe expansion, Idel'chik recommended $K_{fr} = 0$ and calculated value of K_{exp} using Eq. 4 in which $K_1 = 1.02$. Thus, the energy loss coefficient becomes:

$$K = 1.02 \left[\frac{D^2 - 1}{D^2} \right]^2 \tag{16}$$

For a gradual pipe expansion of conical geometry, Idel'chik formulated the friction coefficient:

$$K_{fr} = \frac{\lambda}{8} \operatorname{cosec} \frac{\theta}{2} \left[\frac{D^4 - 1}{D^4} \right] \tag{17}$$

where λ is the frictional coefficient of a unit relative length of pipe (length in section-diameter units) determined as a function of the Reynolds number R from graphs provided and the other parameters are as previously defined.

For the local resistance coefficient due to pipe expansion he proposed the expression:

$$K_{exp} = 3.2\ (\tan \frac{\theta}{2})^{1.25} \left[\frac{D^2 - 1}{D^2} \right]^2, \quad 0° \leq \theta \leq 40° \qquad (18)$$

Eq. 18 is quite similar to one that can be derived from Eq. 4 by substituting an alternate equation for Eq. 12 suggested by Gibson (1911), that is,

$$K_1 = 3.5\ (\tan \frac{\theta}{2})^{1.22}, \quad 7.5° \leq \theta \leq 35° \qquad (19)$$

which yields in the following equation for K:

$$K = 3.5\ (\tan \frac{\theta}{2})^{1.22} \left[\frac{D^2 - 1}{D^2} \right]^2, \quad 7.5° \leq \theta \leq 35° \qquad (20)$$

Similarity between Eqs. 18 and 20 suggests the applicability of Gibson's equations when K_{fr} is small relative to K_{exp}.

Substituting Eqs. 17 and 18 into Eq. 15 gives:

$$K = \frac{\lambda}{8}\ \mathrm{cosec}\ \frac{\theta}{2}\ (\frac{D^4 - 1}{D^4}) + 3.2\ (\tan \frac{\theta}{2})^{1.25}\ (\frac{D^2 - 1}{D^2})^2,$$

$$0° \leq \theta \leq 40° \qquad (21)$$

This equation is for the energy loss coefficient K for gradual pipe expansions of conical geometry having small interior planar angles.

Laliberte, et al. (1983) reported that, in the range $6° \leq \theta \leq 35°$, the values of the energy loss coefficient K for gradual pipe expansion calculated from Eqs. 4 and 12 together and from Eq. 21 match quite closely (± 0.04). And the values of K for an abrupt pipe expansion using Eq. 16 and from Eqs. 4 and 7 together also match very closely. The range $40° \leq \theta \leq 180°$ of the interior planar angle was not covered by Idel'chik's study. But fortunately it is of less practical interest. So Idel'chik's technique for obtaining the energy loss coefficient is useful in the design of irrigation systems. Based on the experiments of Fliegner (1898) and Andres (1906), Parker (1925) suggested a set of values of K_2 in the range $2° \leq \theta \leq 12°$ which are identical with those suggested by King, et al. (1948) and Brater and King (1976) in the range $2° \leq \theta \leq 9°$, but differ in the range $10° \leq \theta \leq 12°$.

Babb and Amorocho (1976) reported the energy loss coefficient K for air flow in a gradual pipe expansion for $\theta = 6°$ and D = 2.0 to be 0.34. This value is larger by a factor of 4 and a factor of 7 than is predicted by Idel'chik's and Tatarinov's equations and by the methods of King, et al. (1948), Brater and King (1976), and Gibson (1911), respectively. Chaturvedi (1963) concluded that energy loss in an axisymmetric expansion reaches its maximum value at $\theta = 60°$ and in the range $60° \leq \theta \leq 180°$ the values of energy loss coefficient are close to the maximum value.

Cermak (1948) found a good correlation between theoretical equations and his data based on experiments with conical diffusers using air for a range of internal planar angle $7.5° \leq \theta \leq 180°$, diameter ratio $1.95 \leq D \leq 6.43$ and Reynolds number $5\ 000 \leq R \leq 150\ 000$.

Rouse and Jezdensky (1966) found the energy loss coefficient K for an abrupt pipe expansion for the range of diameter ratio $1.6 \leq D \leq 3.5$ to be very close to the values estimated by Eq. 4 with $K_1 = 1.00$.

Furuya and Sato (1959) suggested that conical diffusers with an internal planar angle θ of 10° and a suddenly enlarged outlet have significant advantages over the simple conical diffuser of the same length but having an internal planar angle greater than 20°.

And when the interior wall near the separation point is roughened, the energy loss is less than in the case of a smooth wall because of delay of the separation point.

Duggins (1970), using truncated conical diffusers, reported that truncation of the cone yielded a reduced pressure recovery, typically 4% for a 50% truncation. According to Duggins, this result is inconsistent with Gibson's theory. However, he claimed that these findings are in accord with Henderson's theory which postulates that the loss in a truncated diffuser exceeds that in the untruncated diffuser by an amount equal to the loss in a sudden enlargement having the area change that occurs at the truncation. According to Laliberte, et al. (1983), Duggins incorrectly attributes to Gibson an empirical expression which assumes that the energy loss in the first stage is proportional to the change in the velocity head through both stages of the expansion. In reality, however, Gibson assumed a proportionality between energy loss and the change in the velocity head through only the first stage.

2.3 AN ENERGY-EFFICIENT TWO-STAGE PIPE EXPANSION

Gibson (1911) demonstrated that a two-stage pipe expansion consisting of a gradual expansion in the first stage and an abrupt expansion in the second stage (Fig. 3) is the most energy-efficient fitting for a given diameter ratio D and that the energy loss for a two-stage pipe expansion could be minimized by proper selection of diameter at the interface of the two different pipe expansions.

Gibson (1911) formulated an equation for the energy loss as follows:

$$\Delta E = \frac{(V_1-V_2)^2}{2g} \left(\frac{r_2^2}{r_2^2 - r_1^2}\right)^2 \left[K_1 \left(1 - \frac{r_1^2}{(r_1 + \frac{\ell\theta}{2})^2}\right)^2 + \left(\frac{r_1^2}{(r_1 + \frac{\ell\theta}{2})^2} - \frac{r_1^2}{r_2^2}\right)^2\right] \quad (22)$$

where r_1 and r_2 are the approach and the exit pipe radii respectively, θ is the interior angle between the diverging walls of the conical first stage of the two-stage fitting, K_1 is the energy loss coefficient applicable to a velocity head term as explained in Eq. 2 (not $V_1^2/2g$) for the first stage, and ℓ is the length of the pipe expansion.

Gibson successfully validated Eq. 22 by using independently determined values of K_1 and ΔE for different values of approach and exit velocities. However, the only way he was able to develop a method of determining the optimum value of the interior angle θ_o, which produced a minimum energy loss was by a trial-and-error substitution of values of θ in his equation.

Laliberte, et al. (1983) inserted dimensionless lengths and diameters in the Gibson's equation and developed the following equation:

$$K = a\theta^b \left[1 - \frac{1}{(1 + L\theta)^2}\right]^2 + \left[\frac{1}{(1 + L\theta)^2} - \frac{1}{D^2}\right]^2, \ \theta \text{ in rad.} \quad (23)$$

Differentiating Eq. 23 with respect to θ and equating θ to θ_o and $dK/d\theta$ to zero gives:

$$\theta_o^4 + \frac{5}{L}\theta_o^3 + \frac{4}{L^2}\frac{2b+1}{b}\theta_o^2 + \frac{4}{L^3}\frac{b+2}{b}\theta_o + \frac{4}{abL^4\theta_o^b}\left[\frac{(1+L\theta_o)^2}{D^2} - 1\right]$$

$$= 0, \ \theta_o \text{ in rad.} \quad (24)$$

In Eq. 24, values of 1.536 and 1.220 for a and b, respectively, are substituted from Eq. 13. The applicability of this equation is in the range of 0.10 rad. $\leq \theta_0 \leq$ 0.61 rad. This non-linear equation was solved by using Newton's method of iteration to get the approximate optimal value of internal planar angle, that is θ_0.

After getting the optimal value of θ_0 (in radians), the optimal value of the diameter ratio D' at the interface between the first stage and the second stage of the two-stage pipe expansion, that is d'/d_1, is defined by:

$$D' = 1 + L\theta_0 \tag{25}$$

Here, d' is the optimal value of the diameter at the interface between the first stage and the second stage and L is the length ratio l/d_1.

Tables 1 and 2 show values of θ_0 and the optimal value of D' for different values of length ratios L and diameter ratios D, respectively. The optimum internal planar angle θ_0 results in the minimum value of K. The minimum value of K, thus, can be obtained by substituting $\theta = \theta_0$ in Eq. 23. Table 3 presents values of K in an optimally design two-stage pipe expansion for a range of values of dimensionless diameter and length.

CHAPTER III

EQUIPMENT, MATERIALS AND METHODS

3.1 PUMP AND ELECTRIC MOTOR

A single-stage vertical-axis pump was used to deliver water from the sump to the mainline. The specifications for the pump and for a three-phase electric motor required to supply the power to the pump are as follows:

Pump Specifications

Manufactured by:

FAIRBANKS-MORSE

Impeller size	:	0.355 m
Discharge	:	0.221 m^3/s
Total head	:	15.240 m
Speed	:	1770 rpm
Intake diameter	:	0.217 m
Serial no.	:	K3 J260

Electric Motor Specifications

Manufactured by:

BROWN BOVERI (CANADA) LTD., LACHINE
QUEBEC, CANADA

Power	:	44.76 KW
Speed	:	1776 rpm
Current	:	55 A
Voltage	:	575 V
Model	:	365 UPR-4DLHW
Serial no.	:	C32-3638-902

3.2 ORIFICE PLATE

A circular orifice plate installed in the supply line was used to measure the discharge. The orifice diameter was 0.152 m and the pipe diameter was 0.203 m. The discharge through the orifice plate was calculated by using the equation:

$$Q = 22.7\ h^{0.467} \qquad (29)$$

where Q = flow, m^3/s,

h = differential head at orifice, centimetres of mercury,

and 22.7 and 0.467 are the experimental constants.

Differential head at the orifice was measured by using a

U-tube manometer with red meriam having a specific gravity of 2.95 as the measuring liquid. The measured differential head was converted to an equivalent differential head for mercury and then used in Eq. 29 to calculate the discharge. In addition to the measurements using the red meriam manometer, the discharge through the orifice plate was also measured directly by using a previously calibrated mercury manometer which read the discharge in litres per second. Both readings were compared and it was found that, for higher discharges (above 0.040 m^3/s), both readings were nearly the same. For discharges less than 0.040 m^3/s, however, only the red meriam manometer readings were considered because, for the mercury manometer, the low discharge measurements were not within an acceptable limit of error.

3.3 DIFFERENTIAL MANOMETERS

Three differential manometers were used to measure the change in piezometric head along the pipe expansion test section. The manometers were connected with the test section using 'poly-flo' (polyethylene) thermoplastic tubing, T-joints and control valves. Two different setups for the differential manometers were constructed to facilitate measurement of the change in piezometric head for all of the test sections. In the first setup (Fig. 4), two different measuring liquids were used; one was red meriam having a specific gravity of 2.95 and the other liquid was mercury of specific gravity 13.57. Manometers Nos. 1 and 3 were filled with red meriam and Manometer No. 2 was filled with mercury. Manometers Nos. 1 and 3 were used to measure the change in piezometric head upstream and downstream from the pipe expansion, respectively. Manometer No. 2 was used to measure the change in piezometric head between the inlet and exit of the pipe expansion.

In the second setup (Fig. 5), only one manometer filled with red meriam was used to measure the change in piezometric head along the test section successively between upstream tapping points, between the inlet and exit points of the pipe expansion and between the downstream tapping points. The arrangement of the manometers and the pressure taps along the pipe expansion test section for both the first and the second setups is shown in the schematic diagrams (Figs. 4 and 5).

3.4 DIMENSIONS FOR THE PIPE EXPANSION TEST SECTIONS

Altogether, 16 pipe expansion test sections were tested in the Hydraulics Laboratory of the Department of Civil Engineering, University of Manitoba. Four were abrupt pipe expansions each of which featured a different combination of approach and exit diameter. Six gradual pipe expansions and six two-stage pipe expansions were also tested. They were all made of standard steel. The two-stage pipe expansions featured the optimal design criteria suggested by Laliberte, et al. (1983). Dimensions of the pipe expansion test sections are presented in Tables 4 to 6.

3.5 EXPERIMENTAL PROCEDURE

For each test section the experimental procedure was as follows:

1. The test section was welded together with an upstream and downstream pipe expansion and then installed in an existing pipeline in the Hydraulics Laboratory, using a Style 78

Victaulic coupling and a Rockwell 411 coupling.

2. The manometers were connected with the tapping points through 'poly-flo' (polyethylene) thermoplastic tubing, connecting tees and control valves.
3. The pump was used to deliver water from the sump to the mainline. After passing through the test section, the water drained back into the sump.
4. Discharge rates were measured using the manometers which were connected across the orifice plate using 'poly-flo' (polyethylene) thermoplastic tubing.
5. The change in piezometric head along the test section was recorded.
6. Steps 4 and 5 were repeated at different discharge rates.

3.6 COMPUTATION OF THE ENERGY LOSS COEFFICIENT

1. The recorded changes in piezometric head were converted into changes in piezometric head in m of water (Tables 7 to 22).
2. The discharge rates were converted into approach and exit velocities in m/s (Table 23).
3. A FORTRAN IV programming language algorithm was developed to predict piezometric head gradient as a function of discharge in a steel pipe with an assumed absolute roughness coefficient of 4.572×10^{-5} m. This program used the Darcy-Weisbach equation and this equation requires the solution of a non-linear equation to estimate the value of the coefficient of friction f. The Newton-Raphson method of iteration was employed to approximate the value of f. This program

interfaced with the VERSATEC PLOTTER subroutines and plotted the graph between the gradient of piezometric head and discharge for the different pipe diameters tested in this study. Graphs are presented in Appendix A (Figs. A-1 to A-5) and the listing of the computer program algorithm is presented in Appendix B.

4. A second FORTRAN IV programming language algorithm was developed to fit a least-square straight line through the observed change in piezometric head along the horizontal centreline of the pipe expansion. This program plotted the upstream and downstream least-square straight lines simultaneously and then calculated the change in piezometric head between the approach and exit points of the pipe expansion. This program also calculated the velocity head, the energy loss in the pipe expansion and finally determined the energy loss coefficient K. Figs. C-1 to C-22 show the plot of the predicted least-square straight lines as well as the observed change in piezometric head along the test section. The listing of this second computer program algorithm is presented in Appendix C.

CHAPTER IV

RESULTS AND DISCUSSION

A summary of the experimental values of the energy loss coefficient K for the abrupt, gradual and two-stage pipe expansions for each of the velocities tested is shown in Table 24. It is evident from the mean values of the energy loss coefficient K that the gradual pipe expansion is generally more energy-efficient than the abrupt pipe expansion. It is also evident that the two-stage pipe expansion is more energy-efficient than the other fittings (Table 25). This statement is true in general for all values of length ratio and at the higher values of diameter ratio. However, for lower values of diameter ratio, this claim cannot be made. The savings achievable with this optimally designed device are greatest, therefore, at higher dimensionless diameters. However, even at low values of D, the optimally designed two-stage fitting offers opportunity for considerable energy conservation, if it is considered as a replacement for an abrupt pipe expansion.

Examining the experimental values of the energy loss coefficient K (Table 24), it appears that, for the range of velocities attained in the experiments, the energy loss coefficient K does not vary in any regular manner with the velocity. In some cases, the value of K falls off appreciably with decreasing velocities, though, in general, the results do not show any very consistent pattern.

A comparison of the energy loss coefficient K determined experimentally with the predicted values of K (Laliberte, et al. 1983) for all the pipe expansions considered in this study is shown in Table 26. The comparison shows that, for two-stage and gradual pipe expansions with low diameter ratios D, the very low predicted values of K were not achieved in the experiments. Further, for low values of diameter ratios, the experimental values of K for the two-stage pipe expansion were of the same order as the values of K for the gradual pipe expansion. At higher values of diameter ratios D, however, the two-stage pipe expansion exhibited a low value of K as predicted and was considerably more energy-efficient than a gradual pipe expansion having the same diameter ratio D and length ratio L.

The percentage difference in values of the energy loss coefficient K between the predicted results based on the optimal design criteria suggested by Laliberte, et al. (1983) and the experimentally determined results is presented in Table 27.

The deviations from the predicted values of K were between 40 to 400% for two-stage and gradual pipe expansions with low diameter ratios D. However, for the higher diameter ratios the highest deviation from the predicted values of K was 33% (Table 27).

The deviations from the predicted values of K were partly due to the precision in measuring the piezometric head differences and velocity heads. The accuracy in measuring the piezometric head differences and velocity heads were ± 0.000975 m and ± 0.01915 m for red-meriam and mercury manometers, respectively.

The error that has occurred in the measurement of the relevant variables and, therefore, in the calculated values of the energy loss coefficient K is given in Table 28. These values of error show that the experimental setup and methods of measurement and calculation were fairly precise. Even with the highest error taken into consideration, the disagreement between the observed and the predicted values of K for the lower values of diameter ratio D cannot be explained satisfactorily. This implies that the observed variation of values of K is not due to the limitations of the experiment. It is interesting to note that, in those test runs for which there was potential for the maximum error (i.e. when meriam and mercury were used in manometers), the observed values of K agreed reasonably well with the predicted values of K. On the other hand, when the potential for error was less, the observed values of K deviated greatly from the predicted values. This, again, confirms the possibility that the prediction may not be suitable for this range of lower values of diameter ratio D. However, for the higher values of diameter ratio D, the experimental results correspond very closely to the predicted values.

Beside experimental error, there are other factors which might explain the disagreement, at the lower values of diameter ratio D, between observed values and predicted values of the energy loss coefficient K for two-stage pipe expansions. The following points illustrate these factors:

1. The effect of wall friction is not taken into account in Gibson's theory (1911). This assumption is valid for abrupt pipe expansions but, for gradual and two-stage pipe expansions, the wall friction effect in the expansion may be significant, depending on the length of the expansion, the absolute diameters of the approach and exit pipes, the fluid viscosity, the roughness of the wall surface and the state of the fluid flow. In reports of past research, it is claimed that the energy loss coefficient K should reflect both wall friction

losses and internal fluid losses (Idel'chik, 1966).

2. There may be an effect of the absolute magnitude of the pipe diameters on the observed value of energy loss coefficient K. For example, the results for abrupt pipe expansions nos. 1B and 1C, having the same diameter ratios but different absolute values of approach and exit pipe diameter (Table 4), show that, for the smaller absolute pipe diameters, the observed value of K is higher than for the higher absolute pipe diameters. The effect is perhaps due to the proportion of pipe cross-sectional area occupied by the boundary layer being higher for the smaller absolute pipe diameters than for the higher absolute pipe diameters. We do not have sufficient experimental data to frame any definite conclusions concerning the effect of the absolute magnitude of pipe diameters on the value of K for two-stage pipe expansions. However, from the above example, we can speculate that an effect involving the absolute value of pipe diameters similar to that observed for abrupt pipe expansions may exist for both gradual and two-stage pipe expansions.

3. The backward extrapolation of the piezometric pressure heads to the exit point of the pipe expansion represents an idealization which may contribute to the difference between the observed and the predicted values of the energy loss coefficient K. The pressure taps were installed beginning a short distance downstream from the exit point (Figs. 4 and 5) and at several additional downstream points. The extrapolated values of the piezometric pressure heads, of course, are not the true values because, while the velocity

distribution far downstream from the exit point is normally distributed over the entire cross-section represented by the downstream diameter d_2, the velocity profile at the exit point is not normally distributed over the entire cross-section. Instead it is distributed over only the diameter of the interface between the first stage and second stage, that is, over d'.

At the exit point, therefore, the reduction in velocity head has not been fully achieved. However, the extrapolation of the piezometric pressure head measured at the downstream points backward to the exit point of the pipe expansion is an idealization tantamount to assuming that the full reduction of the velocity head has been achieved at the exit point.

In fact, this situation cannot occur at the exit point because there can be no flow across the annular ring represented by the abrupt expansion which is the second stage of the two-stage pipe expansion. As mentioned, the full reduction in the velocity head and the normalization of the velocity profile does not likely occur until some point downstream from the exit point of the pipe expansion. The extent to which the actual flow pattern differs from the idealized condition is undoubtedly a factor accounting for the difference between observed and predicted values of the energy loss coefficient K.

Table 27 indicates that the optimally designed two-stage pipe expansion has substantial potential for energy conservation for the higher diameter ratios. However, for lower diameter ratios, energy conservation is not appreciably greater than that for the gradual pipe expansion. Conceivably, it should be possible to explain this phenomenon by a set of experiments having as an objective the visualization of the flow pattern in the transition zone of the pipe expansion. This would require the visual observation of the flow separation along the pipe expansion by constructing the expansion using a transparent material and by injecting dyes from the side walls of the pipe expansion during fluid flow. Unfortunately, it was impossible, within the constraints of the present study, to investigate this phenomenon. It is, however, hoped that it might be possible to do this in a future study.

To support a recommendation for this investigation, a possible physical explanation of the flow conditions through gradual and two-stage pipe expansions is proposed. In the case of a gradual pipe expansion, part of the velocity head is converted to piezometric pressure head by diverging flow boundaries as illustrated in Fig. 6. However, this conversion of velocity head to piezometric pressure head is more efficient in the case of a two-stage pipe expansion as illustrated in Fig. 7. It is hypothesized that toroidal eddies are formed in a zone of otherwise disorganized flow near the pipe wall immediately downstream from the second stage of a two-stage pipe expansion. It is further hypothesized that these eddies provide a continuously moving surface adjacent to the flow leaving the first stage of the pipe expansion. This phenomenon helps improve the flow condition. The high-velocity fluid leaving the first stage serves as a driving force, by virtue of shear stress, for the rotational motion of these eddies and, in the process, reduces the shear stress at the interface between the main flow leaving the first stage and the fluid in the zone occupied by the toroidal eddies. These toroidal eddies are probably more well developed for higher diameter ratios than that for lower diameter ratios because, for higher diameter ratios and in fact for higher values of absolute diameters, the size of the eddy zone is appreciably larger. For lower values of diameter ratios, and also for lower values of absolute diameters, the eddies in this zone are likely less well developed, the flow being characterized by turbulence which, instead of improving the flow condition in the main flow leaving the first stage, acts to retard it. This phenomenon would naturally be reflected in a higher value of energy loss coefficient K for these situations.

This physical explanation rationalizes the greater energy efficiency of the two-stage pipe expansions for higher diameter ratios and for higher values of absolute diameters. On the other hand, for the lower diameter ratios and for lower values of absolute diameters, the energy efficiency of the two-stage pipe expansions is similar to that of the gradual pipe expansions.

It can be speculated, therefore, that the predicted values of the energy loss coefficient K for two-stage pipe expansions having higher diameter ratios and also those having higher values of absolute diameters should correspond very closely to the experimental values of K. But, for the lower diameter ratios and for lower absolute diameters, the relatively low predicted values of the energy loss coefficient K would not likely be achieved from the experiments. Our study evidently confirmed this speculation and this is perhaps another factor explaining the pattern of the differences between observed and predicted values of the energy loss coefficient K, particularly for the lower diameter ratios, in addition to the three factors described previously.

CHAPTER V

CONCLUSIONS AND SUGGESTIONS FOR FUTURE RESEARCH

5.1 CONCLUSIONS

From this study it can be anticipated that the optimally designed two-stage pipe expansion has substantial potential for energy conservation in reducing the velocity of water as it exits from a centrifugal pump and enters the mainline of an irrigation system.

The very low predicted values of the energy loss coefficient for a two-stage pipe expansion were not achieved when the diameter ratios were small. In this situation the energy loss coefficient was similar to that of a gradual pipe expansion. Therefore, the energy efficiency attained was not appreciably greater than for the gradual pipe expansion.

At higher diameter ratios, however, the agreement between the predicted and the experimental values of the energy loss coefficients was good. Furthermore, at the higher diameter ratios, the observed values were appreciably lower for a two-stage pipe expansion than for a gradual pipe expansion and, of course, considerably lower than for an abrupt pipe expansion.

In situations calling for significant reduction of velocity, therefore, the optimally designed two-stage pipe expansion offers the possibility of accomplishing this objective with less energy loss than with any previously available pipe expansion. This opportunity probably represents the most significant contribution of this study.

5.2 SUGGESTIONS FOR FUTURE RESEARCH

1. Because of limited time and resources, this study did not include other available and commonly used pipe materials and the entire range of diameter and length ratios that was possible. Thus, further tests are suggested to quantify the energy loss coefficient K for the different available materials and the different combinations of diameter and length ratios which are in common use.
2. Since prediction and control of flow separation is of prime interest to hydraulic and fluid power engineers, study is recommended to investigate flow separation and to analyse and visualize the flow pattern in the transition zone by means of a numerical procedure and an experimental study. To visualize the flow pattern the use of a transparent material would be required to prepare the transition zone.
3. The flow conditions in a conical pipe expansion depend on the velocity distribution at the inlet of the pipe expansion as influenced by the initial state of the boundary layer. Therefore, a study is recommended of the various velocity distributions using different lengths of inlet pipe and valves and fittings which are commonly used in irrigation systems.
4. The rise in pressure during the transformation of kinetic energy to pressure energy is not complete at the end of the conical section. Therefore, a study is recommended on the effect of varying the length of the downstream pipe on the maximum pressure recovery.
5. This study did not make any attempt to apply other analytical

approaches in finding the most efficient cross-section for the pipe expansion. Therefore, further study is required using numerical approximation of Navier-Stokes equations to find the qualitative features of fluid flows in the transition zone of a most efficient cross-section and to gain experience on the problems associated with the full Navier-Stokes equations.

REFERENCES

1. Andres, K., "Versüche über die Umsetzung von Wassergeschwendigkeit in Druck", (Experiments on the Conversion of Water Velocity into Pressure), Zeitschrift des Vereines Deutscher Ingenieure, Forschungsarbeiten, Heft 76, Berlin, 1909.

2. Archer, W.H., "Experimental Determination of Loss of Head due to Sudden Enlargement in Circular Pipes", Transactions, ASCE, Vol. 76, Dec., 1913, pp. 999-1026.

3. Babb, A.F., and Amorocho, J., "Mean Energy in Gradually Diverging Flow", Journal of the Hydraulics Division, ASCE, Vol. 102, No. 1445, May, 1976, pp. 581-597.

4. Brater, E.F., and King, H.W., Handbook of Hydraulics for the Solution of Hydraulic Engineering Problems, 6th ed., McGraw-Hill Book Company, Inc., New York, N.Y., 1976, pp. 6-21, 6-22, 6-60, and 6-61.

5. Brightmore, A.W., Proceedings of the Institution of Civil Engineers, Vol. 169, No. 3, 1906, p. 322.

6. Cermak, J.E., "Energy Losses in Conical Diffusers", thesis presented to Colorado State University, at Fort Collins, Colo., in 1948, in partial fulfillment of the requirements for the degree of Master of Science.

7. Chaturvedi, M.C., "Flow Characteristics of Axisymmetric Expansions", Journal of the Hydraulics Division, ASCE, Vol. 89, No. HY3, Proc. Paper No. 3515, May, 1963, pp. 61-92.

8. Duggins, R.K., "The Performance of Truncated Conical Diffusers", J.S.M.E., Vol. 13, No. 2, 1971, pp. 103-109.

9. Furuya, Y., and Sato, T., "Pressure Recovery Efficiency of Short Conical Diffusers and of Roughened Diffusers", Bull. J.S.M.E., 1960, Vol. 3, No. 12, pp. 437-443.

10. Fliegner, A., "Versüche uber das Ausstromen von Luft Durch Konisch-divergente Düsen", Schweiz, Bauztg, 31, 1898.

11. Gibson, A.H., "On the Resistance to Flow of Water Through Pipes or Passages Having Divergent Boundaries", Transactions of the Royal Society of Edinburgh, Edinburgh, Scotland, Vol. 48, Part 1, 1911, pp. 97-116.

12. Handbook of PVC Pipe: Design and Construction, 1st ed., Uni-Bell Pipe Association, Dallas, Tex., 1977, p. 116.

13. Idel'chik, I.E., "Spravochnik po Gidravlicheskim Soprotivleniyam: Koeffitsienty Mestnykh Soprotivlenii i Soprotivleniya Treniya", (Handbook of Hydraulic Resistance: Coefficients of Local Resistance and of Friction), 1960, translated from Russian by Barouch, A., D. Grunaer and the staff of the Israel Program for Scientific Translations, eds., U.S. Department of Commerce, Clearinghouse for Federal Scientific and Technical Information, Springfield, Va., 1966, pp. 151-188, 497-499.

14. King, H.W., Wisler, C.O., and Woodburn, J.G., Hydraulics, 5th ed., John Wiley and Sons, Inc., New York, N.Y., 1948, pp. 206-209.

15. Laliberte, G.E., Shearer, M.N., and English, M.J., "Design of Energy-Efficient Pipe-Size Expansion", Journal of Irrigation and Drainage Engineering, ASCE, Vol. 109, No. 1, Mar., 1983, pp. 13-28.

16. Parker, P. á.M., The Control of Water as Applied to Irrigation, Power, and Town Water Supply Purposes, 2nd ed., George Routledge and Son Ltd., London, U.K., 1925, pp. 796-800.

17. Rouse, H., and Jezdinsky, V., "Fluctuation of Pressure in Conduit Expansions", Journal of the Hydraulics Division, ASCE, Vol. 92, No. HY3, May, 1966, pp. 1-12.

18. Tatarinov, V., "Resistance Coefficients and Flow of Liquids in Pipe Systems", Product Engineering, Vol. 17, No. 5, May, 1946, pp. 406-411.

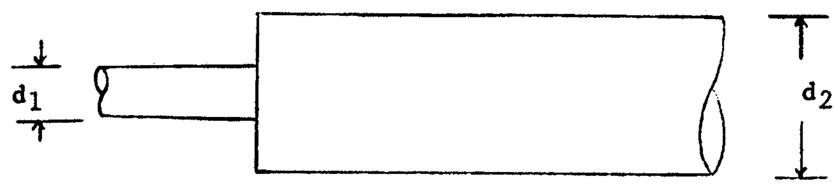

FIG. 1 SCHMATIC OF AN ABRUPT PIPE EXPANSION

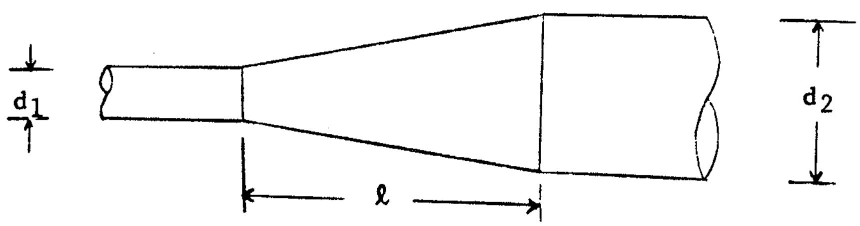

FIG. 2 SCHEMATIC OF A GRADUAL PIPE EXPANSION

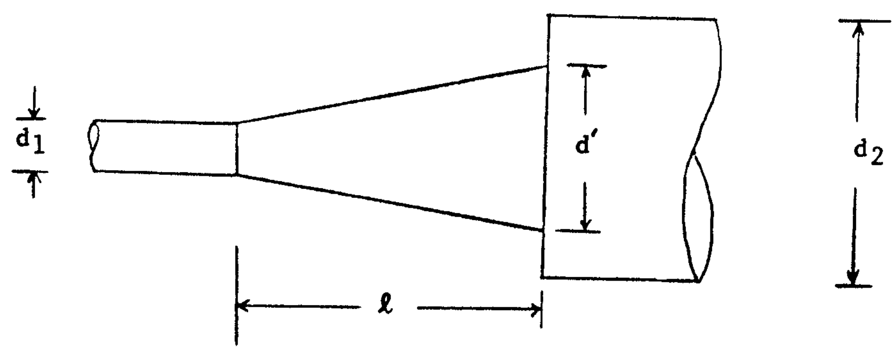

FIG. 3 SCHEMATIC OF A TWO-STAGE PIPE EXPANSION

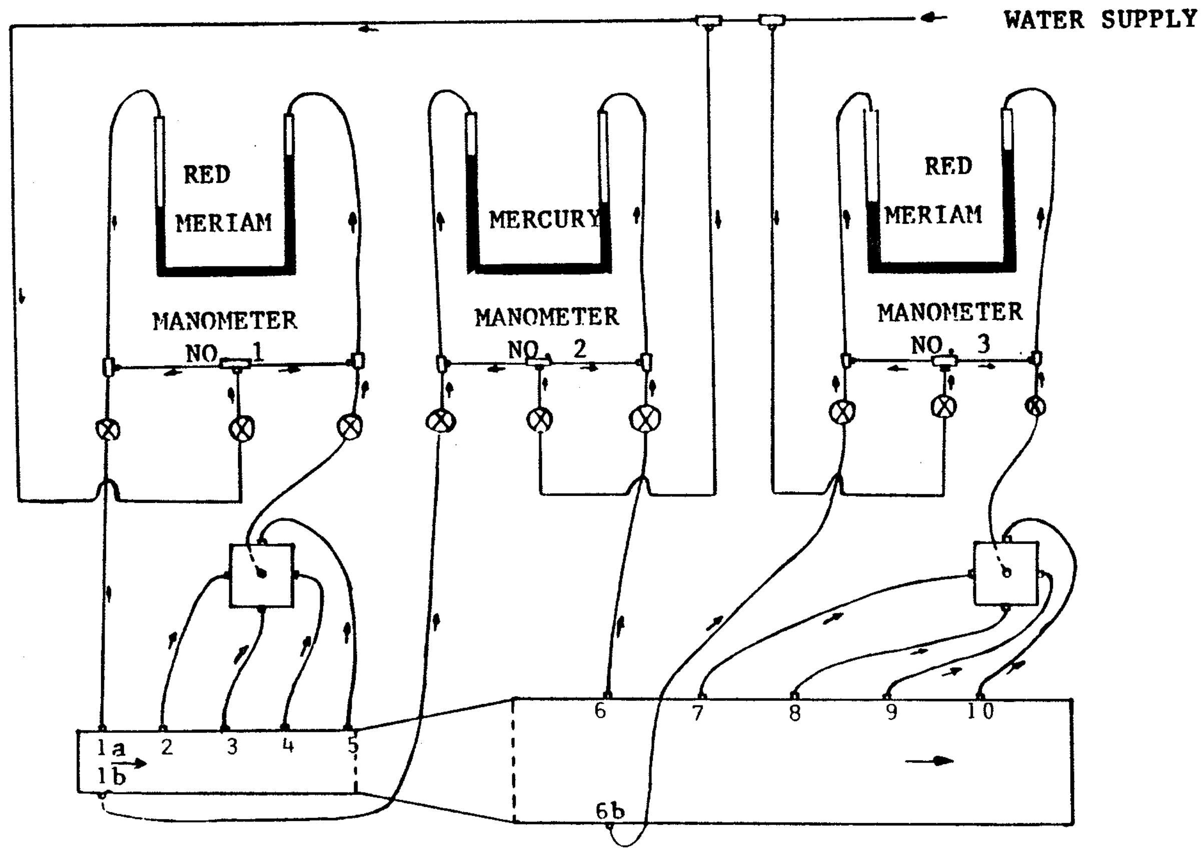

FIG. 4 SCHEMATIC DIAGRAM SHOWING THE ARRANGEMENT OF THE MANOMETERS AND THE PRESSURE TAPS ALONG THE PIPE EXPANSION FOR SETUP 1

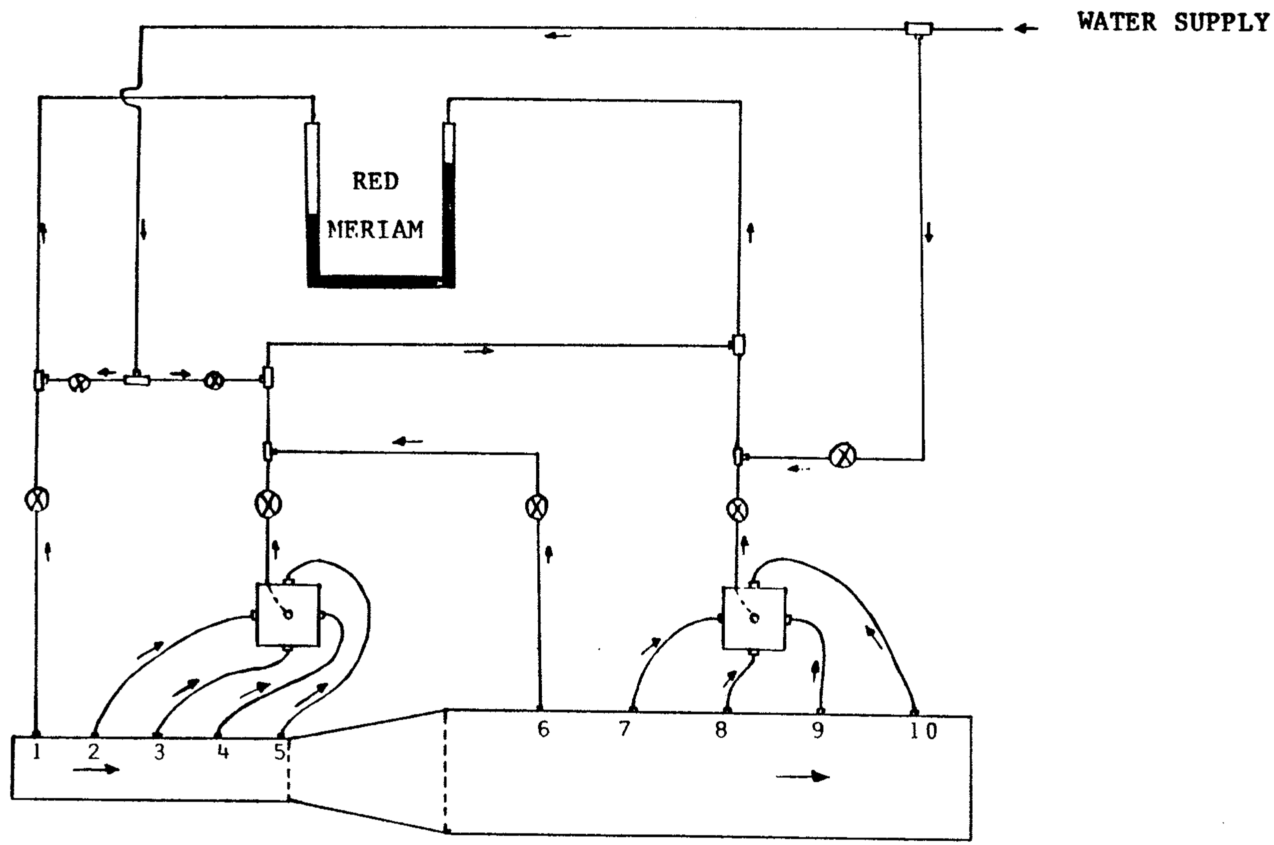

FIG. 5 SCHEMATIC DIAGRAM SHOWING THE ARRANGEMENT OF THE MANOMETER AND THE PRESSURE TAPS ALONG THE PIPE EXPANSION FOR SETUP 2

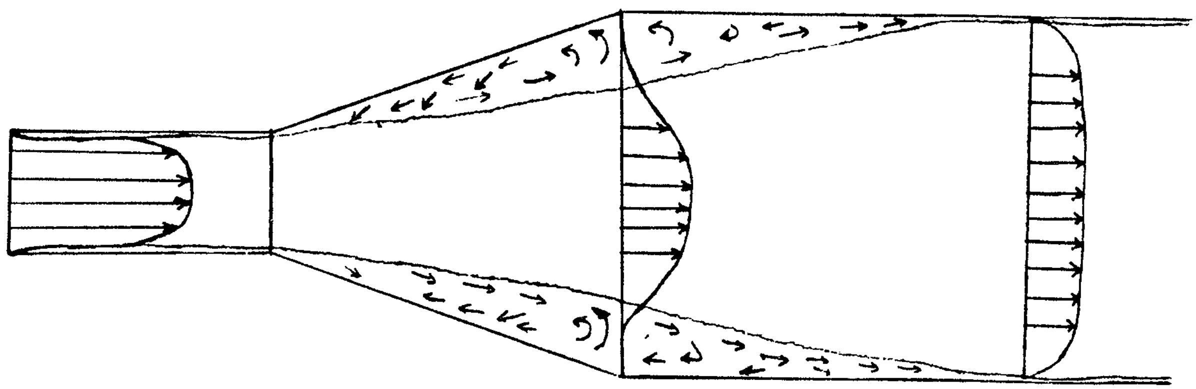

FIG. 6 HYPOTHETICAL FLOW PATTERN IN A GRADUAL PIPE EXPANSION

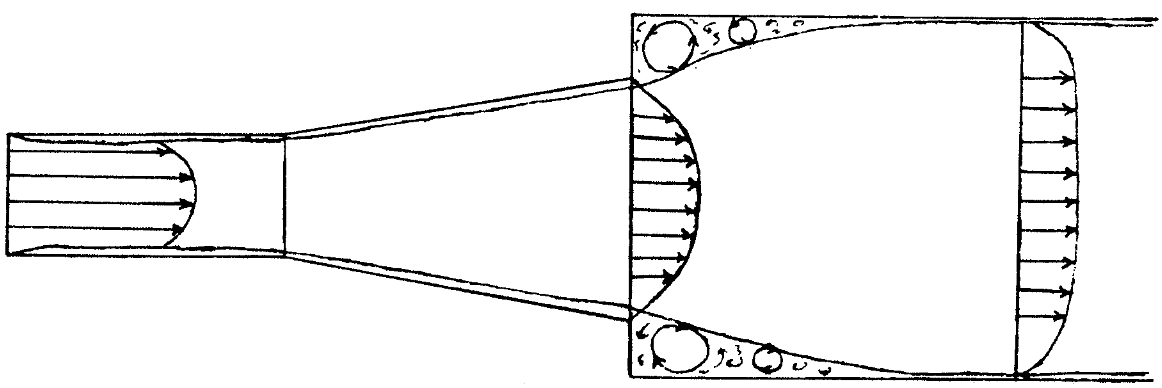

FIG. 7 HYPOTHETICAL FLOW PATTERN IN A TWO-STAGE PIPE EXPANSION

TABLE 1 Values of the optimal angle θ_0 in degrees for a two-stage pipe expansion of optimal design (Laliberte, et al. 1983)

$D = d_2/d_1$	$L = \ell/d_1$			
	1.500	2.000	2.500	3.000
1.111	*	*	*	*
1.250	7°17'	5°47'	*	*
1.333	8°49'	7°06'	5°58'	*
1.429	10°12'	8°18'	7°03'	6°08'
1.500	11°03'	9°03'	7°44'	6°46'
1.600	12°05'	9°58'	8°32'	7°30'
1.667	12°36'	10°26'	9°00'	7°54'
2.000	14°33'	12°12'	10°36'	9°24'
2.500	16°03'	13°31'	11°52'	10°36'
2.667	16°23'	13°48'	12°05'	10°50'
3.000	16°51'	14°16'	12°29'	11°14'
3.333	17°11'	14°33'	14°47'	11°31'

* Outside the range of applicability, $6° \leq \theta_0 \leq 35°$, for Eq. 23.

TABLE 2 Values of the optimal dimensionless diameter D' (the ratio of the optimal diameter d' at the interface to the inlet diameter d_1, that is, d'/d_1) in a two-stage pipe expansion of optimal design. (Laliberte, et al. 1983).

$D = d_2/d_1$	$L = \ell/d_1$			
	1.500	2.000	2.500	3.000
1.111	*	*	*	*
1.250	1.190	1.202	*	*
1.333	1.231	1.248	1.260	*
1.429	1.267	1.290	1.308	1.321
1.500	1.290	1.316	1.338	1.354
1.600	1.316	1.348	1.372	1.393
1.667	1.330	1.364	1.392	1.414
2.000	1.381	1.426	1.462	1.492
2.500	1.420	1.472	1.518	1.555
2.667	1.429	1.482	1.528	1.567
3.000	1.441	1.498	1.545	1.588
3.333	1.450	1.508	1.558	1.603

* Outside the range of applicability, $0.10 \leq \Theta \leq 0.61$, for Eq. 23.

TABLE 3 Values of the energy loss coefficient K for use in Eq. 1 associated with a two-stage pipe expansion of optimal design (Laliberte, et al. 1983).

$D = d_2/d_1$	$L = \ell/d_1$			
	1.500	2.000	2.500	3.000
1.111	*	*	*	*
1.250	0.02	0.01	*	*
1.333	0.03	0.02	0.02	*
1.429	0.04	0.04	0.03	0.02
1.500	0.06	0.05	0.04	0.03
1.600	0.08	0.06	0.05	0.05
1.667	0.09	0.07	0.06	0.05
2.000	0.14	0.12	0.10	0.09
2.500	0.20	0.17	0.15	0.13
2.667	0.21	0.18	0.16	0.14
3.000	0.23	0.20	0.18	0.16
3.333	0.25	0.21	0.19	0.17

* Outside the range of applicability, $0.10 \leq \theta \leq 0.61$, for Eq. 23.

TABLE 4 Dimensions for the abrupt pipe expansions

Pipe Expansion No.	Approach Diameter d_1 m	Exit Diameter d_2 m	$D = d_2/d_1$
1A	0.152	0.203	1.333
IB	0.102	0.203	2.000
1C	0.051	0.102	2.000
1D	0.038	0.127	3.333

TABLE 5 Dimensions for the gradual pipe expansions

Pipe Expansion No.	Approach Diameter d_1 m	Exit Diameter d_2 m	$D = d_2/d_1$	Pipe Expansion Centreline Length ℓ m	$L = \ell/d_1$
2A	0.152	0.203	1.333	0.457	3.000
2B	0.152	0.203	1.333	0.305	2.000
2C	0.152	0.203	1.333	0.229	1.500
2D	0.102	0.203	2.000	0.305	3.000
2E	0.102	0.203	2.000	0.203	2.000
2F	0.102	0.203	2.000	0.152	1.500

TABLE 6 Dimensions for the two-stage pipe expansions

Pipe Expansion No.	Approach Diameter d_1 (m)	Exit Diameter d_2 (m)	$D = d_2/d_1$	Pipe Expansion Centreline Length ℓ (m)	$L = \ell/d_1$
3A	0.152	0.203	1.333	0.457	3.000
3B	0.152	0.203	1.333	0.305	2.000
3C	0.152	0.203	1.333	0.229	1.500
3D	0.102	0.203	2.000	0.305	3.000
3E	0.102	0.203	2.000	0.203	2.000
3F	0.102	0.203	2.000	0.152	1.500

TABLE 7 Observed change in piezometric head along the pipe expansion No. 1A for different discharge rates

Press. Tap No.	Axial Distance m	Change in Piezometric Head for Test Number, m		
		Test No. 1	Test No. 2	Test No. 3
1	0.0000	0.0000	0.0000	0.0000
2	0.2540	-0.0058	-0.0034	-0.0029
3	0.5080	-0.0097	-0.0058	-0.0039
4	0.7620	-0.0370	-0.0214	-0.0159
5	1.0160	-0.0624*	-0.0283*	-0.0195*
6	1.4224	+0.2554*	+0.1540*	+0.1150*
7	1.9304	+0.2944	+0.1813	+0.1345
8	2.4384	+0.2925	+0.1784	+0.1326
9	2.6924	+0.2808	+0.1716	+0.1287
10	2.9464	+0.2749	+0.1696	+0.1267

* These data points were not considered in the computation of energy loss coefficient K.

TABLE 8 Observed change in piezometric head along the pipe expansion No. 1B for different discharge rates

Press. Tap No.	Axial Distance m	Change in Piezometric Head for Test Number, m			
		Test No. 1	Test No. 2	Test No. 3	Test No. 4
1	0.0000	0.0000	0.0000	0.0000	0.0000
2	0.0762	-0.0462	-0.0302	-0.0195	-0.0146
3	0.1524	-0.0624	-0.0390	-0.0273	-0.0195
4	0.2286	-0.1371	-0.0877	-0.0595	-0.0390
5	0.2921	-0.0984*	-0.0663 *	-0.0438*	-0.0312*
6	0.6858	+0.4980*	+0.3448*	+0.2107*	+0.1341*
7	1.1938	+1.4852	+0.9942	+0.6241	+0.4006
8	1.7018	+1.5368	+1.0195	+0.6358	+0.4181
9	1.9558	+1.5173	+1.0087	+0.6280	+0.4109
10	2.2098	+1.5023	+1.0019	+0.6241	+0.4051

* These data points were not considered in the computation of energy loss coefficient K.

TABLE 9 Observed change in piezometric head along the pipe expansion No. 1C for different discharge rates

Press. Tap No.	Axial Distance m	Change in Piezometric Head for Test Number, m			
		Test No. 1	Test No. 2	Test No. 3	Test No. 4
1	0.0000	0.0000	0.0000	0.0000	0.0000
2	0.2032	-0.2106	-0.1521	-0.1121	-0.0780
3	0.4064	-0.3399	-0.2565	-0.1882	-0.1316
4	0.6096	-0.5869	-0.4329	-0.3178	-0.2213
5	0.8128	-0.7345	-0.5538	-0.3997	-0.2788
6	1.2192	-0.4214*	-0.3256*	-0.2346*	-0.1724*
7	1.6002	+0.0524	+0.0253	+0.0217	+0.0050
8	1.8542	+0.0319	+0.0162	+0.0149	+0.0011
9	2.1082	+0.0260	+0.0097	+0.0110	-0.0008
10	2.3622	+0.0426	+0.0194	+0.0149	-0.0027

* These data points were not considered in the computation of energy loss coefficient K.

TABLE 10 Observed change in piezometric head along the pipe expansion No. 1D for different discharge rates

Press. Tap No.	Axial Distance m	Change in Piezometric Head for Test Number, m			
		Test No. 1	Test No. 2	Test No. 3	Test No. 4
1	0.0000	0.0000	0.0000	0.000	0.0000
2	0.2032	-0.5128	-0.6552	-0.1959	-0.5427
3	0.4064	-1.2044	-1.5463	-0.4134	-1.1310
4	0.6096	-2.1105	-2.7436	-0.7059	-1.9480
5	0.8128	-2.4186	-3.1590	-0.8443	-2.3127
6	1.2192	-1.4175*	-1.8773*	-0.4693*	-1.0248*
7	1.6002	-1.0641	-1.3937	-0.3516	-0.7382
8	1.8542	-1.0685	-1.4015	-0.3572	-0.7440
9	2.1082	-1.0776	-1.4093	-0.3630	-0.7470
10	2.3622	-1.0822	-1.4171	-0.3669	-0.7518

* These data points were not considered in the computation of energy loss coefficient K.

TABLE 11 Observed change in piezometric head along the pipe expansion No. 2A for different discharge rates

Press. Tap No.	Axial Distance m	Change in Piezometric Head for Test Number, m			
		Test No. 1	Test No. 2	Test No. 3	Test No. 4
1	0.0000	0.0000	0.0000	0.0000	0.0000
2	0.2540	-0.0351	-0.0234	-0.0156	-0.0117
3	0.5080	-0.0526	-0.0351	-0.0234	-0.0136
4	0.7620	-0.0604	-0.0409	-0.0273	-0.0175
5	1.0160	-0.0682	-0.0468	-0.0312	-0.0214
6	1.8796	+0.3958	+0.2613	+0.1735	+0.1092
7	2.3876	+0.3880	+0.2574	+0.1716	+0.1072
8	2.8956	+0.3822	+0.2515	+0.1696	+0.1053
9	3.1496	+0.3685	+0.2437	+0.1657	+0.1014
10	3.4036	+0.3646	+0.2398	+0.1638	+0.0994

TABLE 12 Observed change in piezometric head along the pipe expansion No. 2B for different discharge rates

Press. Tap No.	Axial Distance m	Change in Piezometric Head for Test Number, m				
		Test No. 1	Test No. 2	Test No. 3	Test No. 4	Test No. 5
1	0.0000	0.0000	0.0000	0.0000	0.0000	0.0000
2	0.2540	-0.0058	-0.0039	-0.0039	-0.0029	-0.0029
3	0.5080	-0.0156	-0.0117	-0.0087	-0.0048	-0.0039
4	0.7620	-0.0409	-0.0273	-0.0195	-0.0156	-0.0117
5	1.0160	-0.0721*	-0.0507*	-0.0351*	-0.0273*	-0.0214*
6	1.7272	+0.3900*	+0.2730*	+0.1794*	+0.1443*	+0.1092*
7	2.2352	+0.3939	+0.2769	+0.1794	+0.1443	+0.1111
8	2.7432	+0.3880	+0.2710	+0.1755	+0.1423	+0.1092
9	2.9972	+0.3744	+0.2613	+0.1716	+0.1365	+0.1053
10	3.2512	+0.3724	+0.2574	+0.1696	+0.1365	+0.1033

* These data points were not considered in the computation of energy loss coefficient K.

TABLE 13 Observed change in piezometric head along the pipe expansion No. 2C for different discharge rates

Press. Tap No.	Axial Distance m	Change in Piezometric Head for Test Number, m			
		Test No. 1	Test No. 2	Test No. 3	Test No. 4
1	0.0000	0.0000	0.0000	0.0000	0.0000
2	0.2540	-0.0078	-0.0058	-0.0039	-0.0039
3	0.5080	-0.0195	-0.0136	-0.0117	-0.0078
4	0.7620	-0.0516	-0.0351	-0.0243	-0.0146
5	1.0160	-0.0858	-0.0624	-0.0419	-0.0263
6	1.6510	+0.4118	+0.2873	+0.1915	+0.1149
7	2.1590	+0.4089	+0.2854	+0.1910	+0.1149
8	2.6670	+0.4011	+0.2815	+0.1896	+0.1134
9	2.9210	+0.3884	+0.2727	+0.1828	+0.1110
10	3.1750	+0.3865	+0.2698	+0.1798	+0.1095

TABLE 14 Observed change in piezometric head along the pipe expansion No. 2D for different discharge rates

Press. Tap No.	Axial Distance m	Change in Piezometric Head for Test Number, m				
		Test No. 1	Test No. 2	Test No. 3	Test No. 4	Test No. 5
1	0.0000	0.0000	0.0000	0.0000	0.0000	0.0000
2	0.0762	-0.0351	-0.0195	-0.0136	-0.0117	-0.0097
3	0.2286	-0.1131	-0.0760	-0.0516	-0.0351	-0.0195
4	0.3048	-0.1443	-0.0955	-0.0643	-0.0438	-0.0273
5	0.3683	-0.3042*	-0.2047*	-0.1404*	-0.0887*	-0.0448*
6	1.0668	+3.4865*	+2.2413*	+1.4559*	+0.9195*	+0.5363*
7	1.5748	+3.6366	+2.3495	+1.5222	+0.9653	+0.5636
8	2.0828	+3.6308	+2.3329	+1.5163	+0.9604	+0.5607
9	2.3368	+3.6171	+2.3251	+1.5085	+0.9585	+0.5578
10	2.5908	+3.6113	+2.3193	+1.5038	+0.9555	+0.5558

* These data points were not considered in the computation of energy loss coefficient K.

TABLE 15 Observed change in piezometric head along the pipe expansion No. 2E for different discharge rates

Press. Tap No.	Axial Distance m	Change in Piezometric Head for Test Number, m				
		Test No. 1	Test No. 2	Test No. 3	Test No. 4	Test No. 5
1	0.0000	0.0000	0.0000	0.0000	0.0000	0.0000
2	0.0763	-0.0507	-0.0341	-0.0243	-0.0175	-0.0117
3	0.1524	-0.0916	-0.0604	-0.0399	-0.0273	-0.0185
4	0.2286	-0.1345	-0.0926	-0.0604	-0.0438	-0.0243
5	0.2921	-0.5762 *	-0.3861 *	-0.2661 *	-0.1521 *	-0.0955 *
6	0.5334	+2.5669 *	+1.7624 *	+1.1589 *	+0.7662 *	+0.4214 *
7	1.3970	+2.7502	+1.8813	+1.2360	+0.8179	+0.4526
8	1.9050	+2.7346	+1.8774	+1.2292	+0.8150	+0.4487
9	2.1590	+2.7210	+1.8735	+1.2251	+0.8052	+0.4448
10	2.4130	+2.7171	+1.8696	+1.2194	+0.7974	+0.4428

* These data points were not considered in the computation of energy loss coefficient K.

TABLE 16 Observed change in piezometric head along the pipe expansion No. 2F for different discharge rates

Press. Tap No.	Axial Distance m	Change in Piezometric Head for Test Number, m					
		Test No. 1	Test No. 2	Test No. 3	Test No. 4	Test No. 5	Test No. 6
1	0.0000	0.0000	0.0000	0.0000	0.0000	0.0000	0.0000
2	0.0763	-0.0975	-0.0750	-0.0380	-0.0273	-0.1111	-0.0195
3	0.1524	-0.1248	-0.1014	-0.0546	-0.0370	-0.1443	-0.0263
4	0.2286	-0.2301	-0.1813	-0.0955	-0.0643	-0.2613	-0.0429
5	0.2921	-0.5733*	-0.4368*	-0.2252*	-0.1462*	-0.6103*	-0.0955*
6	0.8382	+1.8582*	+1.4176*	+0.8045*	+0.5364*	+2.1264*	+0.3831*
7	1.3462	+1.9810	+1.5073	+0.8601	+0.5754	+2.2628	+0.4075
8	1.8542	+1.9634	+1.5033	+0.8562	+0.5754	+2.2551	+0.4075
9	2.1082	+1.9556	+1.4936	+0.8474	+0.5675	+2.2453	+0.4036
10	2.3622	+1.9498	+1.4897	+0.8455	+0.5646	+2.2453	+0.4026

* These data points were not considered in the computation of energy loss coefficient K.

TABLE 17 Observed change in piezometric head along the pipe expansion No. 3A for different discharge rates

Press. Tap No.	Axial Distance m	Change in Piezometric Head for Test Number, m					
		Test No. 1	Test No. 2	Test No. 3	Test No. 4	Test No. 5	Test No. 6
1	0.0000	0.0000	0.0000	0.0000	0.0000	0.0000	0.0000
2	0.2540	-0.0273	-0.0195	-0.0136	-0.0097	-0.0058	-0.0019
3	0.5080	-0.0487	-0.0331	-0.0195	-0.0136	-0.0097	-0.0058
4	0.7620	-0.0565	-0.0390	-0.0234	-0.0175	-0.0136	-0.0078
5	1.0160	-0.0604*	-0.0429 *	-0.0253*	-0.0195 *	-0.0156*	-0.0097*
6	1.8796	+0.3695*	+0.2574 *	+0.1638*	+0.1228 *	+0.0916*	+0.0604*
7	2.3876	+0.3763	+0.2593	+0.1638	+0.1228	+0.0916	+0.0604
8	2.8956	+0.3705	+0.2554	+0.1618	+0.1189	+0.0897	+0.0585
9	3.1496	+0.3510	+0.2476	+0.1540	+0.1150	+0.0877	+0.0565
10	3.4036	+0.3490	+0.2437	+0.1521	+0.1131	+0.0858	+0.0565

* These data points were not considered in the computation of energy loss coefficient K.

TABLE 18 Observed change in piezometric head along the pipe expansion No. 3B for different discharge rates

Press. Tap No.	Axial Distance m	Change in Piezometric Head for Test Number, m					
		Test No. 1	Test No. 2	Test No. 3	Test No. 4	Test No. 5	Test No. 6
1	0.0000	0.0000	0.0000	0.0000	0.0000	0.0000	0.0000
2	0.2540	-0.0351	-0.0214	-0.0136	-0.0078	-0.0058	-0.0039
3	0.5080	-0.0526	-0.0351	-0.0214	-0.0136	-0.0097	-0.0058
4	0.7620	-0.0565	-0.0370	-0.0253	-0.0156	-0.0126	-0.0087
5	1.0160	-0.0643	-0.0448	-0.0292	-0.0175	-0.0156	-0.0107
6	1.7272	+0.3724*	+0.2554*	+0.1677*	+0.1092*	+0.0858*	+0.0546*
7	2.2352	+0.3763	+0.2574	+0.1686	+0.1092	+0.0838	+0.0546
8	2.7432	+0.3705	+0.2535	+0.1638	+0.1072	+0.0838	+0.0507
9	2.9972	+0.3549	+0.2437	+0.1560	+0.1053	+0.0819	+0.0468
10	3.2512	+0.3510	+0.2398	+0.1560	+0.1033	+0.0799	+0.0468

* These data points were not considered in the computation of energy loss coefficient K.

TABLE 19 Observed change in piezometric head along the pipe expansion No. 3C for different discharge rates

Press. Tap No.	Axial Distance m	Change in Piezometric Head for Test Number, m			
		Test No. 1	Test No. 2	Test No. 3	Test No. 4
1	0.0000	0.0000	0.0000	0.0000	0.0000
2	0.2540	-0.0058	-0.0019	-0.0019	-0.0010
3	0.5080	-0.0156	-0.0078	-0.0058	-0.0019
4	0.7620	-0.0448	-0.0292	-0.0156	-0.0058
5	1.0160	-0.0780	-0.0507	-0.0351	-0.0117
6	1.6510	+0.4017*	+0.2593*	+0.1540*	+0.0604*
7	2.1590	+0.4075	+0.2613	+0.1560	+0.0624
8	2.6669	+0.4017	+0.2554	+0.1540	+0.0624
9	2.9209	+0.3861	+0.2457	+0.1482	+0.0604
10	3.1750	+0.3822	+0.2437	+0.1482	+0.0604

* These data points were not considered in the computation of energy loss coefficient K.

TABLE 20 Observed change in piezometric head along the pipe expansion No. 3D for different discharge rates

Press. Tap No.	Axial Distance m	Change in Piezometric Head for Test Number, m			
		Test No. 1	Test No. 2	Test No. 3	Test No. 4
1	0.0000	0.0000	0.0000	0.0000	0.0000
2	0.1524	-0.0624	-0.0331	-0.0195	-0.0087
3	0.2286	-0.1725	-0.1101	-0.0760	-0.0438
4	0.3048	-0.1901	-0.1228	-0.0867	-0.0526
5	0.3683	-0.2145	-0.1374	-0.0955	-0.0604
6	1.0668	+2.9884*	+2.0114*	+1.4175*	+0.8428*
7	1.5748	+3.2419 *	+2.1830*	+1.5384*	+0.9160*
8	2.0828	+3.2624	+2.1918	+1.5462	+0.9199
9	2.3368	+3.2458	+2.1869	+1.5404	+0.9150
10	2.5908	+3.2399	+2.1830	+1.5384	+0.9130

* These data points were not considered in the computation of energy loss coefficient K.

TABLE 21 Observed change in piezometric head along the pipe expansion No. 3E for different discharge rates

Press. Tap No.	Axial Distance m	Change in Piezometric Head for Test Number, m			
		Test No. 1	Test No. 2	Test No. 3	Test No. 4
1	0.0000	0.0000	0.0000	0.0000	0.0000
2	0.0762	-0.0507	-0.0360	-0.0224	-0.0175
3	0.1524	-0.0682	-0.0507	-0.0321	-0.0224
4	0.2286	-0.1131	-0.0848	-0.0507	-0.0351
5	0.2921	-0.2847*	-0.2076*	-0.1209*	-0.0799*
6	0.8890	+2.9692*	+2.1551*	+1.1972*	+0.8045*
7	1.3970	+3.2734*	+2.3793*	+1.3279*	+0.8903*
8	1.9050	+3.3037	+2.4008	+1.3376	+0.9020
9	2.1590	+3.2861	+2.3949	+1.3318	+0.8962
10	2.4130	+3.2812	+2.3871	+1.3279	+0.8942

* These data points were not considered in the computation of energy loss coefficient K.

TABLE 22 Observed change in piezometric head along the pipe expansion No. 3F for different discharge rates

Press. Tap No.	Axial Distance m	Change in Piezometric Head for Test Number, m			
		Test No. 1	Test No. 2	Test No. 3	Test No. 4
1	0.0000	0.0000	0.0000	0.0000	0.0000
2	0.0762	-0.6708	-0.2886	-0.1540	-0.0887
3	0.2286	-0.9399 *	-0.4953 *	-0.3120 *	-0.1608 *
4	0.3048	-0.8063	-0.4095	-0.2301	-0.1287
5	0.3683	-1.0237	-0.5460	-0.3147	-0.1852
6	0.9144	+2.0880 *	+1.5133 *	+1.0919 *	+0.6321 *
7	1.4224	+2.4624 *	+1.7766 *	+1.2654 *	+0.7374 *
8	1.9304	+2.4800	+1.7980	+1.2713	+0.7452
9	2.1844	+2.4683	+1.7863	+1.2654	+0.7384
10	2.4384	+2.4644	+1.7824	+1.2606	+0.7355

* These data points were not considered in the computation of energy loss coefficient K.

TABLE 23 Approach and exit velocity for pipe expansions tested

Pipe Expansion No.	Test Number 1		2		3		4		5		6	
	Approach Velocity (m/s)	Exit Velocity (m/s)	Approach Velocity (m/s)	Exit Velocity (m/s)	Approach Velocity (m/s)	Exit Velocity (m/s)	Approach Velocity (m/s)	Exit Velocity (m/s)	Approach Velocity (m/s)	Exit Velocity (m/s)	Approach Velocity (m/s)	Exit Velocity (m/s)
1A	3.918	2.204	3.076	1.730	2.709	1.524	-	-	-	-	-	-
1B	9.395	2.372	7.658	1.934	6.089	1.537	4.978	1.256	-	-	-	-
1C	7.610	1.902	6.534	1.633	5.816	1.454	5.042	1.260	-	-	-	-
1D	16.194	1.457	14.047	1.264	14.464	1.301	-	-	-	-	-	-
2A	3.995	2.247	3.258	1.833	2.668	1.501	2.145	1.206	-	-	-	-
2B	3.900	2.194	3.285	1.847	2.705	1.521	2.417	1.359	2.180	1.226	-	-
2C	4.122	2.323	3.374	1.901	2.750	1.550	2.133	1.202	-	-	-	-
2D	9.887	2.496	8.101	2.045	6.595	1.665	5.348	1.350	4.050	1.022	-	-
2E	9.403	2.374	7.843	1.980	6.338	1.600	5.169	1.305	4.002	1.010	-	-
2F	9.609	2.426	9.075	2.291	7.981	2.015	5.945	1.501	4.848	1.224	4.026	1.016
3A	3.860	2.171	3.221	1.812	2.635	1.482	2.299	1.293	2.035	1.144	1.696	0.954
3B	4.001	2.255	3.152	1.776	2.631	1.483	2.220	1.251	1.918	1.081	1.644	0.926
3C	4.012	2.256	3.243	1.824	2.563	1.441	1.641	0.923	-	-	-	-
3D	9.099	2.297	7.592	1.917	6.292	1.588	4.951	1.250	-	-	-	-
3E	9.212	2.326	7.920	1.999	5.956	1.504	4.893	1.235	-	-	-	-
3F	9.276	2.342	7.866	1.986	6.377	1.610	4.983	1.258	-	-	-	-

TABLE 24 Experimental values of the energy loss coefficient K for pipe expansions tested

Pipe Expansion No.	Value of K for Test Number					
	Test No. 1	Test No. 2	Test No. 3	Test No. 4	Test No. 5	Test No. 6
1A	0.207	0.214	0.226	-	-	-
1B	0.558	0.557	0.561	0.565	-	-
1C	0.612	0.613	0.621	0.629	-	-
1D	0.735	0.732	0.722	-	-	-
2A	0.073	0.076	0.068	0.083	-	-
2B	0.060	0.068	0.081	0.079	0.105	-
2C	0.096	0.071	0.063	0.058	-	-
2D	0.160	0.189	0.203	0.224	0.210	-
2E	0.279	0.292	0.284	0.262	0.322	-
2F	0.389	0.396	0.383	0.378	0.382	0.370
3A	0.061	0.059	0.091	0.098	0.113	0.145
3B	0.072	0.078	0.086	0.090	0.105	0.167
3C	0.077	0.079	0.090	0.080	-	-
3D	0.108	0.135	0.115	0.145	-	-
3E	0.131	0.142	0.151	0.150	-	-
3F	0.136	0.200	0.172	0.208	-	-

TABLE 25 Experimental average values of the energy loss coefficient K for pipe expansions tested

Pipe Expansion No.	$D = d_2/d_1$	$L = \ell/d_1$	Average Value of K
1A	1.333	-	0.21
1B	2.000	-	0.56
1C	2.000	-	0.61
1D	3.333	-	0.73
2A	1.333	3.000	0.08
2B	1.333	2.000	0.08
2C	1.333	1.500	0.07
2D	2.000	3.000	0.20
2E	2.000	2.000	0.29
2F	2.000	1.500	0.38
3A	1.333	3.000	0.09
3B	1.333	2.000	0.10
3C	1.333	1.500	0.08
3D	2.000	3.000	0.12
3E	2.000	2.000	0.14
3F	2.000	1.500	0.17

TABLE 26 Comparison of the experimental values of the energy loss coefficient K with the predicted values of K (Laliberte, et al. 1983)

Type of Pipe Expansion	Pipe Expansion No.	$D = d_2/d_1$	$L = \ell/d_1$	Average Value of K	
				Experimental	Predicted
Abrupt	1A	1.333	-	0.21	0.19
"	1B	2.000	-	0.56	0.56
"	1C	2.000	-	0.61	0.56
"	1D	3.333	-	0.73	0.83
Gradual	2A	1.333	3.000	0.08	0.02
"	2B	1.333	2.000	0.08	0.03
"	2C	1.333	1.500	0.07	0.05
"	2D	2.000	3.000	0.20	0.22
"	2E	2.000	2.000	0.29	0.36
"	2F	2.000	1.500	0.38	0.50
Two-stage	3A	1.333	3.000	0.09	$\leq$0.02
"	3B	1.333	2.000	0.10	0.02
"	3C	1.333	1.500	0.08	0.03
"	3D	2.000	3.000	0.12	0.09
"	3E	2.000	2.000	0.14	0.12
"	3F	2.000	1.500	0.17	0.14

TABLE 27 Percentage difference in values of the energy loss coefficient K between the predicted (Laliberte, et al. 1983) and the experimental results

Type of Pipe Expansion	Pipe Expansion No.	$D = d_2/d_1$	$L = \ell/d_1$	Average Value of K		Percentage difference in value of K
				Experimental	Predicted	
Abrupt	1A	1.333	-	0.21	0.19	11
"	1B	2.000	-	0.56	0.56	0
"	1C	2.000	-	0.61	0.56	9
"	1D	3.333	-	0.73	0.83	-12
Gradual	2A	1.333	3.000	0.08	0.02	300
"	2B	1.333	2.000	0.08	0.03	167
"	2C	1.333	1.500	0.07	0.05	40
"	2D	2.000	3.000	0.20	0.22	-9
"	2E	2.000	2.000	0.29	0.36	-19
"	2F	2.000	1.500	0.38	0.50	-24
Two-stage	3A	1.333	3.000	0.09	$\leq$0.02	350
"	3B	1.333	2.000	0.10	0.02	400
"	3C	1.333	1.500	0.08	0.03	167
"	3D	2.000	3.000	0.12	0.09	33
"	3E	2.000	2.000	0.14	0.12	16
"	3F	2.000	1.500	0.17	0.14	21

TABLE 28 Error in measurement and calculation of energy loss coefficient K

Pipe Expansion No.	Test No.	$E_{\Delta h}$	E_q	E_v	E_{vh}	$E_{\Delta p}$	$E_{\Delta E}$	E_{Ko}	Abs.E_{Ko}	K_o	K_o ± Abs.E_{Ko}	K_p	$\frac{K_o-K_p}{K_p}$
1A	1	0.0025	0.0012	0.0012	0.0023	0.0040	0.0167	0.0179	0.0037	0.207	0.207 ± 0.0037	0.19	0.089
"	2	0.0041	0.0019	0.0019	0.0038	0.0065	0.0265	0.0285	0.0061	0.214	0.214 ± 0.0061	0.19	0.126
"	3	0.0054	0.0025	0.0025	0.0050	0.0086	0.0325	0.0351	0.0079	0.226	0.226 ± 0.0079	0.19	0.189
1B	1	0.0021	0.0010	0.0010	0.0020	0.0110	0.0108	0.0118	0.0066	0.558	0.558 ± 0.0066	0.56	-0.004
"	2	0.0033	0.0015	0.0015	0.0031	0.0165	0.0164	0.0179	0.0100	0.557	0.557 ± 0.0100	0.56	-0.005
"	3	0.0053	0.0025	0.0025	0.0050	0.0263	0.0259	0.0285	0.0160	0.561	0.561 ± 0.0160	0.56	0.002
"	4	0.0081	0.0038	0.0038	0.0076	0.0398	0.0387	0.0426	0.0241	0.565	0.565 ± 0.0241	0.56	0.009
1C	1	0.0622	0.0286	0.0286	0.0579	0.0195	0.0991	0.1314	0.0804	0.612	0.612 ± 0.0804	0.56	0.093
"	2	0.0856	0.0391	0.0391	0.0797	0.0265	0.1359	0.1821	0.1117	0.613	0.613 ± 0.1117	0.56	0.095
"	3	0.1093	0.0497	0.0497	0.1018	0.0343	0.1711	0.2323	0.1442	0.621	0.621 ± 0.1442	0.56	0.109
"	4	0.1476	0.0664	0.0664	0.1372	0.0468	0.2273	0.3146	0.1979	0.629	0.629 ± 0.1979	0.56	0.123
1D	1	0.0426	0.0197	0.0197	0.0397	0.0030	0.0773	0.0990	0.0727	0.735	0.735 ± 0.0727	0.83	-0.114
"	2	0.0574	0.0264	0.0264	0.0535	0.0040	0.1053	0.1353	0.0991	0.732	0.732 ± 0.0991	0.83	-0.118
"	3	0.0540	0.0249	0.0249	0.0504	0.0043	0.0884	0.1161	0.0838	0.722	0.722 ± 0.0838	0.83	-0.130
2A	1	0.0024	0.0011	0.0011	0.0022	0.0030	0.0451	0.0463	0.0034	0.073	0.073 ± 0.0034	0.02	2.650
"	2	0.0037	0.0017	0.0017	0.0034	0.0045	0.0661	0.0679	0.0052	0.076	0.076 ± 0.0052	0.02	2.800
"	3	0.0056	0.0026	0.0026	0.0052	0.0066	0.1120	0.1148	0.0078	0.068	0.068 ± 0.0078	0.02	2.400
"	4	0.0088	0.0041	0.0041	0.0082	0.0105	0.1430	0.1477	0.0123	0.083	0.083 ± 0.0123	0.02	3.150

TABLE 28: CONTINUED

2B	1	0.0025	0.0012	0.0012	0.0023	0.0031	0.0577	0.0589	0.0035	0.060	0.060 ± 0.0035	0.03	1.000
"	2	0.0036	0.0017	0.0017	0.0034	0.0044	0.0729	0.0747	0.0051	0.068	0.068 ± 0.0051	0.03	1.267
"	3	0.0054	0.0025	0.0025	0.0050	0.0066	0.0910	0.0938	0.0076	0.081	0.081 ± 0.0076	0.03	1.700
"	4	0.0068	0.0032	0.0032	0.0064	0.0082	0.1178	0.1214	0.0096	0.079	0.079 ± 0.0096	0.03	1.633
"	5	0.0085	0.0040	0.0040	0.0079	0.0105	0.1093	0.1137	0.0119	0.105	0.105 ± 0.0119	0.03	2.500
2C	1	0.0022	0.0010	0.0010	0.0021	0.0368	0.2389	0.2402	0.0231	0.096	0.096 ± 0.0231	0.05	0.920
"	2	0.0034	0.0016	0.0016	0.0032	0.0527	0.4814	0.4837	0.0343	0.071	0.071 ± 0.0343	0.05	0.420
"	3	0.0052	0.0024	0.0024	0.0049	0.0783	0.8185	0.8230	0.0518	0.063	0.063 ± 0.0518	0.05	0.260
"	4	0.0089	0.0041	0.0041	0.0083	0.1291	1.4841	1.4944	0.0867	0.058	0.058 ± 0.0867	0.05	0.160
2D	1	0.0019	0.0009	0.0009	0.0018	0.0048	0.0336	0.0345	0.0055	0.160	0.160 ± 0.0055	0.22	-0.273
"	2	0.0029	0.0014	0.0014	0.0027	0.0075	0.0424	0.0438	0.0083	0.189	0.189 ± 0.0083	0.22	-0.141
"	3	0.0045	0.0021	0.0021	0.0042	0.0115	0.0615	0.0637	0.0129	0.203	0.203 ± 0.0129	0.22	-0.077
"	4	0.0070	0.0032	0.0032	0.0065	0.0182	0.0819	0.0854	0.0191	0.224	0.224 ± 0.0191	0.22	0.018
"	5	0.0125	0.0058	0.0058	0.0117	0.0308	0.1578	0.1646	0.0346	0.210	0.210 ± 0.0346	0.22	-0.045
2E	1	0.0021	0.0010	0.0010	0.0020	0.0063	0.0215	0.0225	0.0063	0.279	0.279 ± 0.0063	0.36	-0.225
"	2	0.0031	0.0015	0.0015	0.0029	0.0093	0.0295	0.0310	0.0091	0.292	0.292 ± 0.0091	0.36	-0.189
"	3	0.0049	0.0023	0.0023	0.0046	0.0140	0.0467	0.0491	0.0139	0.284	0.284 ± 0.0139	0.36	-0.211
"	4	0.0075	0.0035	0.0035	0.0070	0.0209	0.0727	0.0765	0.0200	0.262	0.262 ± 0.0200	0.36	-0.272
"	5	0.0128	0.0060	0.0060	0.0120	0.0377	0.1034	0.1100	0.0354	0.322	0.322 ± 0.0354	0.36	-0.106
2F	1	0.0023	0.0011	0.0011	0.0021	0.0081	0.0166	0.0177	0.0069	0.389	0.389 ± 0.0069	0.50	-0.222
"	2	0.0030	0.0014	0.0014	0.0028	0.0106	0.0212	0.0226	0.0090	0.396	0.396 ± 0.0090	0.50	-0.208
"	3	0.0056	0.0026	0.0026	0.0052	0.0188	0.0398	0.0425	0.0163	0.383	0.383 ± 0.0163	0.50	-0.234
"	4	0.0086	0.0040	0.0040	0.0080	0.0279	0.0611	0.0654	0.0247	0.378	0.378 ± 0.0247	0.50	-0.244
"	5	0.0020	0.0009	0.0009	0.0019	0.0072	0.0151	0.0160	0.0061	0.382	0.382 ± 0.0061	0.50	-0.236
"	6	0.0127	0.0059	0.0059	0.0118	0.0399	0.0911	0.0976	0.0361	0.370	0.370 ± 0.0361	0.50	-0.260

TABLE 28: CONTINUED

3A	1	0.0026	0.0012	0.0012	0.0024	0.0031	0.0581	0.0594	0.0036	0.061	0.061 ± 0.0036	0.02	2.050
"	2	0.0037	0.0017	0.0017	0.0035	0.0045	0.0871	0.0890	0.0053	0.059	0.059 ± 0.0053	0.02	1.950
"	3	0.0057	0.0027	0.0027	0.0053	0.0070	0.0856	0.0885	0.0081	0.091	0.091 ± 0.0081	0.02	3.550
"	4	0.0076	0.0035	0.0035	0.0071	0.0094	0.1050	0.1089	0.0107	0.098	0.098 ± 0.0107	0.02	3.900
"	5	0.0098	0.0046	0.0046	0.0092	0.0123	0.1170	0.1222	0.0138	0.113	0.113 ± 0.0138	0.02	4.650
"	6	0.0144	0.0067	0.0067	0.0134	0.0187	0.1326	0.1403	0.0203	0.145	0.145 ± 0.0203	0.02	6.250
3B	1	0.0025	0.0012	0.0012	0.0023	0.0031	0.0342	0.0355	0.0026	0.072	0.072 ± 0.0026	0.02	2.600
"	2	0.0037	0.0017	0.0017	0.0034	0.0045	0.1572	0.1592	0.0124	0.078	0.078 ± 0.0124	0.02	2.900
"	3	0.0057	0.0026	0.0026	0.0053	0.0069	0.1023	0.1052	0.0090	0.086	0.086 ± 0.0090	0.02	3.300
"	4	0.0086	0.0040	0.0040	0.0081	0.0104	0.0964	0.1008	0.0091	0.090	0.090 ± 0.0091	0.02	3.500
"	5	0.0109	0.0051	0.0051	0.0102	0.0133	0.1623	0.1682	0.0177	0.105	0.105 ± 0.0177	0.02	4.250
"	6	0.0154	0.0072	0.0072	0.0144	0.0208	0.1222	0.1303	0.0218	0.167	0.167 ± 0.0218	0.02	7.350
3C	1	0.0024	0.0011	0.0011	0.0022	0.0030	0.0426	0.0437	0.0034	0.077	0.077 ± 0.0034	0.03	1.567
"	2	0.0037	0.0017	0.0017	0.0034	0.0046	0.0641	0.0659	0.0052	0.079	0.079 ± 0.0052	0.03	1.633
"	3	0.0061	0.0028	0.0028	0.0056	0.0074	0.0915	0.0946	0.0085	0.090	0.090 ± 0.0085	0.03	2.000
"	4	0.0154	0.0072	0.0072	0.0144	0.0178	0.2565	0.2656	0.0212	0.080	0.080 ± 0.0212	0.03	1.667
3D	1	0.0023	0.0011	0.0011	0.0021	0.0053	0.0595	0.0607	0.0066	0.108	0.108 ± 0.0066	0.09	0.200
"	2	0.0033	0.0016	0.0016	0.0031	0.0079	0.0687	0.0704	0.0095	0.135	0.135 ± 0.0095	0.09	0.500
"	3	0.0050	0.0023	0.0023	0.0046	0.0113	0.1179	0.1205	0.0139	0.115	0.115 ± 0.0139	0.09	0.278
"	4	0.0082	0.0038	0.0038	0.0077	0.0189	0.1527	0.1571	0.0228	0.145	0.145 ± 0.0228	0.09	0.611
3E	1	0.0022	0.0010	0.0010	0.0021	0.0054	0.0478	0.0489	0.0064	0.131	0.131 ± 0.0064	0.12	0.092
"	2	0.0031	0.0014	0.0014	0.0029	0.0074	0.0599	0.0614	0.0087	0.142	0.142 ± 0.0087	0.12	0.183
"	3	0.0056	0.0026	0.0026	0.0052	0.0132	0.1005	0.1034	0.0156	0.151	0.151 ± 0.0156	0.12	0.258
"	4	0.0084	0.0039	0.0039	0.0078	0.0195	0.1503	0.1548	0.0232	0.150	0.150 ± 0.0232	0.12	0.250

TABLE 28: CONTINUED

3F	1	0.0022	0.0010	0.0010	0.0020	0.0053	0.0454	0.0465	0.0063	0.136	0.136 ± 0.0063	0.14	-0.029
"	2	0.0031	0.0014	0.0014	0.0029	0.0080	0.0432	0.0447	0.0089	0.200	0.200 ± 0.0089	0.14	0.429
"	3	0.0048	0.0022	0.0022	0.0045	0.0118	0.0766	0.0790	0.0136	0.172	0.172 ± 0.0136	0.14	0.229
"	4	0.0081	0.0038	0.0038	0.0076	0.0203	0.1049	0.1091	0.0227	0.208	0.208 ± 0.0227	0.14	0.486

Footnotes:

$E_{\Delta h}$ Relative error in measurement of pressure head across the orifice plate

E_q Relative error in calculation of discharge

E_v Relative error in calculation of average discharge velocity

E_{vh} Relative error in calculation of velocity head

$E_{\Delta p}$ Relative error in measurement of pressure head across the pipe expansion

$E_{\Delta E}$ Relative error in calculation of energy loss across the pipe expansion

E_{Ko} Relative error in calculation of observed energy loss coefficient

Abs.E_{Ko} Absolute error in calculation of observed energy loss coefficient

K_o Observed energy loss coefficient

K_p Predicted energy loss coefficient

APPENDIX A

GRADIENT OF PIEZOMETRIC HEAD AS A FUNCTION OF DISCHARGE IN A STEEL PIPE

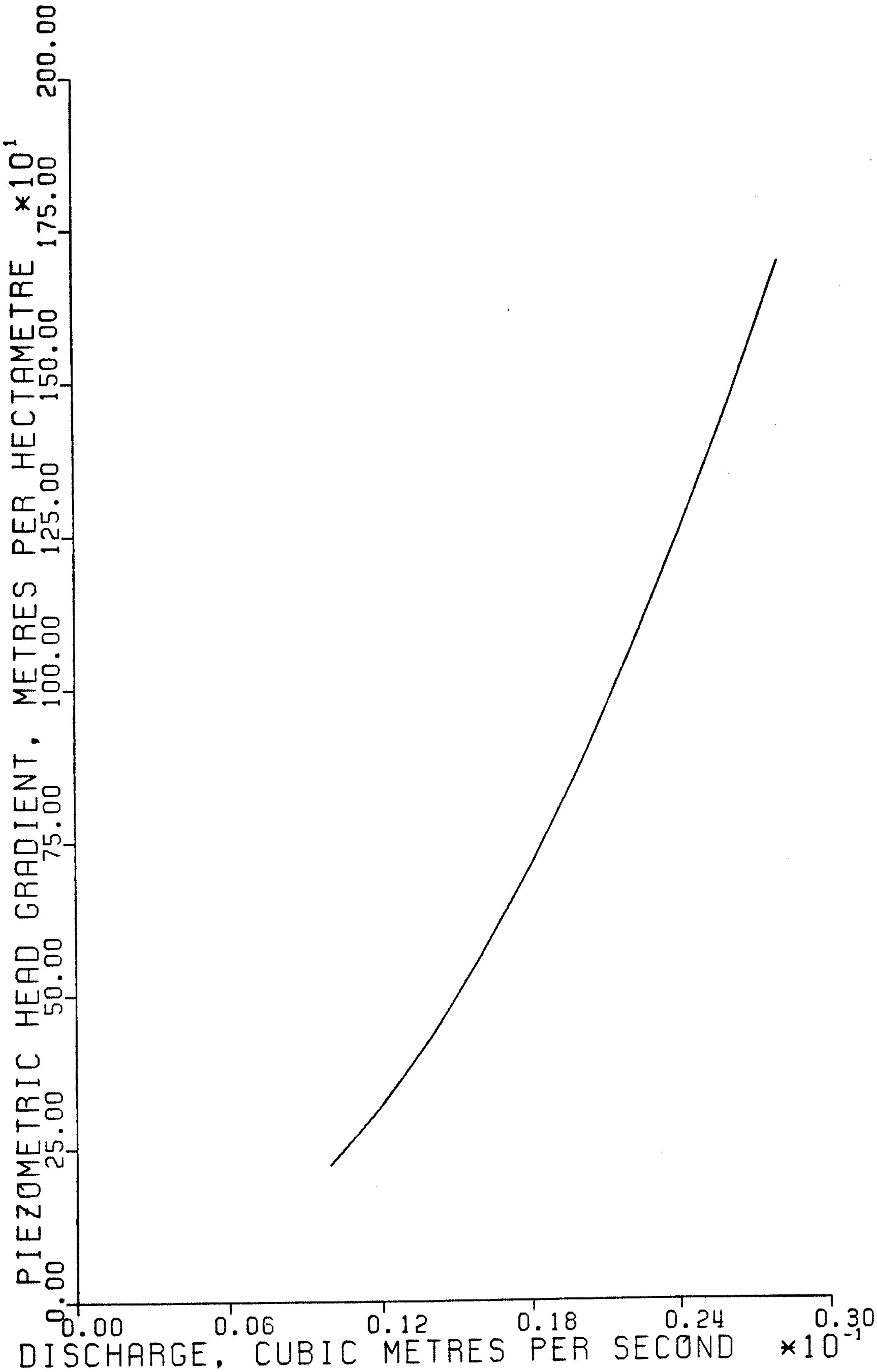

FIG. A-1 GRADIENT OF PIEZOMETRIC HEAD AS A FUNCTION OF DISCHARGE IN A 0.038-m DIAMETER STEEL PIPE WITH AN ABSOLUTE ROUGHNESS COEFFICIENT OF 4.572×10^{-5} m.

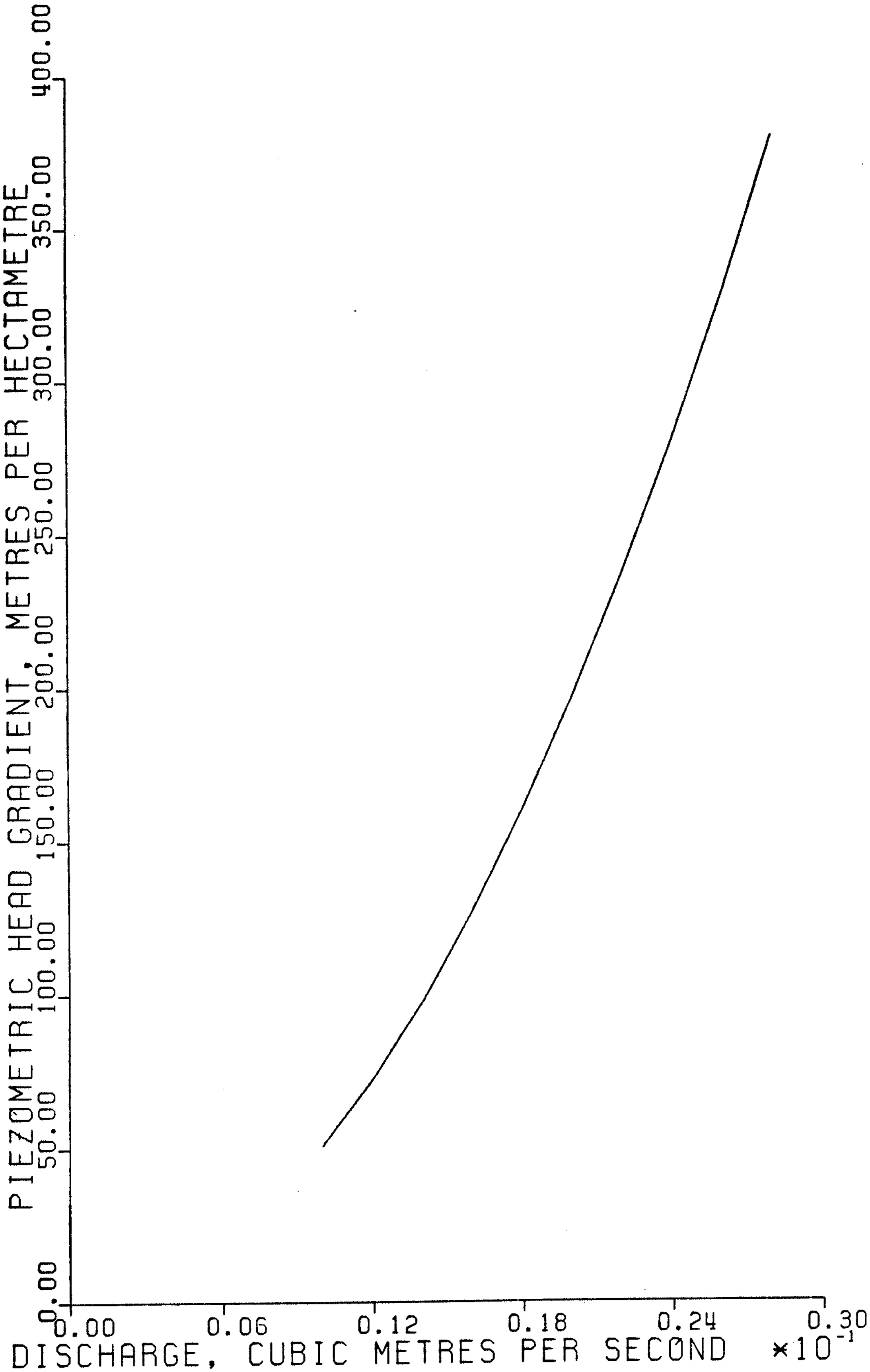

FIG. A-2 GRADIENT OF PIEZOMETRIC HEAD AS A FUNCTION OF DISCHARGE IN A 0.051-m DIAMETER STEEL PIPE WITH AN ABSOLUTE ROUGHNESS COEFFICIENT OF 4.572×10^{-5} m.

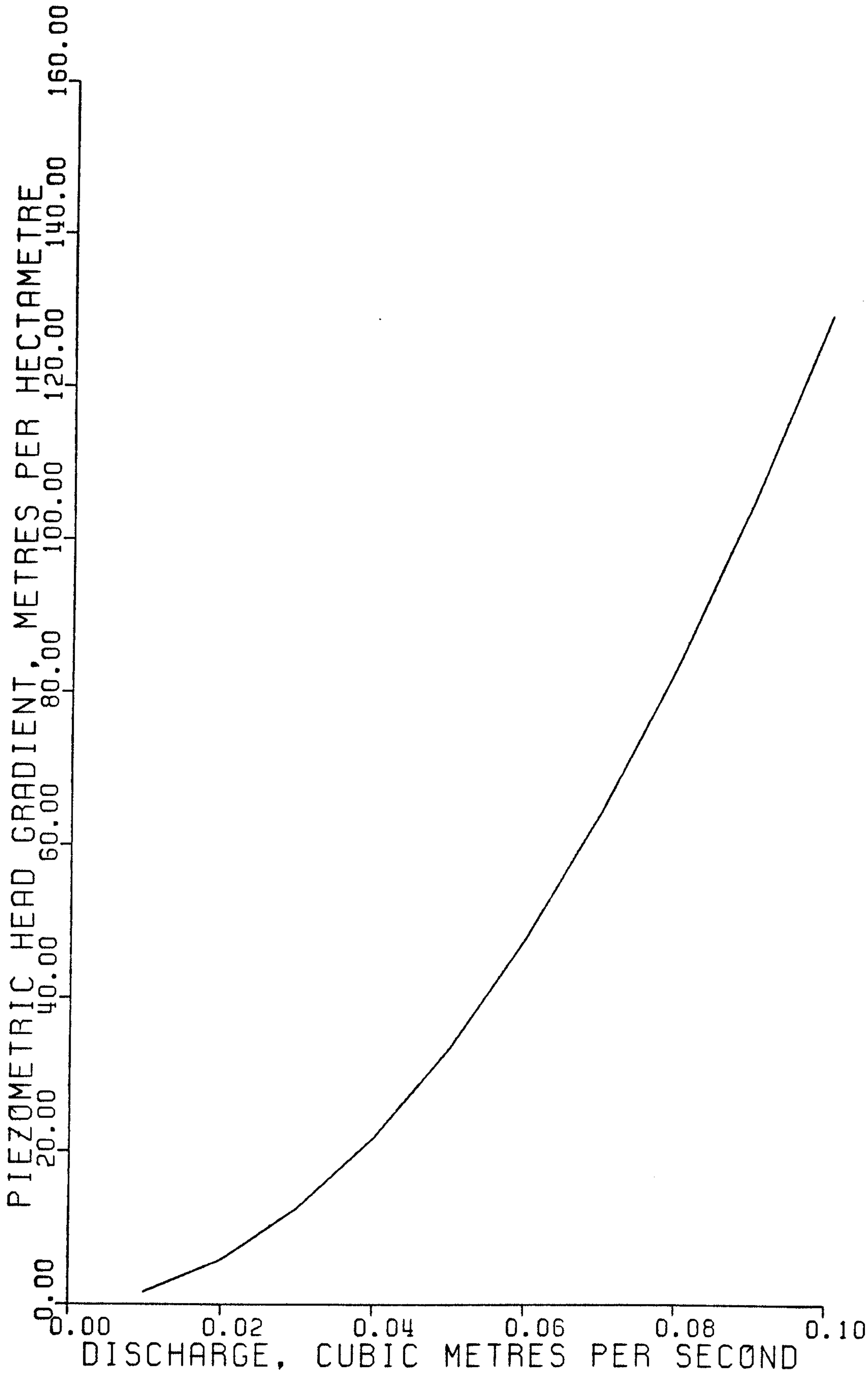

FIG. A-3 GRADIENT OF PIEZOMETRIC HEAD AS A FUNCTION OF DISCHARGE IN A 0.102-m DIAMETER STEEL PIPE WITH AN ABSOLUTE ROUGHNESS COEFFICIENT OF 4.572×10^{-5} m.

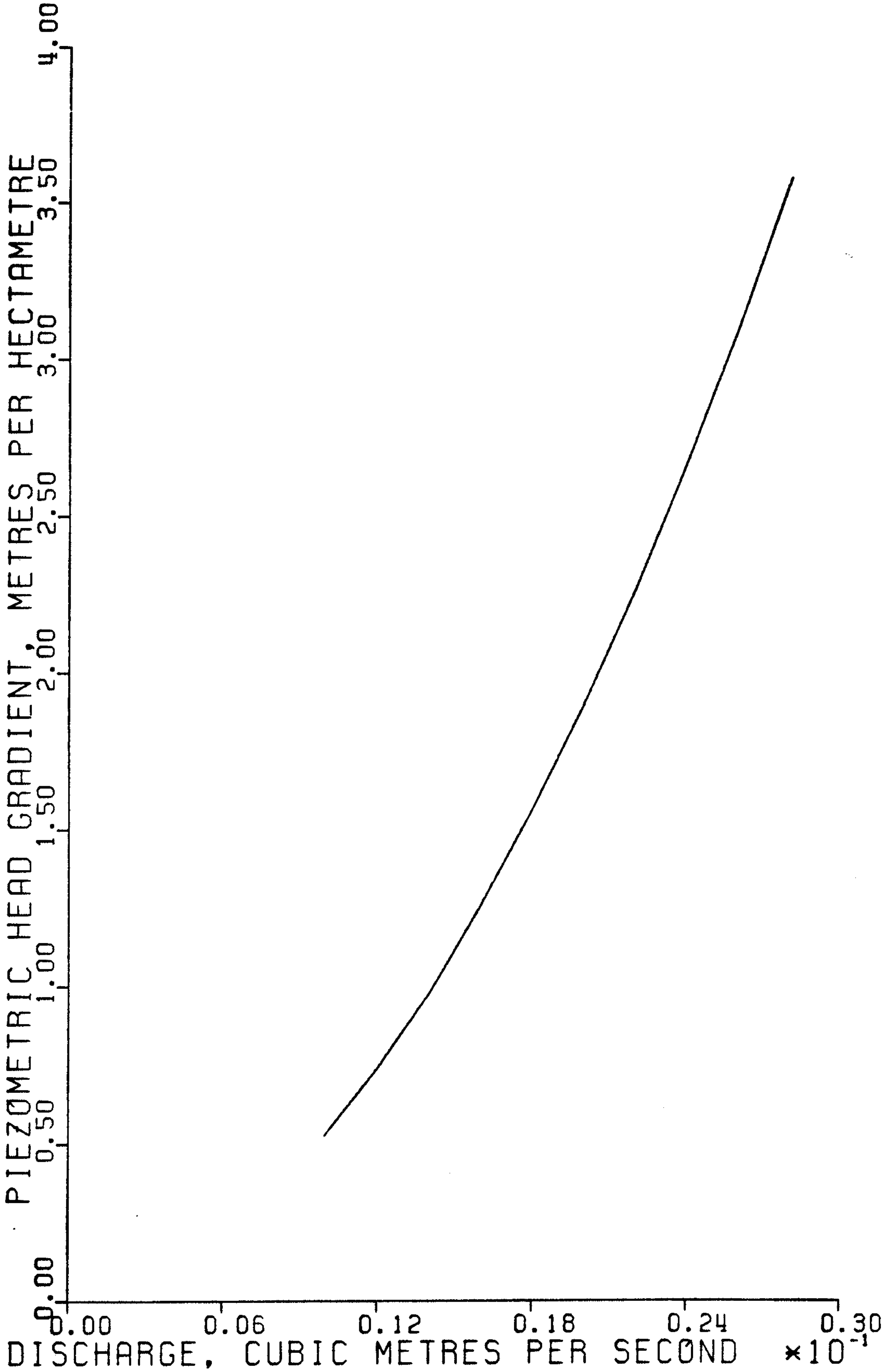

FIG. A-4 GRADIENT OF PIEZOMETRIC HEAD AS A FUNCTION OF DISCHARGE IN A 0.152-m DIAMETER STEEL PIPE WITH AN ABSOLUTE ROUGHNESS COEFFICIENT OF 4.572 x 10^{-5} m.

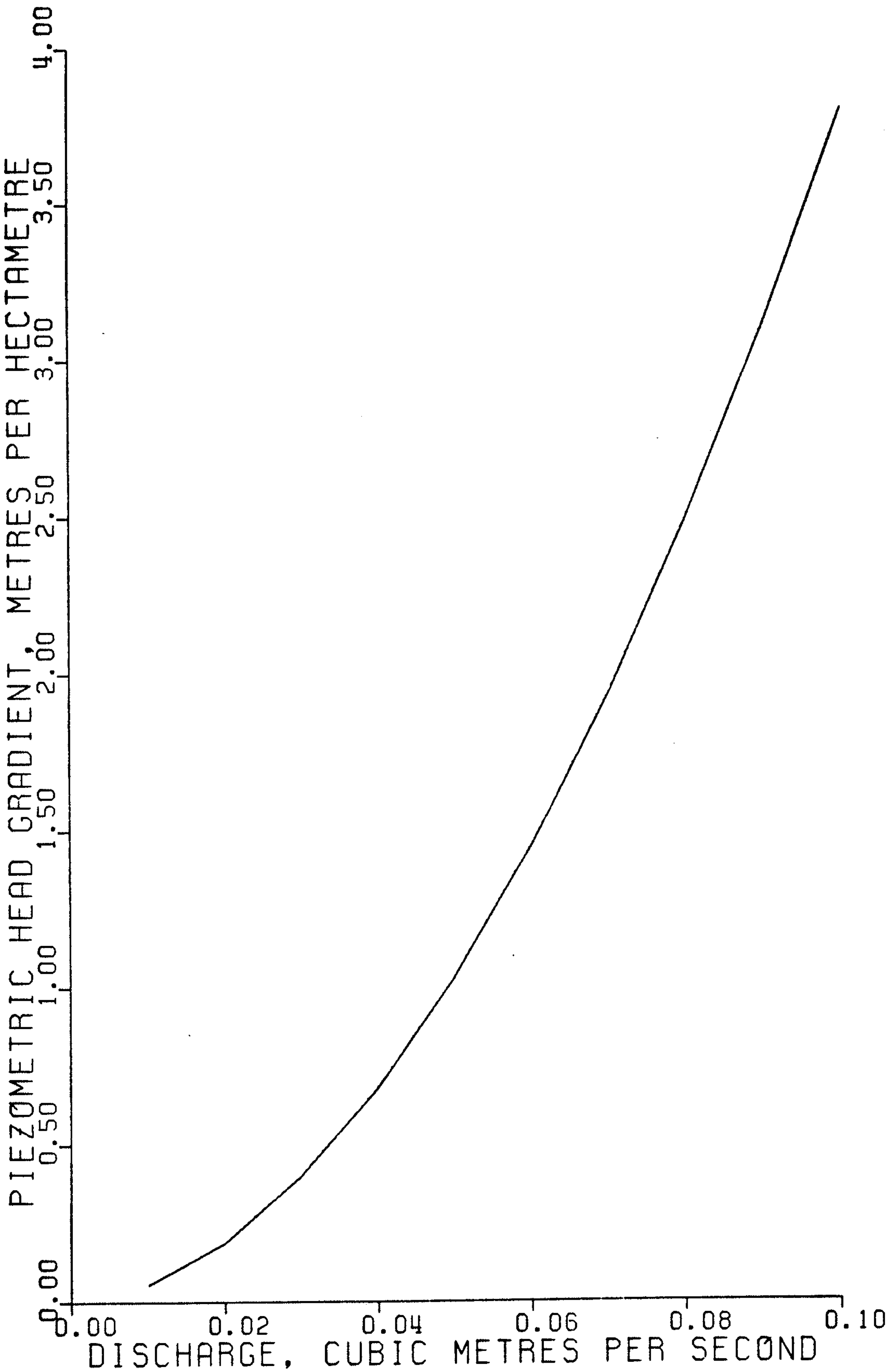

FIG. A-5 GRADIENT OF PIEZOMETRIC HEAD AS A FUNCTION OF DISCHARGE IN A 0.203-m DIAMETER STEEL PIPE WITH AN ABSOLUTE ROUGHNESS COEFFICIENT OF 4.572×10^{-5} m.

APPENDIX B

ALGORITHM TO CALCULATE PIEZOMETRIC HEAD AS A FUNCTION OF DISCHARGE IN A STEEL PIPE

APPENDIX B ALGORITHM TO CALCULATE GRADIENT OF PIEZOMETRIC HEAD AS A FUNCTION OF DISCHARGE IN A STEEL PIPE

```
C ... PROGRAM TO CALCULATE GRADIENT OF PIEZOMETRIC HEAD AS A
C ... FUNCTION OF DISCHARGE IN A STEEL PIPE WITH AN ASSUMED
C ... ABSOLUTE ROUGHNESS COEFFICIENT OF 4.572X10E-5 METERS.
C ... A - CROSS-SECTIONAL AREA, M**2
C ... E - ABSOLUTE ROUGHNESS OF PIPE, M.
C ... F - COEFFICIENT OF FRICTION, CALCULATED BY
C ...     'DARCY-WEISBACH' EQUATION.
C ... FL - LENGTH OF PIPE, M.
C ... G - ACCELARATION DUE TO GRAVITY, M/S**2
C ... HL - HEAD LOSS DUE TO FRICTION IN THE PIPE, M.
C ... Q - DISCHARGE RATE, M**3/S.
C ... RE - REYNOLD'S NUMBER.
C ... V - FLOW VELOCITY, M/S.
C ....VIS - KINEMATIC VISCOSITY OF WATER AT ROOM
C ....      TEMPERATURE (20 C), M**2/S.
C .........................................................
      REAL*8 RE,VIS,E
10    READ(5,*) D,Q,FL,VIS,E,G
      A =0.78539816*D*D
111   V = Q/A
      RE=V*D/VIS
      IF (RE .GT. 2100) GO TO 3
      F = 64/RE
      GO  TO 1
3     EVIS = E/VIS
      ELOG =  18.7*DLOG10(2.71828183)
      ED = E/D
      F =  1./(1.14-2.*ALOG10(ED))**2
      PAR =  V*SQRT(F/8.)*EVIS
      IF  (PAR .GT. 100) GO TO 1
      NCT =0
2     FS = SQRT(F)
      FZ =  0.5/(F*FS)
      ARG =  ED + 9.35/(RE*FS)
      FF   = 1./FS - 1.14 + 2.*ALOG10(ARG)
      DF   = FZ + ELOG*FZ/(ARG*RE)
      DIF =FF/DF
      F   = F+DIF
      NCT  = NCT+1
      IF (ABS(DIF) .GT. 0.00001 .AND. NCT .LT. 15) GO TO 2
1     HL   = F*FL*V*V/(2.*G*D)
      SL   =HL/FL
      WRITE (6,101) Q,D,FL,F,HL,SL
 101  FORMAT (1X,'Q =',F10.4,1X,'D ='F10.4,1X,'L =',F10.2,1X,
     $'F =',F10.5,1X,'HEADLOSS =',F10.4,1X,'SLOPE =',F10.4)
      IF(Q .GE. .25) GO TO 4
      Q=Q+0.002
      GO TO 111
4     STOP
      END
```

APPENDIX C

ALGORITHM TO FIT A LEAST-SQUARE STRAIGHT LINE THROUGH THE OBSERVED CHANGE IN PIEZOMETRIC HEAD ALONG THE HORIZONTAL CENTRELINE OF THE PIPE EXPANSION AND TO CALCULATE THE ENERGY LOSS COEFFICIENT K

APPENDIX C ALGORITHM TO FIT A LEAST-SQUARE STRAIGHT LINE THROUGH THE OBSERVED CHANGE IN PIEZOMETRIC HEAD ALONG THE HORIZONTAL CENTRE-LINE OF THE PIPE EXPANSION AND TO CALCULATE THE ENERGY LOSS COEFFICIENT K

```
C ..... PROGRAM FOR LEAST SQUARE STRAIGHT LINE FITTING AND
C ..... REGRESSION COEFFICIENT FOR THE UNOBSTRUCTED UPSTREAM
C ..... PIPE SECTION.
C ..... X : DISTANCE ALONG THE PIPE SECTION.
C ..... Y : PRESSURE DIFFERENCES BETWEEN THE 1ST TAPPING
C .....     POINT AND THE REST ALL TAPPING POINTS.
C ..... N : NUMBER OF TAPPING POINTS EXCLUDING THE 1ST ONE.
C ...........................................................
      DIMENSION X(5),Y(5)
      READ (5,*) N,BETA1
      DO 11 I = 1,N
      READ (5,*) X(I),Y(I)
11    CONTINUE
      SUMX=0.0
      SUMY=0.0
      SUMXSQ=0.0
      SUMYSQ=0.0
      SUMXY=0.0
      DO 10 I= 1,N
      SUMX=SUMX+X(I)
      SUMY=SUMY+Y(I)
      SUMXSQ=SUMXSQ+X(I)*X(I)
      SUMYSQ=SUMYSQ+Y(I)*Y(I)
      SUMXY=SUMXY+X(I)*Y(I)
10    CONTINUE
      XBAR=SUMX/N
      YBAR=SUMY/N
      SXX=SUMXSQ-(SUMX*SUMX)/N
      SYY=SUMYSQ-(SUMY*SUMY)/N
      SXY=SUMXY-(SUMX*SUMY)/N
C     BETA1=SXY/SXX
      BETA0=YBAR-BETA1*XBAR
      R=SXY/(SQRT(SXX*SYY))
      DO 111 J= 1,N
      WRITE (6,*) X(J),Y(J)
111   CONTINUE
      DELTAP=BETA0+BETA1*1.0414
      WRITE (6,*)
      WRITE (6,*) BETA0,BETA1,DELTAP,R
      STOP
      END
```

APPENDIX C CONTINUED

```
C ..... PROGRAM FOR LEAST SQUARE STRAIGHT LINE FITTING AND
C ..... REGRESSION COEFFICIENT FOR THE UNOBSTRUCTED DOWNSTREAM
C ..... PIPE SECTION.
C ..... X : DISTANCE ALONG THE PIPE SECTION.
C ..... Y : PRESSURE DIFFERENCES BETWEEN THE 1ST TAPPING
C .....     POINT AND THE REST ALL TAPPING POINTS.
C ..... N : NUMBER OF TAPPING POINTS EXCLUDING THE 1ST ONE.
C ...........................................................
      DIMENSION X(5),Y(5)
      READ (5,*) N,BETA1
      DO 11 I = 1,N
      READ (5,*) X(I),Y(I)
11    CONTINUE
      SUMX=0.0
      SUMY=0.0
      SUMXSQ=0.0
      SUMYSQ=0.0
      SUMXY=0.0
      DO 10 I= 1,N
      SUMX=SUMX+X(I)
      SUMY=SUMY+Y(I)
      SUMXSQ=SUMXSQ+X(I)*X(I)
      SUMYSQ=SUMYSQ+Y(I)*Y(I)
      SUMXY=SUMXY+X(I)*Y(I)
10    CONTINUE
      XBAR=SUMX/N
      YBAR=SUMY/N
      SXX=SUMXSQ-(SUMX*SUMX)/N
      SYY=SUMYSQ-(SUMY*SUMY)/N
      SXY=SUMXY-(SUMX*SUMY)/N
C     BETA1=SXY/SXX
      BETA0=YBAR-BETA1*XBAR
      R=SXY/(SQRT(SXX*SYY))
      DO 111 J= 1,N
      WRITE (6,*) X(J),Y(J)
111   CONTINUE
      DELTAP=BETA0+BETA1*1.27
      WRITE (6,*)
      WRITE (6,*) BETA0,BETA1,DELTAP,R
      STOP
      END
```

APPENDIX C CONTINUED

```
      DIMENSION IBUF(4000),XARRAY(12),YARRAY(12),XUS(7),
     $YUS(7),XDS(7),YDS(7),XU(4),YU(4),XD(4),YD(4),XBE(4),
     $YBE(4),XA(11),YA(11),XB(4),YB(4),XC(4),YC(4),XUP(6),
     $YUP(6),XDN(6),YDN(6),XUD(4),YUD(4),X1(4),Y1(4)
      CALL PLOTS (IBUF,4000)
      READ (5,*) (XARRAY(I),YARRAY(I),I=1,10)
      WRITE(6,*) (XARRAY(I),YARRAY(I),I=1,10)
      CALL PLOT(0.0,-5.0,-3)
      CALL PLOT(0.5,2.5,-3)
      XARRAY(11)=0.0
      XARRAY(12)=0.35
      YARRAY(11)=-0.40
      YARRAY(12)=1.0/5.0
      CALL AXIS (0.0,-.75,'CENTRELINE DISTANCE, METRES',
     $-27,10.0,0.0,XARRAY(11),XARRAY(12))
      CALL AXIS (-0.5,0.0,'CHANGE IN PIEZOMETRIC HEAD,
     $METRES',34,5.0,90.0,YARRAY(11),YARRAY(12))
      READ(5,*) N,NN,FL,DL,TL,BETAUS,BETADS,D1,D2
      DO 10 I=1,N
      XUS(I)=XARRAY(I)
      YUS(I)=YARRAY(I)
      XDS(I)=XARRAY(5+I)
      YDS(I)=YARRAY(5+I)
 10   CONTINUE
      DO 11 I=6,7
      XUS(I)=XARRAY(5+I)
      YUS(I)=YARRAY(5+I)
      XDS(I)=XARRAY(5+I)
      YDS(I)=YARRAY(5+I)
 11   CONTINUE
      IF(NN .EQ. 4)GO TO 100
      CALL LINE (XUS,YUS,5,1,-1,2)
      CALL LINE (XDS,YDS,5,1,-1,0)
      GO TO 200
  100 DO 13 I=1,NN
      XUP(I)=XARRAY(I)
      YUP(I)=YARRAY(I)
      XDN(I)=XARRAY(6+I)
      YDN(I)=YARRAY(6+I)
  13  CONTINUE
      DO 14 I=5,6
      XUP(I)=XARRAY(6+I)
      YUP(I)=YARRAY(6+I)
      XDN(I)=XARRAY(6+I)
      YDN(I)=YARRAY(6+I)
  14  CONTINUE
```

APPENDIC C CONTINUED

```
      DO 15 I=1,2
      XUD(I)=XARRAY(4+I)
      YUD(I)=YARRAY(4+I)
      XUD(2+I)=XARRAY(10+I)
      YUD(2+I)=YARRAY(10+I)
   15 CONTINUE
      CALL LINE (XUP,YUP,4,1,-1,2)
      CALL LINE (XDN,YDN,4,1,-1,0)
      CALL LINE (XUD,YUD,2,1,-1,11)
C     X1(1)=0.0
C     X1(2)=2.95
C     Y1(1)=0.0
C     Y1(2)=0.0
C     X1(3)=XARRAY(11)
C     X1(4)=XARRAY(12)
C     Y1(3)=YARRAY(11)
C     Y1(4)=YARRAY(12)
C     CALL DASHLN (X1,Y1,2,1,10)
  200 SUMXUS=0.0
      SUMYUS=0.0
      SUMXDS=0.0
      SUMYDS=0.0
C     K=N-1
      DO 12 I=1,N
      SUMXUS=SUMXUS+XUS(I)
      SUMYUS=SUMYUS+YUS(I)
      SUMXDS=SUMXDS+XDS(I)
      SUMYDS=SUMYDS+YDS(I)
   12 CONTINUE
      XBARUS=SUMXUS/N
      YBARUS=SUMYUS/N
      XBARDS=SUMXDS/N
      YBARDS=SUMYDS/N
      BETA0U=YBARUS-BETAUS*XBARUS
      BETA0D=YBARDS-BETADS*XBARDS
      XU(1)=0.0
      YU(1)=BETA0U
      XU(2)=FL
      YU(2)=BETA0U+BETAUS*XU(2)
      XU(3)=XUS(6)
      YU(3)=YUS(6)
      XU(4)=XUS(7)
      YU(4)=YUS(7)
```

APPENDIX C CONTINUED

```
C.................................................
      XD(1)=FL+DL
      YD(1)=BETA0D+BETADS*XD(1)
      XD(2)=TL
      YD(2)=BETA0D+BETADS*XD(2)
      XD(3)=XU(3)
      YD(3)=YU(3)
      XD(4)=XU(4)
      YD(4)=YU(4)
      CALL LINE (XU,YU,2,1,0,0)
      CALL LINE (XD,YD,2,1,0,0)
      XBE(1)=FL
      YBE(1)=YU(2)
      XBE(2)=FL+DL
      YBE(2)=YD(1)
      XBE(3)=XD(3)
      YBE(3)=YD(3)
      XBE(4)=XD(4)
      YBE(4)=YD(4)
      CALL DASHLN(XBE,YBE,2,1,10)
      XA(1)=0.0
      YA(1)=-(D1/2.)
      XA(2)=XA(1)
      YA(2)=D1/2.
      XA(3)=FL
      YA(3)=D1/2.
      XA(4)=FL+DL
      YA(4)=D2/2.
      XA(5)=TL
      YA(5)=YA(4)
      XA(6)=XA(5)
      YA(6)=-(D2/2.)
      XA(7)=FL+DL
      YA(7)=YA(6)
      XA(8)=XA(3)
      YA(8)=-(D1/2.)
      XA(9)=XA(1)
      YA(9)=YA(1)
      XA(10)=0.0
      YA(10)=0.0
      XA(11)=XARRAY(12)
      YA(11)=XARRAY(12)
      CALL LINE (XA,YA,9,1,0,0)
```

APPENDIX C CONTINUED

```
      XB(1)=0.0
      YB(1)=0.0
      XB(2)=TL
      YB(2)=0.0
      XB(3)=XA(10)
      YB(3)=YA(10)
      XB(4)=XA(11)
      YB(4)=YA(11)
      CALL DASHLN (XB,YB,2,1,10)
      XC(1)=FL
      YC(1)=-(D1/2.)
      XC(2)=XC(1)
      YC(2)=D1/2.
      XC(3)=XB(3)
      YC(3)=YB(3)
      XC(4)=XB(4)
      YC(4)=YB(4)
      CALL DASHLN (XC,YC,2,1,10)
      X1(1)=FL+DL
      Y1(1)=-(D2/2.)
      X1(2)=X1(1)
      Y1(2)=D2/2.
      X1(3)=XC(3)
      Y1(3)=YC(3)
      X1(4)=XC(4)
      Y1(4)=YC(4)
      CALL DASHLN(X1,Y1,2,1,10)
      CALL SYMBOL(-.42,-1.85,.14,75HFIG. 2.9 CHANGE IN
     $PIEZOMETRIC HEAD ALONG THE HORIZONTAL CENTRELINE
     $OF PIPE,0.0,75)
      CALL SYMBOL(0.84,-2.10,0.14,64HEXPANSION NO. 2B
     $UNDER THE VELOCITY CONDITIONS OF TEST NO. 2B-5.,
     $0.0,64)
      CALL PLOT (12.0,0.0,999)
      STOP
      END
C .......................................................
C .... PROGRAM FOR COMPUTING THE ENERGY LOSS COEFFICIENT K
C .......................................................
      READ (5,*) A1,A2,D,N
      DO 11 I= 1,N
      READ (5,*) Q,P1B,P1E
      PBE = (-(P1B)+P1E)
      V1  = Q/A1
      V2  = Q/A2
      VHEAD = (V1*V1)/(2*9.81)
      ELOSS = PBE+VHEAD*((D**4-1)/(D**4))
      ELCOE = ELOSS/VHEAD
      WRITE (6,*) I,Q,V1,V2,ELCOE
 11    CONTINUE
      STOP
      END
```

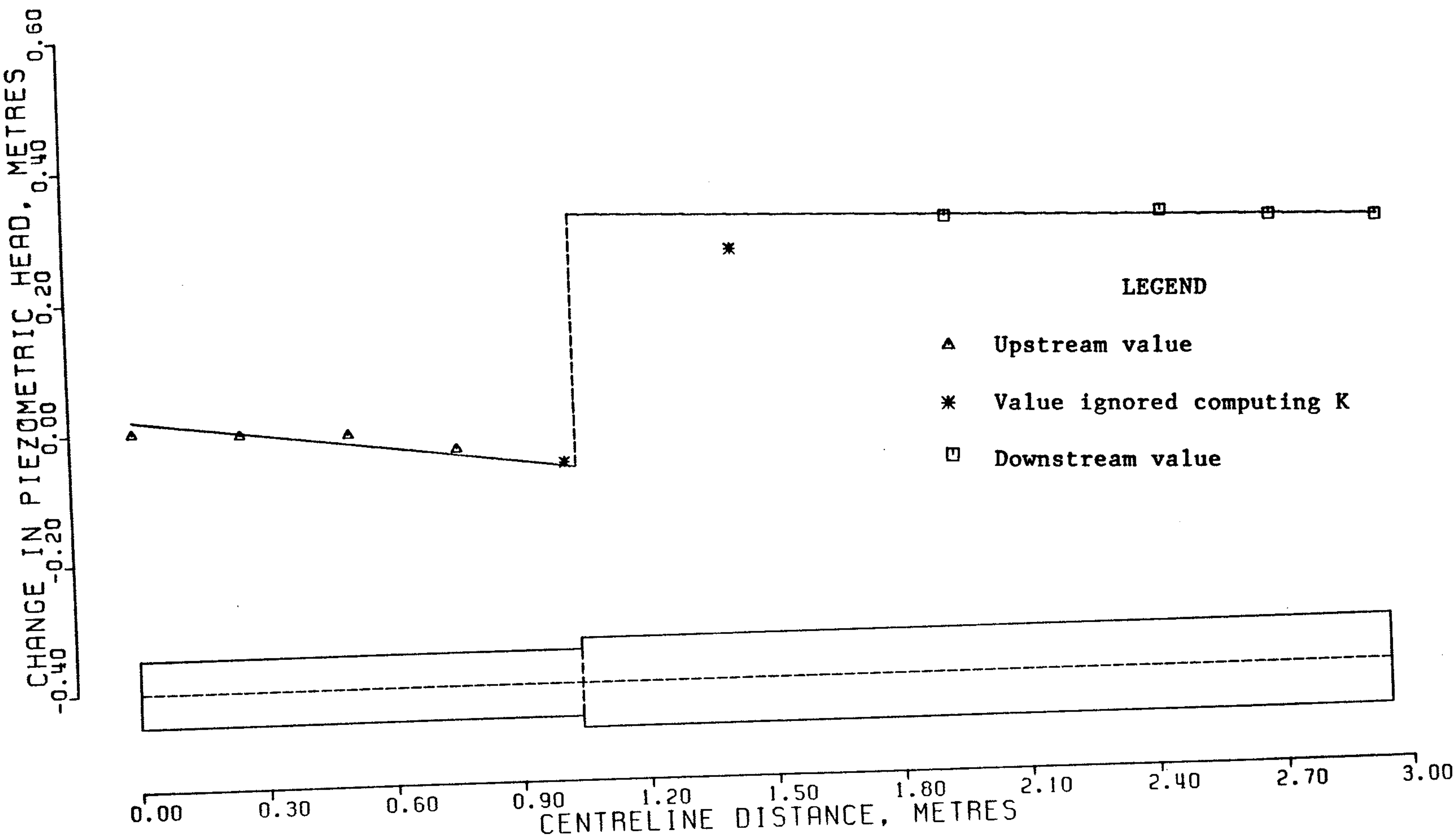

FIG. C-1 CHANGE IN PIEZOMETRIC HEAD ALONG THE HORIZONTAL CENTRELINE OF PIPE EXPANSION NO. 1A UNDER THE VELOCITY CONDITIONS OF TEST NO. 1

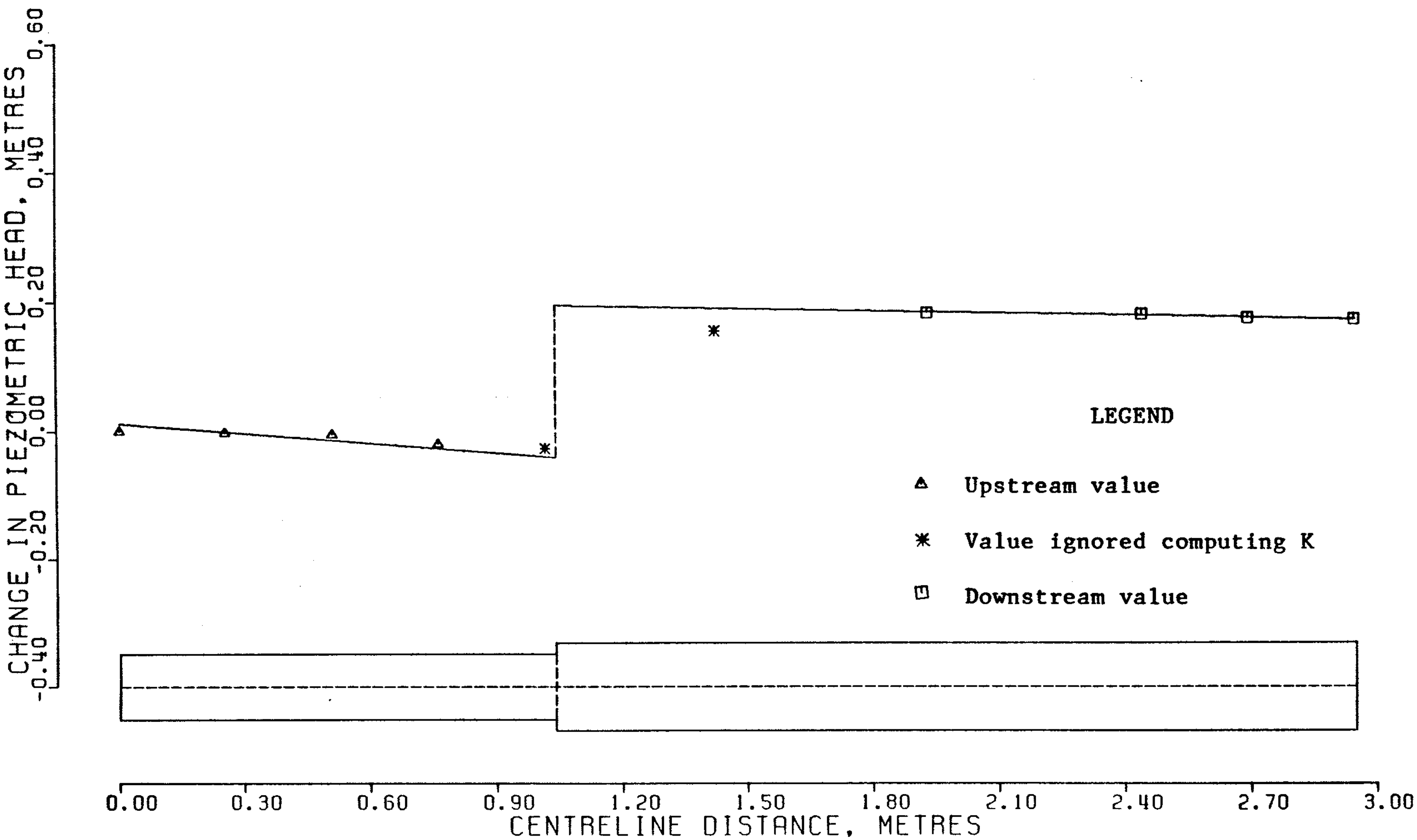

FIG. C-2 CHANGE IN PIEZOMETRIC HEAD ALONG THE HORIZONTAL CENTRELINE OF PIPE EXPANSION NO. 1A UNDER THE VELOCITY CONDITIONS OF TEST NO. 2

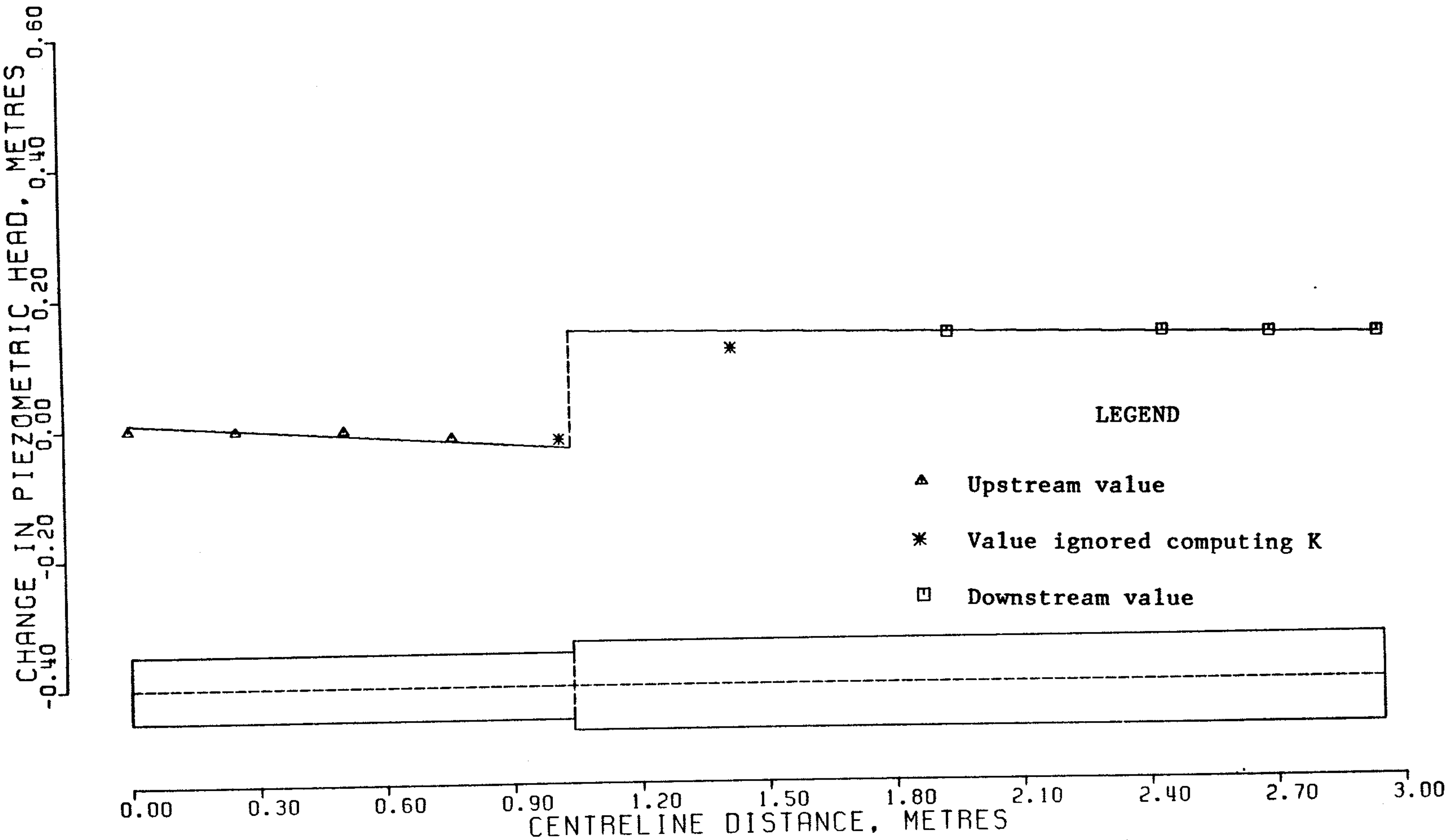

FIG. C-3 CHANGE IN PIEZOMETRIC HEAD ALONG THE HORIZONTAL CENTRELINE OF PIPE EXPANSION NO. 1A UNDER THE VELOCITY CONDITIONS OF TEST NO. 3

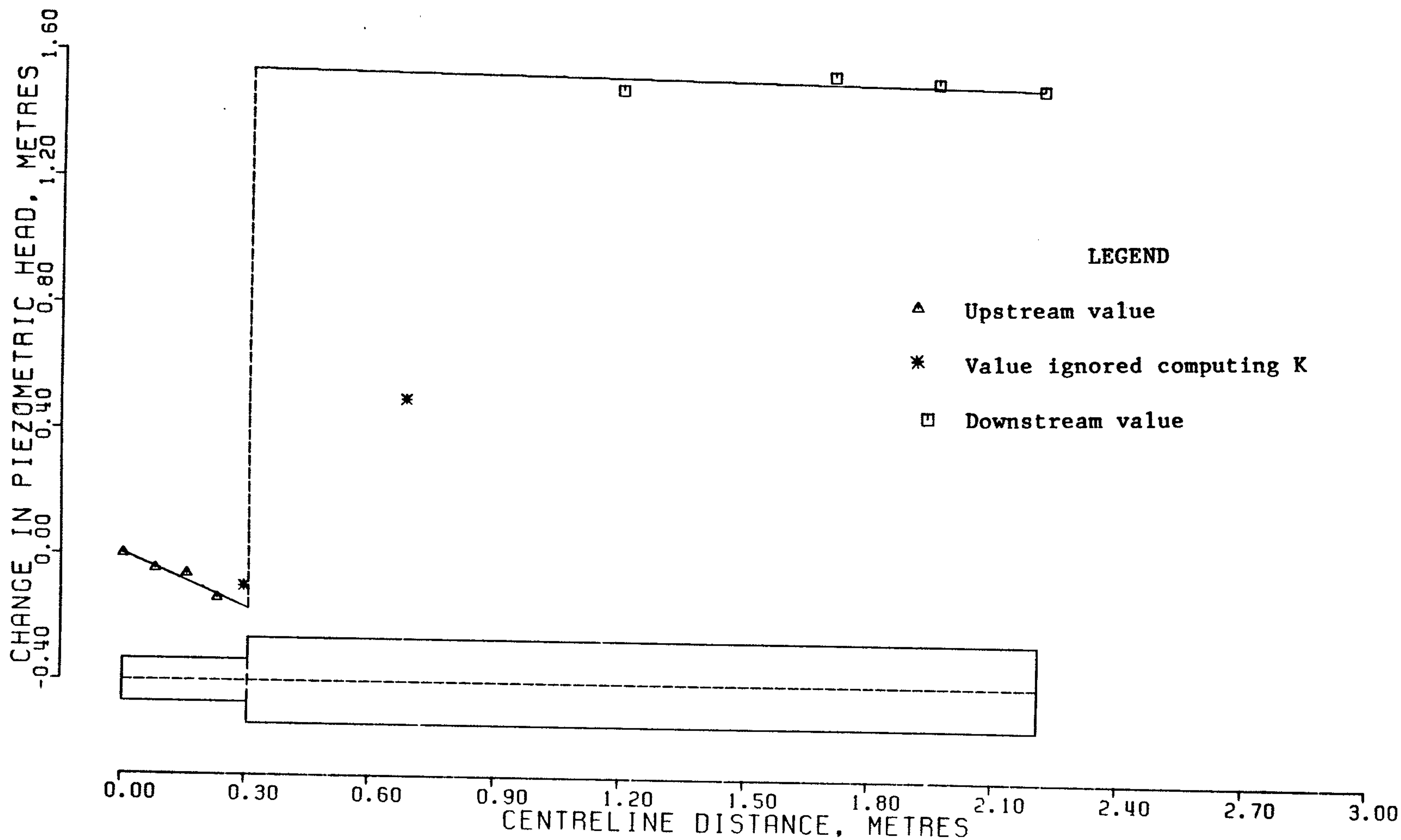

FIG. C-4 CHANGE IN PIEZOMETRIC HEAD ALONG THE HORIZONTAL CENTRELINE OF PIPE EXPANSION NO. 1B UNDER THE VELOCITY CONDITIONS OF TEST NO. 1

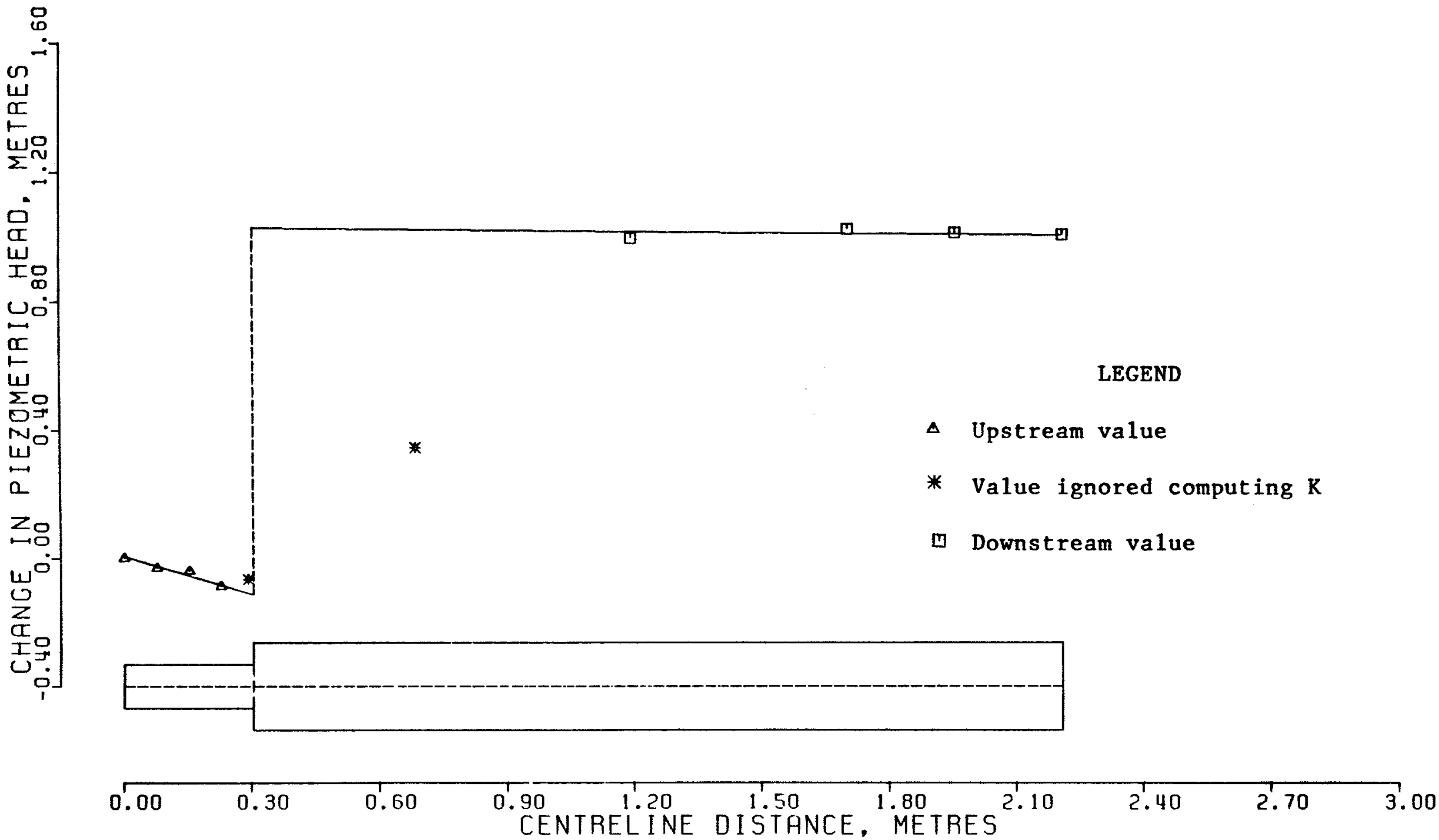

FIG. C-5 CHANGE IN PIEZOMETRIC HEAD ALONG THE HORIZONTAL CENTRELINE OF PIPE EXPANSION NO. 1B UNDER THE VELOCITY CONDITIONS OF TEST NO. 2

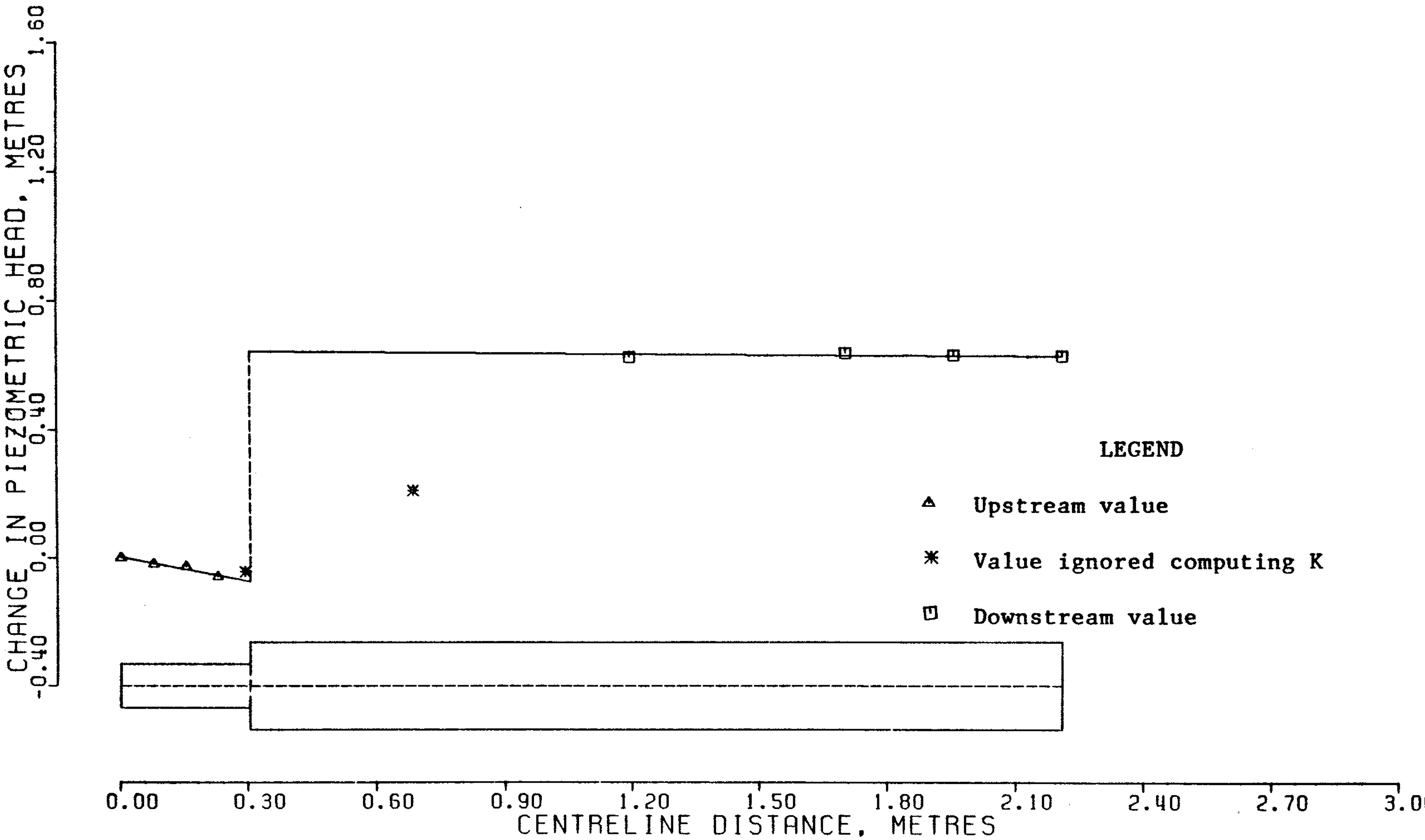

FIG. C-6 CHANGE IN PIEZOMETRIC HEAD ALONG THE HORIZONTAL CENTRELINE OF PIPE EXPANSION NO. 1B UNDER THE VELOCITY CONDITIONS OF TEST NO. 3

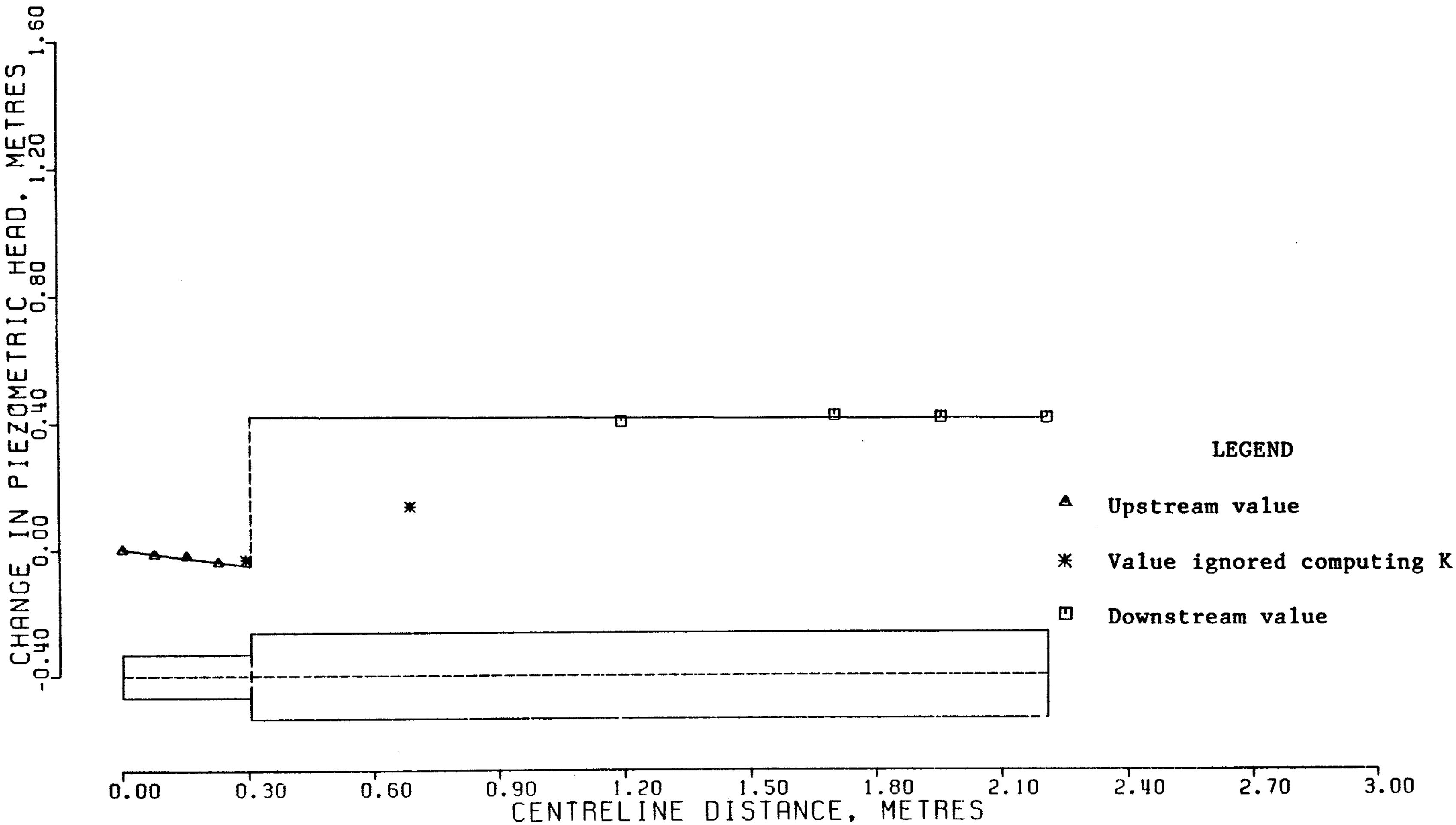

FIG. C-7 CHANGE IN PIEZOMETRIC HEAD ALONG THE HORIZONTAL CENTRELINE OF PIPE EXPANSION NO. 1B UNDER THE VELOCITY CONDITIONS OF TEST NO. 4

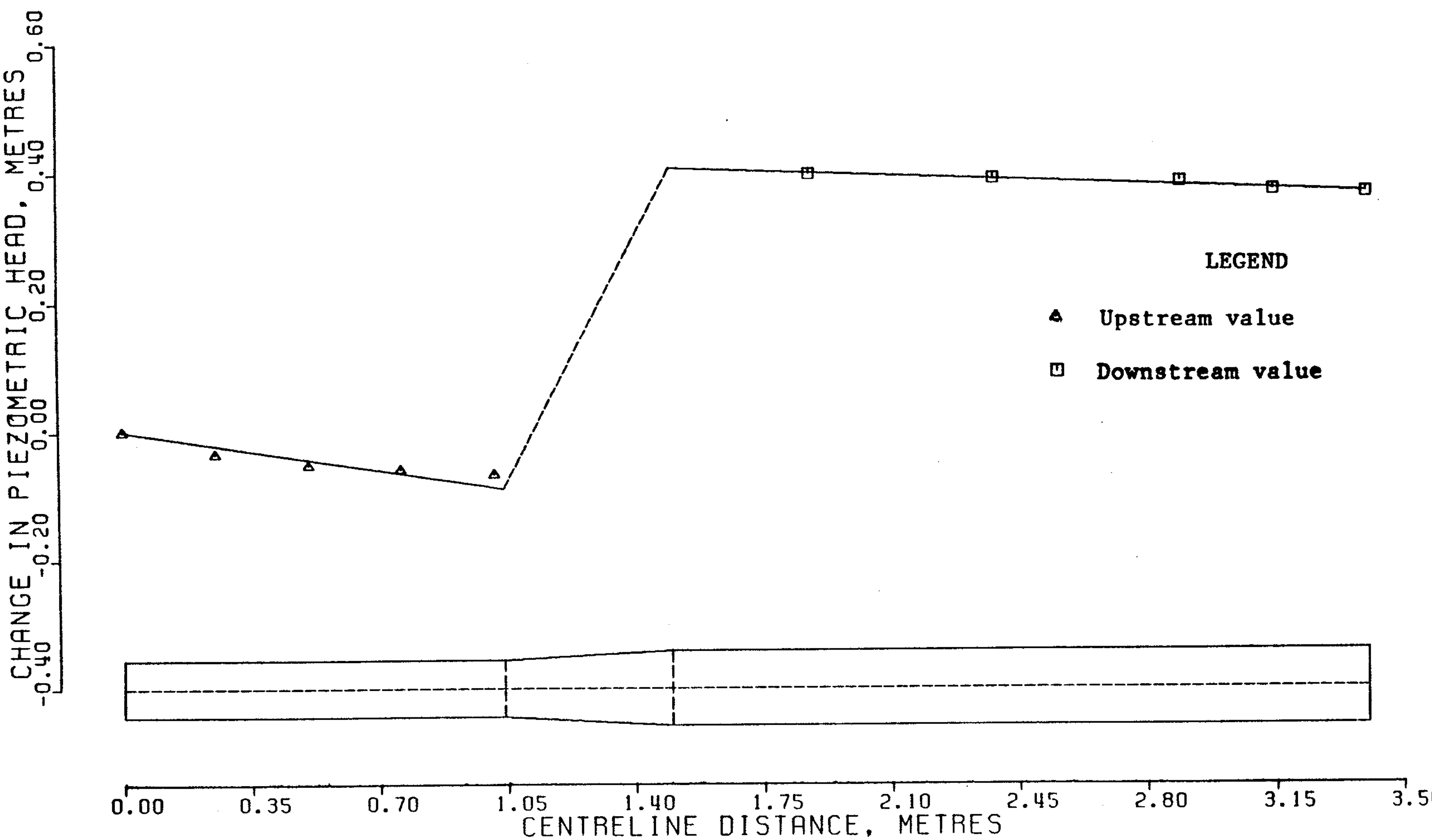

FIG. C-8 CHANGE IN PIEZOMETRIC HEAD ALONG THE HORIZONTAL CENTRELINE OF PIPE EXPANSION NO. 2A UNDER THE VELOCITY CONDITIONS OF TEST NO. 1

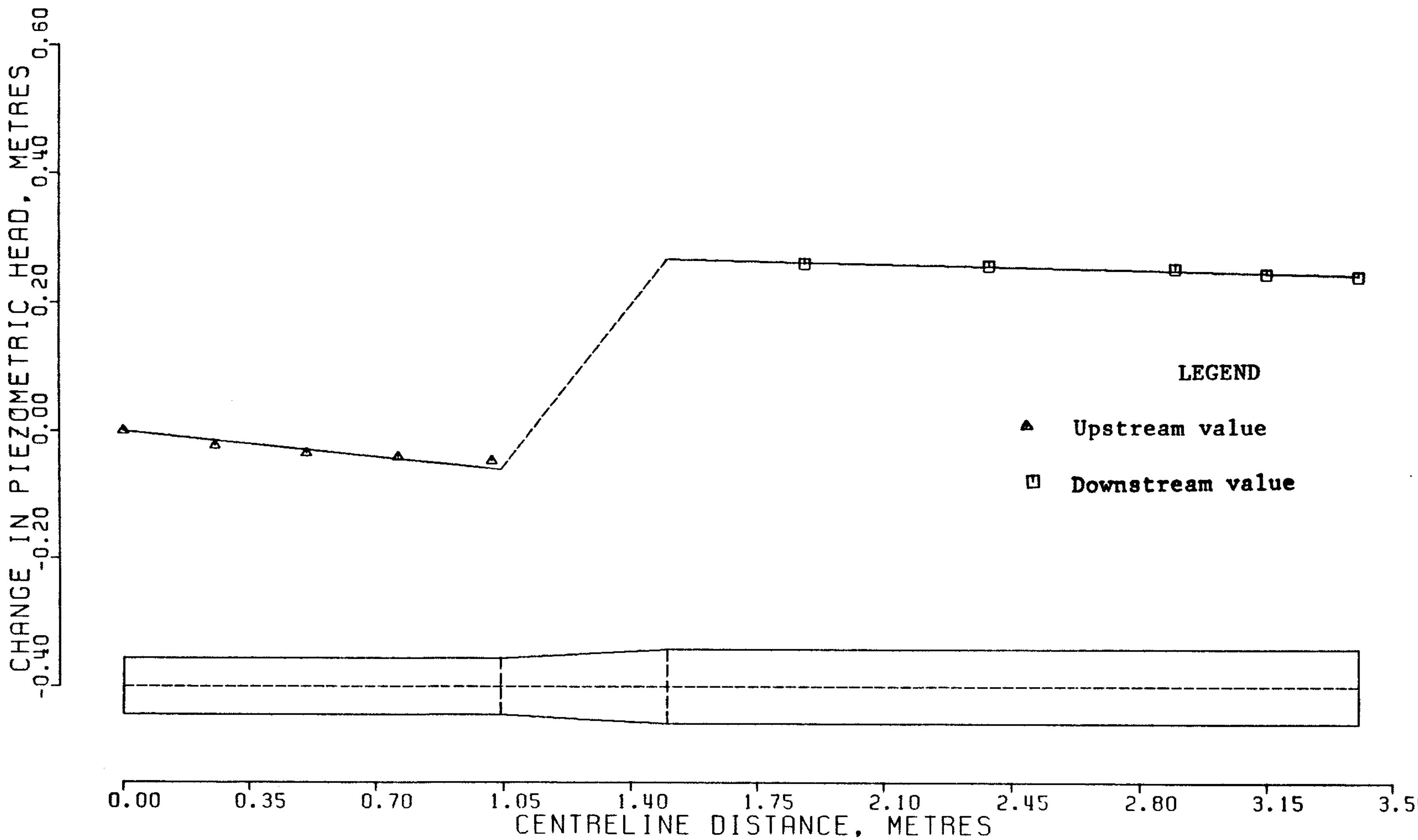

FIG. C-9 CHANGE IN PIEZOMETRIC HEAD ALONG THE HORIZONTAL CENTRELINE OF PIPE EXPANSION NO. 2A UNDER THE VELOCITY CONDITIONS OF TEST NO. 2

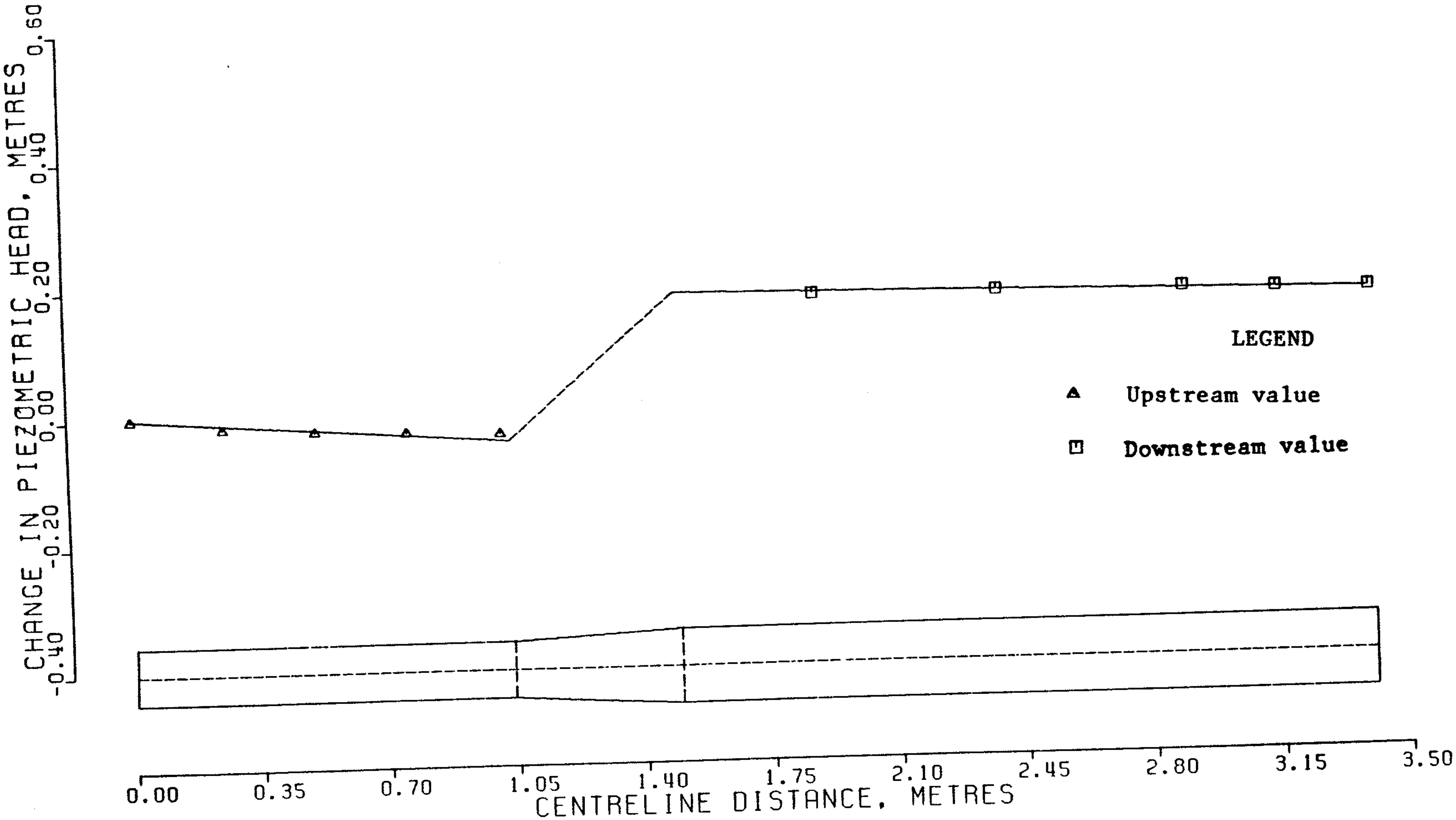

FIG. C-10 CHANGE IN PIEZOMETRIC HEAD ALONG THE HORIZONTAL CENTRELINE OF PIPE EXPANSION NO. 2A UNDER THE VELOCITY CONDITIONS OF TEST NO. 3

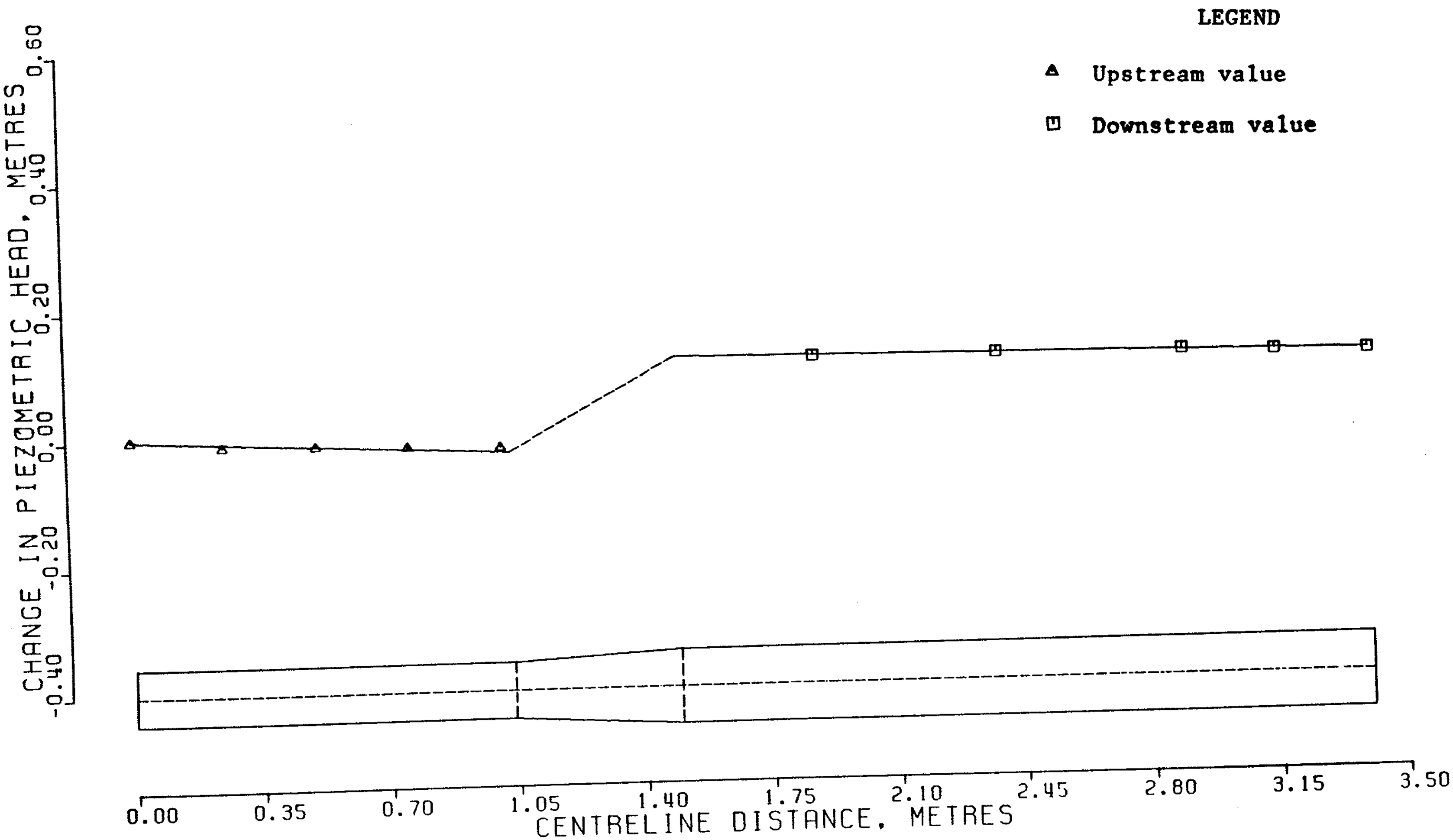

FIG. C-11 CHANGE IN PIEZOMETRIC HEAD ALONG THE HORIZONTAL CENTRELINE OF PIPE EXPANSION NO. 2A UNDER THE VELOCITY CONDITIONS OF TEST NO. 4

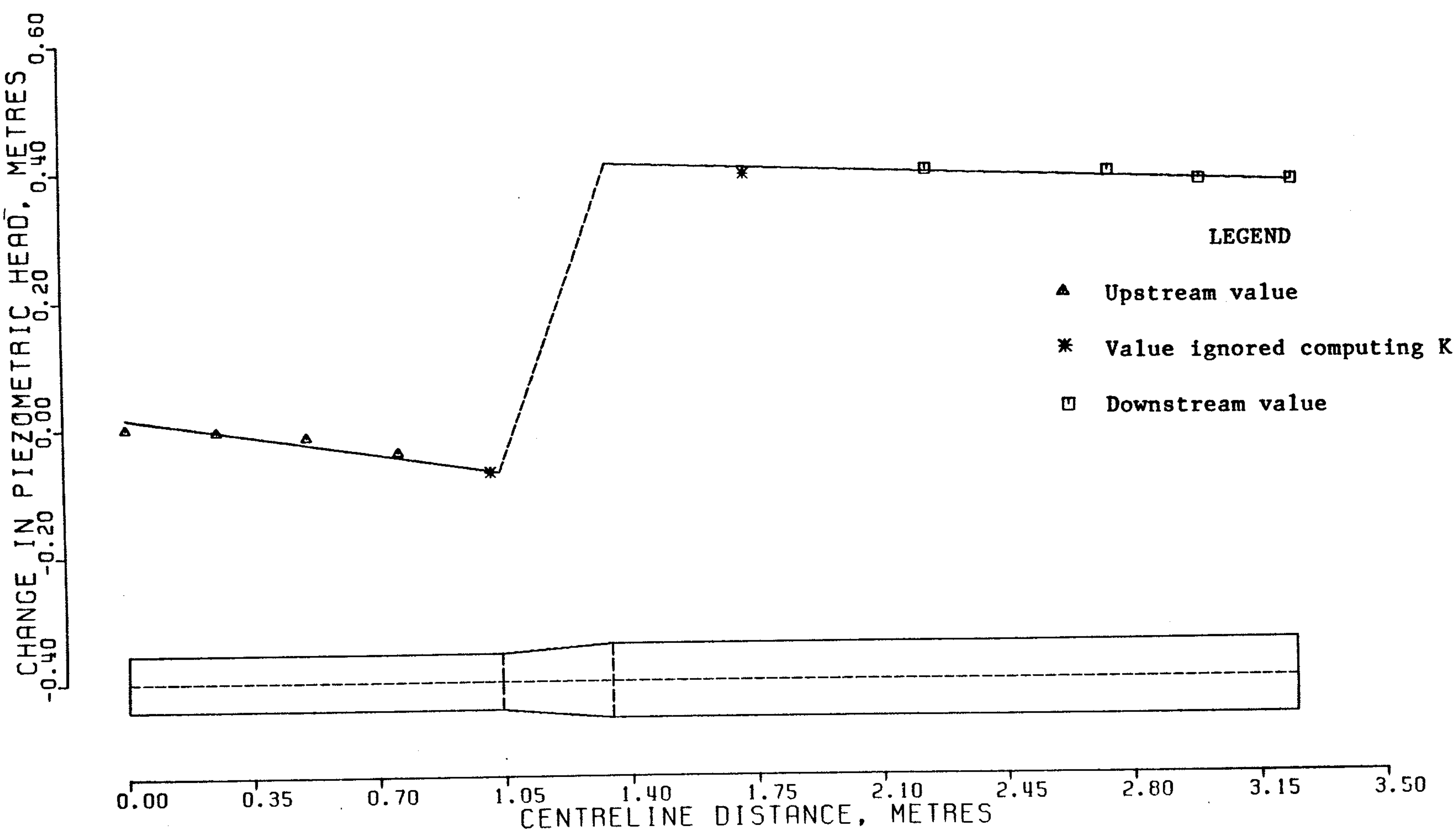

FIG. C-12 CHANGE IN PIEZOMETRIC HEAD ALONG THE HORIZONTAL CENTRELINE OF PIPE EXPANSION NO. 2B UNDER THE VELOCITY CONDITIONS OF TEST NO. 1

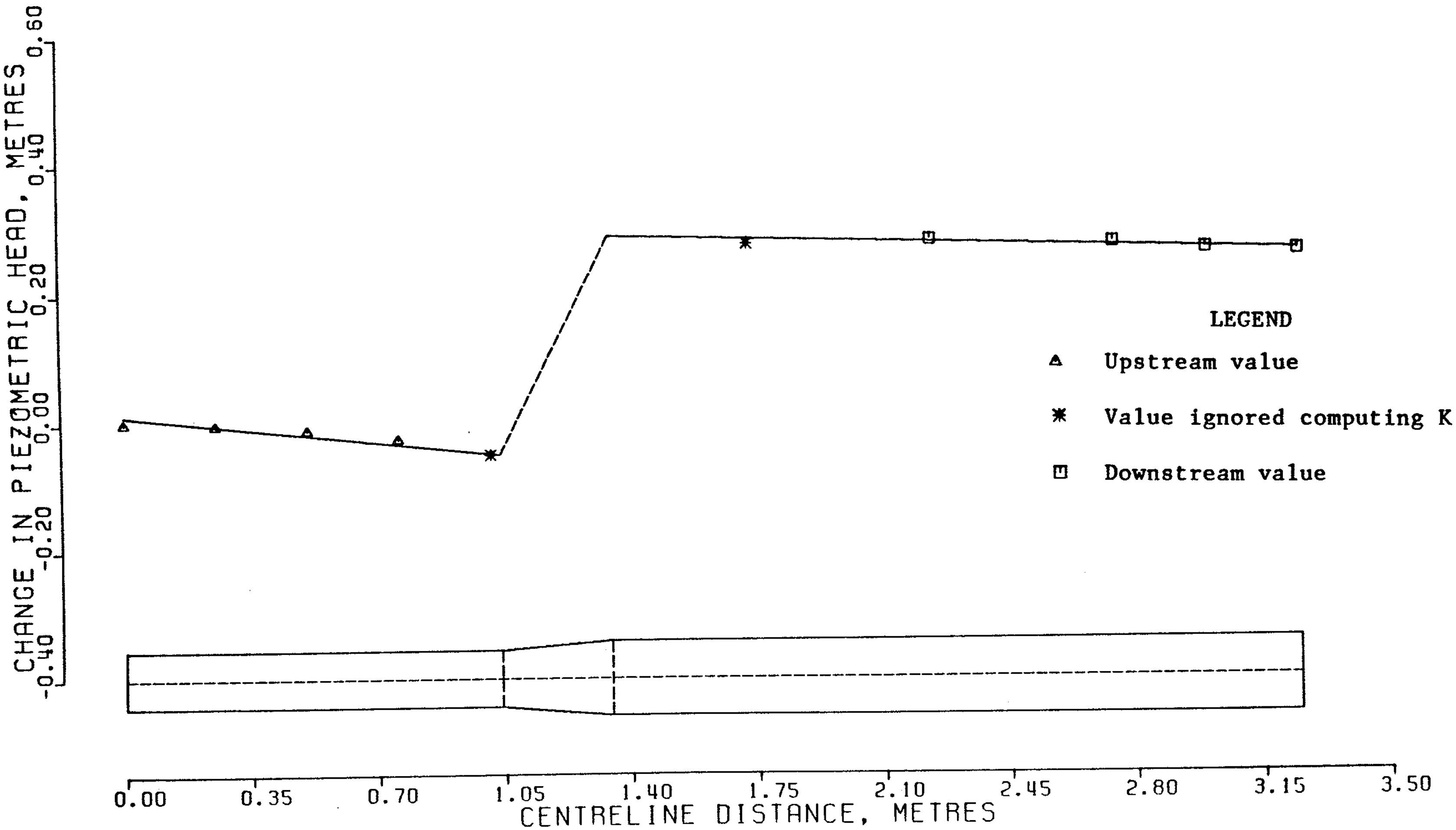

FIG. C-13 CHANGE IN PIEZOMETRIC HEAD ALONG THE HORIZONTAL CENTRELINE OF PIPE EXPANSION NO. 2B UNDER THE VELOCITY CONDITIONS OF TEST NO. 2

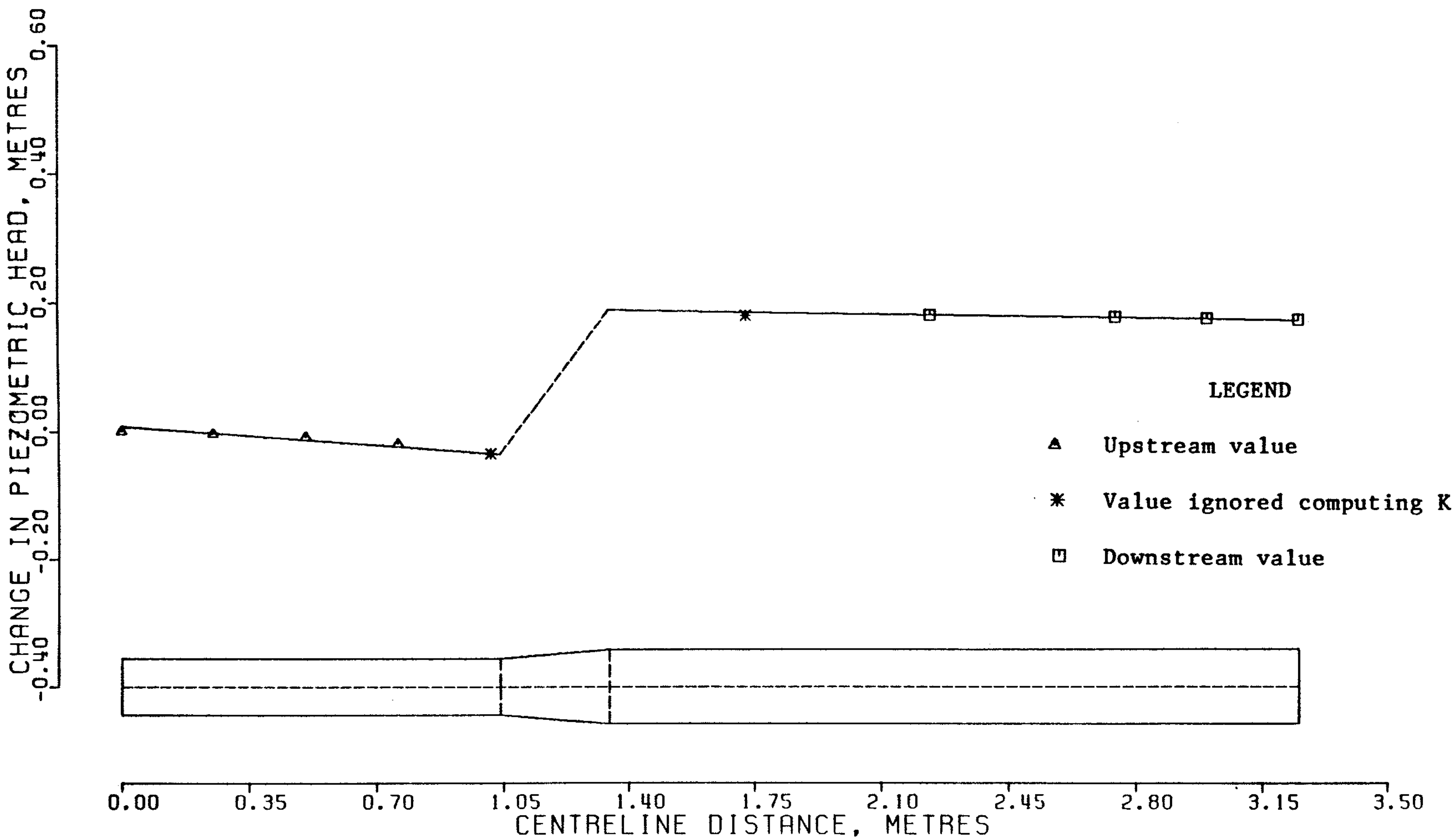

FIG. C-14 CHANGE IN PIEZOMETRIC HEAD ALONG THE HORIZONTAL CENTRELINE OF PIPE EXPANSION NO. 2B UNDER THE VELOCITY CONDITIONS OF TEST NO. 3

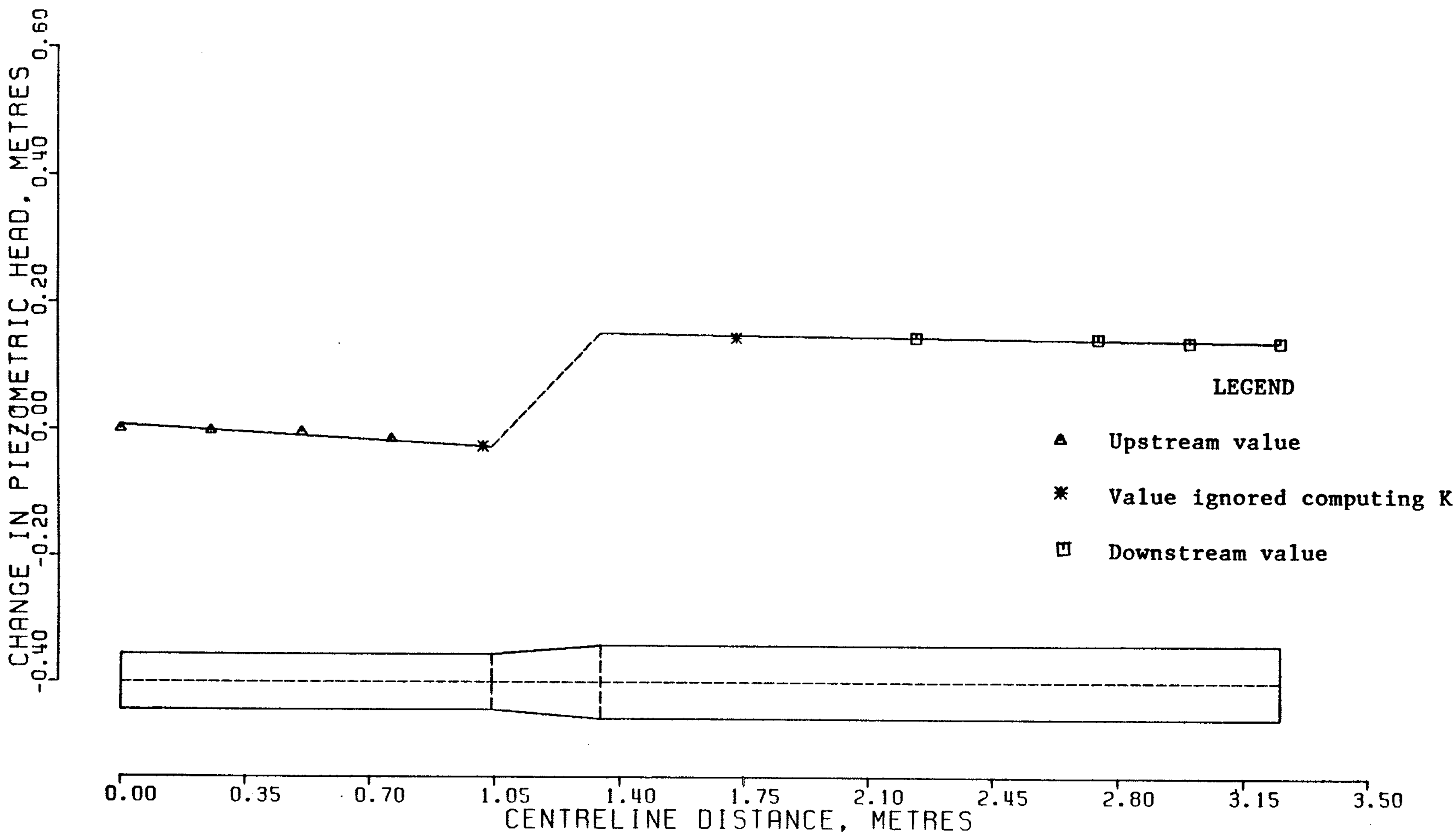

FIG. C-15 CHANGE IN PIEZOMETRIC HEAD ALONG THE HORIZONTAL CENTRELINE OF PIPE EXPANSION NO. 2B UNDER THE VELOCITY CONDITIONS OF TEST NO. 4

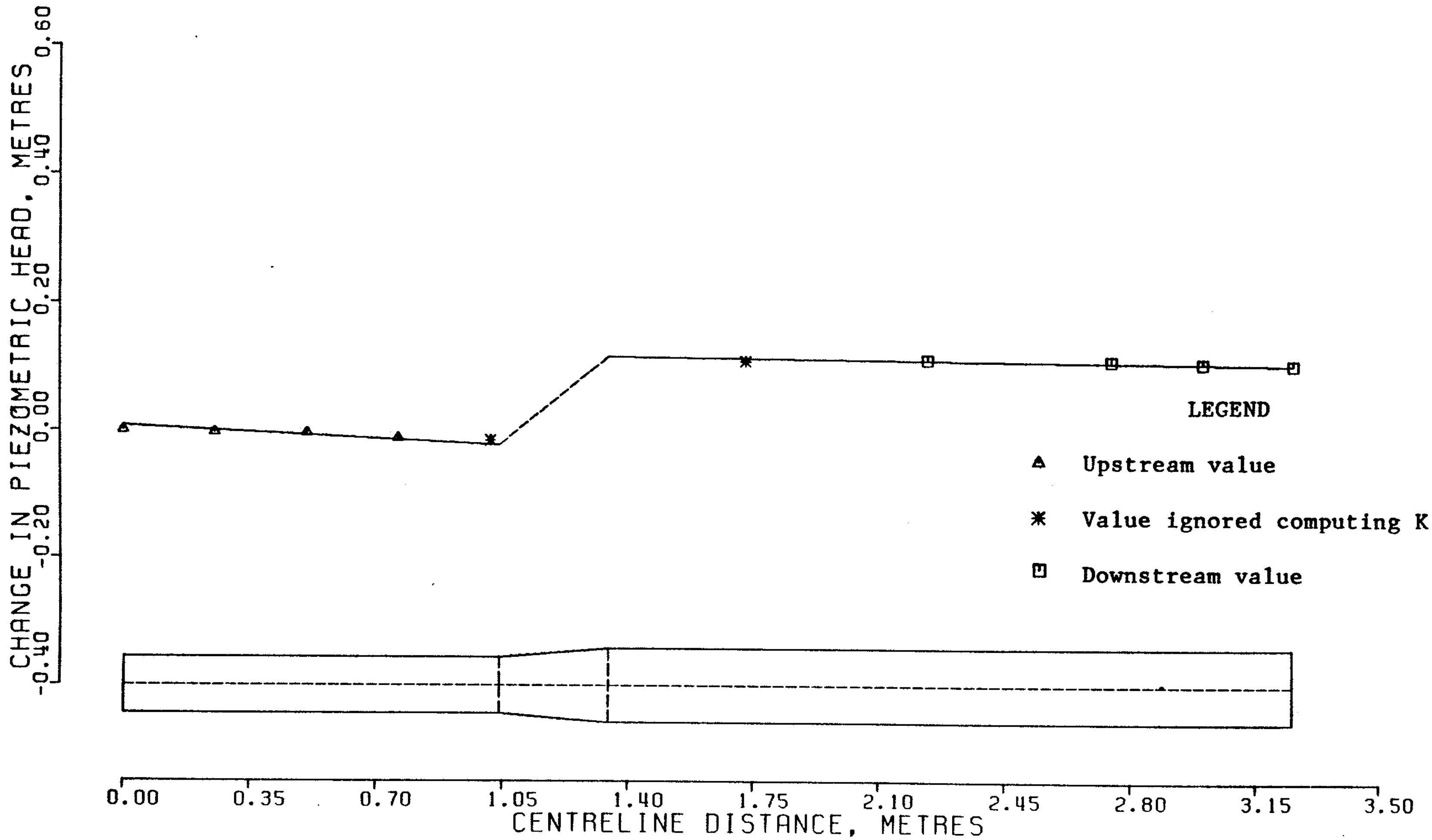

FIG. C-16 CHANGE IN PIEZOMETRIC HEAD ALONG THE HORIZONTAL CENTRELINE OF PIPE EXPANSION NO. 2B UNDER THE VELOCITY CONDITIONS OF TEST NO. 5

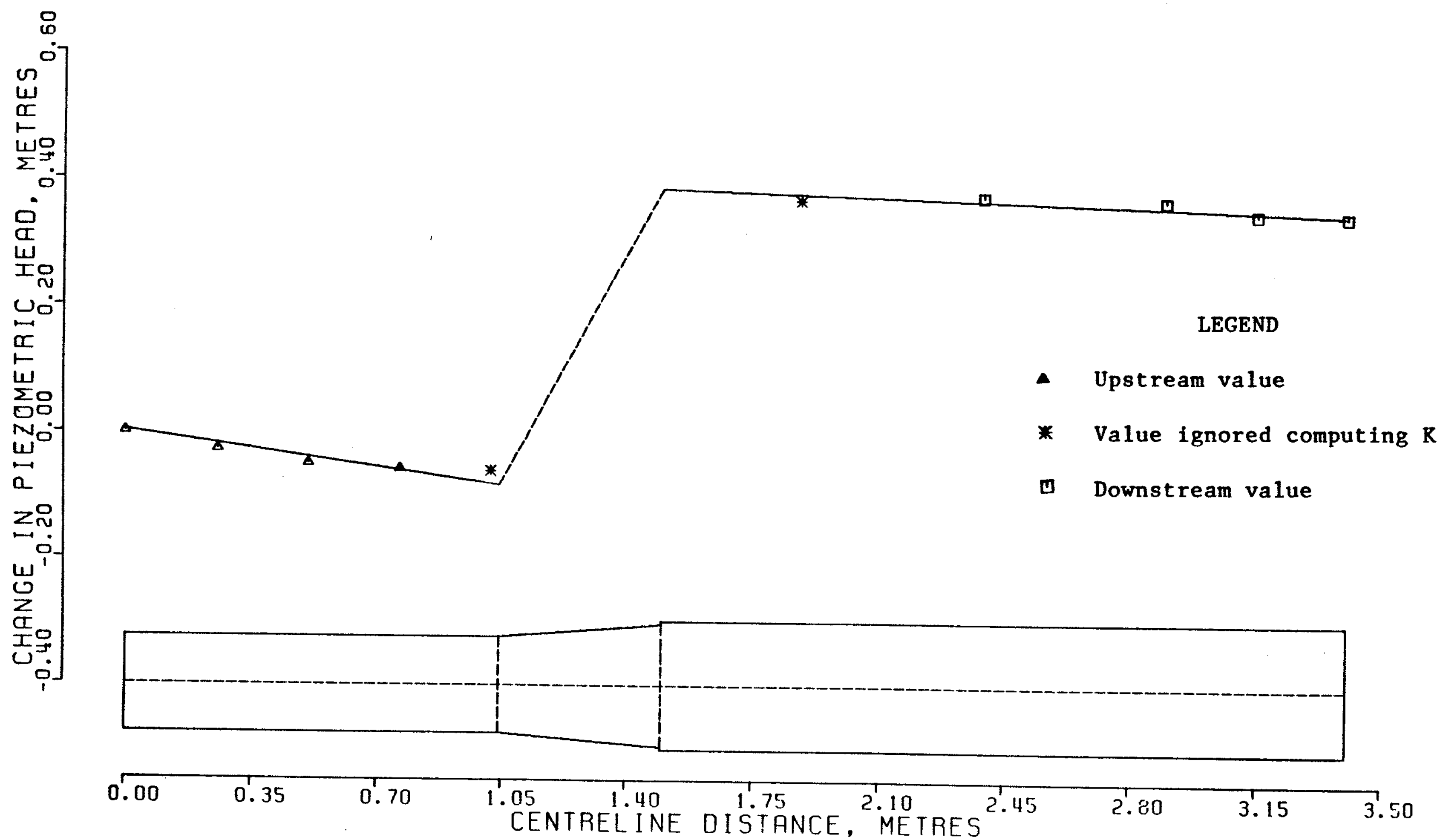

FIG. C-17 CHANGE IN PIEZOMETRIC HEAD ALONG THE HORIZONTAL CENTRELINE OF PIPE EXPANSION NO. 3A UNDER THE VELOCITY CONDITIONS OF TEST NO. 1

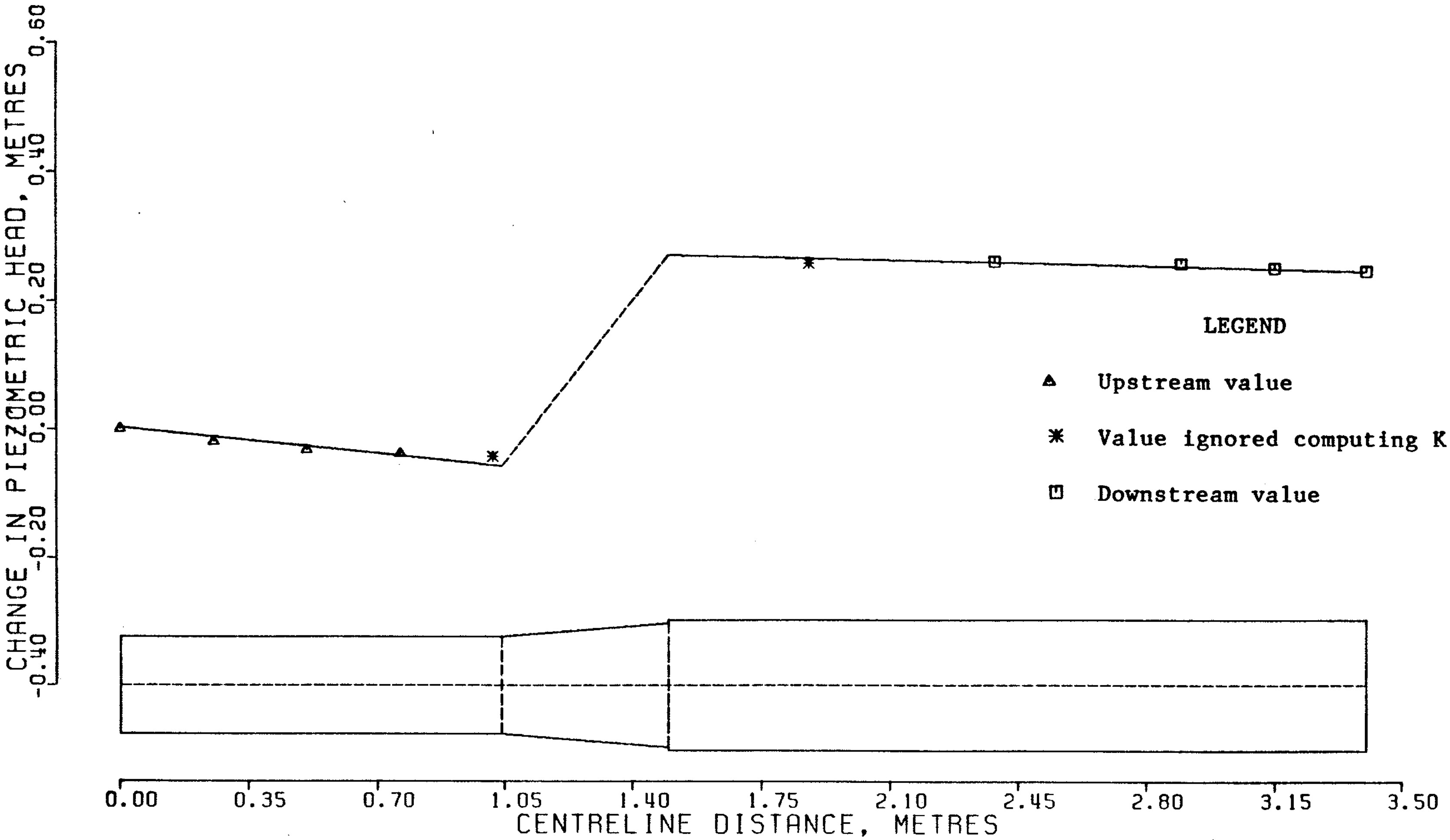

FIG. C-18 CHANGE IN PIEZOMETRIC HEAD ALONG THE HORIZONTAL CENTRELINE OF PIPE EXPANSION NO. 3A UNDER THE VELOCITY CONDITIONS OF TEST NO. 2

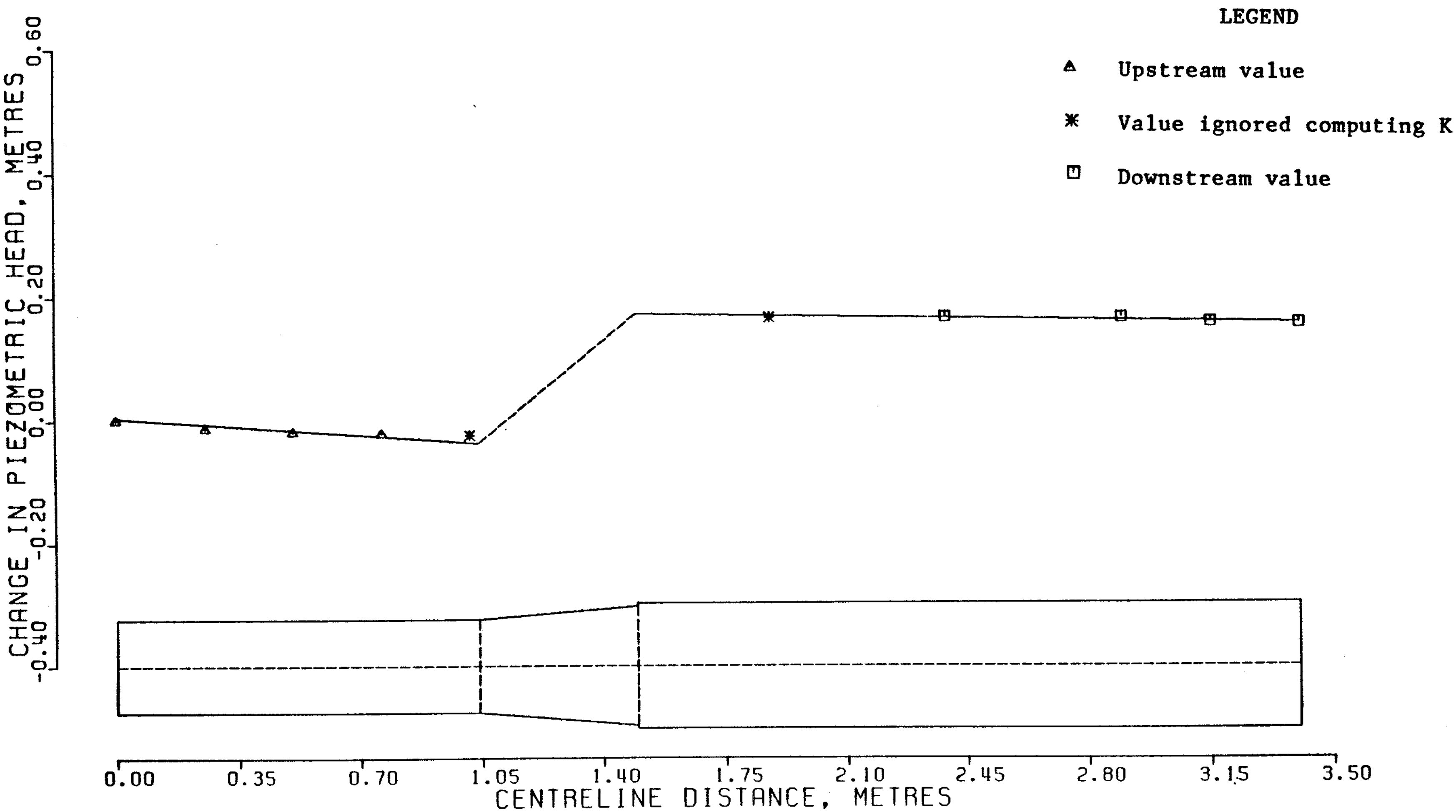

FIG. C-19 CHANGE IN PIEZOMETRIC HEAD ALONG THE HORIZONTAL CENTRELINE OF PIPE EXPANSION NO. 3A UNDER THE VELOCITY CONDITIONS OF TEST NO.3

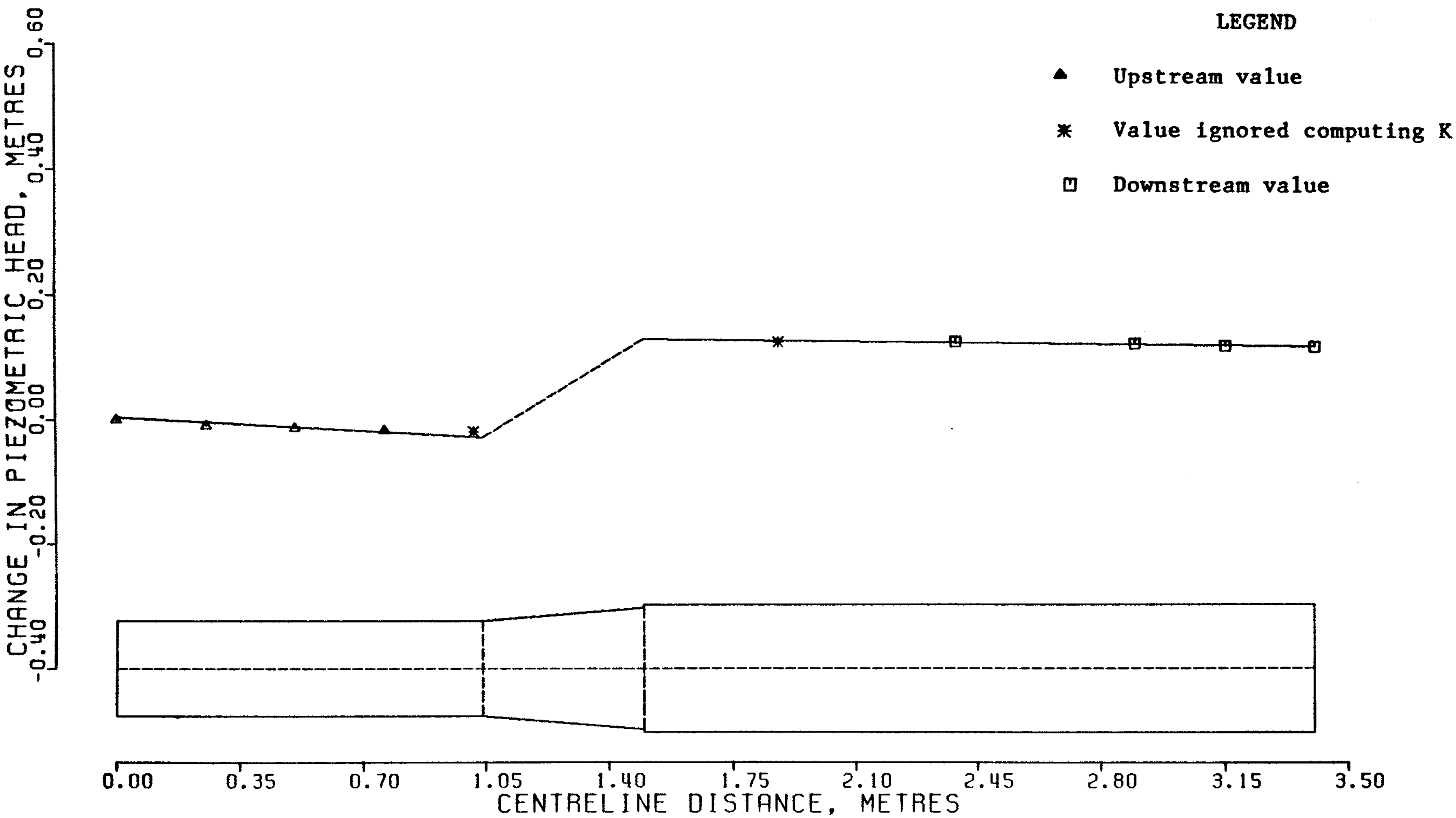

FIG. C-20 CHANGE IN PIEZOMETRIC HEAD ALONG THE HORIZONTAL CENTRELINE OF PIPE EXPANSION NO. 3A UNDER THE VELOCITY CONDITIONS OF TEST NO. 4

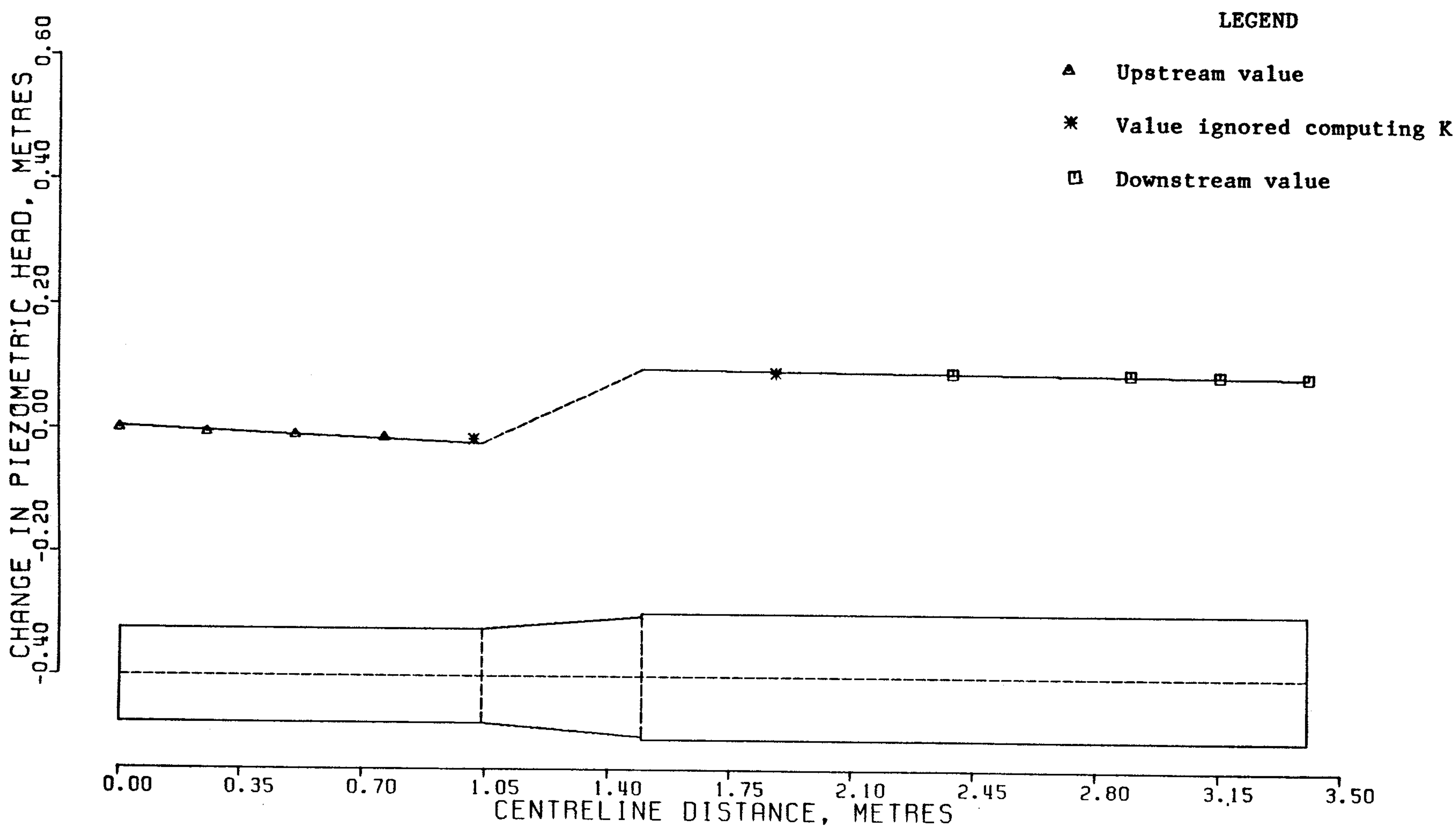

FIG. C-21 CHANGE IN PIEZOMETRIC HEAD ALONG THE HORIZONTAL CENTRELINE OF PIPE EXPANSION NO. 3A UNDER THE VELOCITY CONDITIONS OF TEST NO. 5

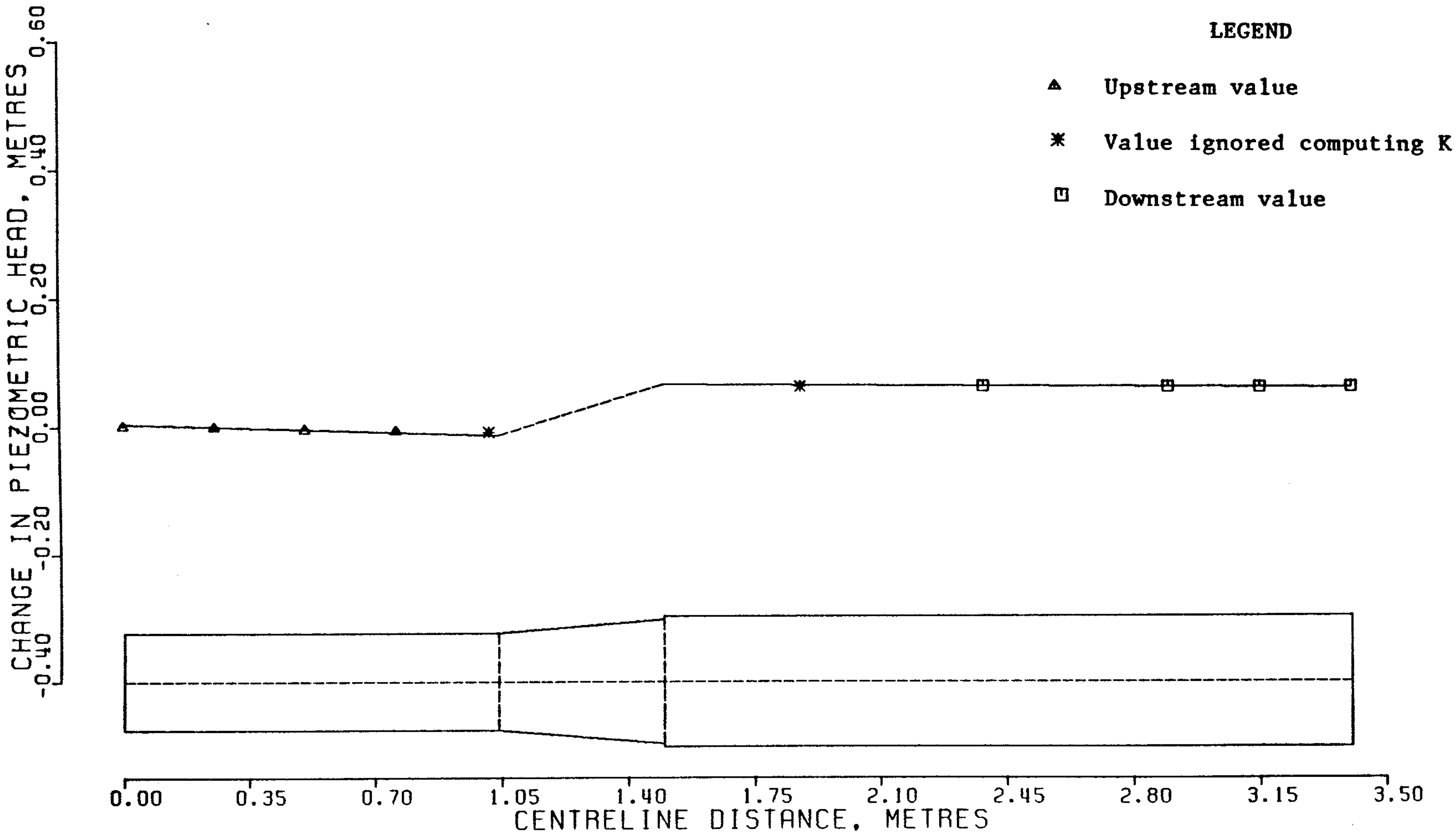

FIG. C-22 CHANGE IN PIEZOMETRIC HEAD ALONG THE HORIZONTAL CENTRELINE OF PIPE EXPANSION NO. 3A UNDER THE VELOCITY CONDITIONS OF TEST NO. 6

APPENDIX D

ALGORITHM TO CALCULATE THE ERRORS INCURRED IN THE MEASUREMENT OF PRESSURE HEAD AND IN THE CALCULATION OF WATER DISCHARGE, AVERAGE DISCHARGE VELOCITY, ENERGY LOSS ΔE AND ENERGY LOSS COEFFICIENT K

APPENDIX D ALGORITHM TO CALCULATE THE ERRORS INCURRED IN THE MEASUREMENT OF PRESSURE HEAD AND IN THE CALCULATION OF WATER DISCHARGE, AVERAGE DISCHARGE VELOCITY, ENERGY LOSS ΔE AND ENERGY LOSS COEFFICIENT K

```
C  ..........................................................
C ....PROGRAM TO CALCULATE THE ERRORS INCURRED IN THE
C ....MEASUREMENT OF PRESSURE HEAD AND IN THE CALCULATION
C ....OF WATER DISCHARGE, AVERAGE DISCHARGE VELOCITY, ENERGY
C ....LOSS AND ENERGY LOSS COEFFICIENT K
C  ..........................................................
      REAL EH,EQ,EV,EHEAD,EP,C,H,EDELE,EK,ABEK,K,KP,LTK,UTK
      READ(5,*) X,Y,D
      WRITE(6,*)
      WRITE(6,*)
      DO 11 N=1,24
       READ(5,*) DELH,DELP,V1,K,KP
      EH=X/DELH
      EQ=(1+EH)**0.467-1
      EV=EQ
      EHEAD=2*EV+EV*EV
      EP=Y/DELP
      C=1-(1/(D**4))
      H=((V1*V1)/(2*981))
      EDELE=(EP*DELP)/(-DELP+H*C)+(EHEAD*H*C)/(-DELP+H*C)
      EK=(EDELE+EV)/(1-EV)
      ABEK=EK*K
      LTK=K - ABEK
      UTK=K + ABEK
      DOPK=K - KP
      REK=DOPK/KP
      WRITE(6,100)N,EH,EQ,EV,EHEAD,EP,EDELE,EK,ABEK,K,K,
     $ABEK,KP,REK
100   FORMAT(1X,I2,2X,F6.4,2X,F6.4,2X,F6.4,2X,F6.4,2X,F6.4,
     $2X,F6.4,2X,F6.4,2X,F6.4,2X,F5.3,2X,F5.3,2X,F6.4,2X,
     $F5.2,2X,F6.3/)
 11   CONTINUE
      STOP
      END
```